



# Kent Academic Repository

**Alkhas, Sharif (2018) *Superoscillations in non-monochromatic naturally occurring waves*. Master of Science by Research (MScRes) thesis, University of Kent,.**

## Downloaded from

<https://kar.kent.ac.uk/67109/> The University of Kent's Academic Repository KAR

## The version of record is available from

## This document version

UNSPECIFIED

## DOI for this version

## Licence for this version

CC BY (Attribution)

## Additional information

## Versions of research works

### Versions of Record

If this version is the version of record, it is the same as the published version available on the publisher's web site. Cite as the published version.

### Author Accepted Manuscripts

If this document is identified as the Author Accepted Manuscript it is the version after peer review but before type setting, copy editing or publisher branding. Cite as Surname, Initial. (Year) 'Title of article'. To be published in *Title of Journal*, Volume and issue numbers [peer-reviewed accepted version]. Available at: DOI or URL (Accessed: date).

## Enquiries

If you have questions about this document contact [ResearchSupport@kent.ac.uk](mailto:ResearchSupport@kent.ac.uk). Please include the URL of the record in KAR. If you believe that your, or a third party's rights have been compromised through this document please see our [Take Down policy](https://www.kent.ac.uk/guides/kar-the-kent-academic-repository#policies) (available from <https://www.kent.ac.uk/guides/kar-the-kent-academic-repository#policies>).

---

# Superoscillations in non-monochromatic naturally occurring waves

---

*by Sharif Alkhass*



UNIVERSITY OF KENT  
SCHOOL OF PHYSICAL SCIENCES

THESIS SUBMITTED FOR THE DEGREE OF RESEARCH MASTERS OF SCIENCE IN  
PHYSICS TO THE UNIVERSITY OF KENT

Supervisor: Professor Paul Strange

# Nomenclature

## Greek Alphabet

$\alpha$	alpha
$\beta$	beta
$\chi$	chi
$\Delta$	delta
$\delta$	delta
$\epsilon$	epsilon
$\eta$	eta
$\Gamma$	gamma
$\gamma$	gamma
$\iota$	iota
$\kappa$	kappa
$\Lambda$	lambda
$\lambda$	lambda
$\mu$	mu
$\nu$	nu
$\Omega$	omega
$\omega$	omega
$\Phi$	phi
$\phi$	phi
$\Pi$	pi
$\pi$	pi

---

$\Psi$	psi
$\psi$	psi
$\rho$	rho
$\Sigma$	sigma
$\tau$	tau
$\Theta$	theta
$\theta$	theta
$\Upsilon$	upsilon
$v$	upsilon
$\varpi$	varpi
$\Xi$	xi
$\xi$	xi
$\zeta$	zeta

### Mathematical Expressions

*	complex conjugate
$\langle x \rangle$	average of $x$
$\delta$	Dirac delta function
$\frac{\partial y}{\partial x}$	Partial derivative with respect to $x$
$\Im$	Imaginary part
$\int$	Integral operator
$\Re$	Real part
$\Sigma$	summation
$E$	expectation value
$exp/e$	Exponential function
$i$	$\sqrt{-1}$
$\ln$	Natural logarithm

### Physical Constants

$\hbar$	$\frac{2\pi}{h}$
---------	------------------

---

---

$c$  Speed of light  $\approx 3 \times 10^8 m s^{-1}$

$h$  Planck's constant  $\approx 6.62607004 \times 10^{-34} J s$

**Physical Variables**

$k$  wavenumber  $m^{-1}$

$m$  mass kg

$t$  time s

# Abstract

It is well known that one might describe a wave or a function in terms of its Fourier components, therefore a function would be labelled as superoscillatory if it oscillates faster than the fastest Fourier component. This phenomena is known to be caused by the fine destructive interference between the Fourier components of a wave. There is a vast amount of literature on this special phenomena, however the main focus of this thesis will be studying and analysing the works of Sir Michael Berry, Sandu Popescu, Mark Dennis, and J.Lindberg [1][2][3][4][5], focusing mainly on naturally occurring superoscillations through the superposition of a large number of waves. In particular, investigating the effects of changing the band-width of the waves on the fractional superoscillatory area of the resultant wave as well as the effects of varying the number of waves (Fourier components) superimposing.

In the papers by Mark Dennis et al [5] [4], an in depth description is given for superoscillations in speckle patterns, through the derivation of a joint probability density function of both intensity and phase gradient. Through this, a superoscillating fraction of  $\frac{1}{5}$  is found for a disk spectrum in addition an expression is found for an annular spectrum. The main work conducted for this thesis builds on this through a range of computational methods, specifically investigating the fraction of superoscillations obtained from the superposition of two dimensional non-monochromatic waves. An interesting result found shows that the fractional area which exhibit superoscillations is given to be much smaller than  $\frac{1}{5}$  for an annular spectrum as described in [5]. The calculations conducted here describes the effect of changing the bandwidth; in which the wavenumber of the individual waves are chosen from, has on the fraction of superoscillations. In addition the effect of varying the lowest wavenumber in the spectrum, as well as the number of sources, is provided. The study of all the papers mentioned earlier involves a vast amount of statistical analysis, ranging from Gaussian and speckle statistics to probability theory.

# Acknowledgements

First and foremost I would like to thank my lecturer Professor Paul Strange for letting me undergo this research under his supervision. Ever since my undergraduate course I have always had a passion towards theoretical physics, and have long wanted to further my study with research. After meeting Paul I knew that he was an ideal choice as a supervisor for my postgraduate study, his passion and devotion to the field is truly inspiring.

Thank you to my fellow research colleagues Jack Herklots and Greg Smith for their help and support throughout my research. I am going to miss all the random yet hilarious conversations between the two, as they have never failed to make me laugh. I wish them both the best of luck for their future, they are most definitely destined for greatness.

I would also like to thank my family for supporting me during my study, and who throughout my life helped me pursue my true passions in life, they showed me that one is truly capable of anything when you set your mind to it. I would also like to give a special thanks to one of my best friends and colleague Rob Butler who has inspired me to pursue further education, he will never be forgotten. Last but not least I would like to give my thanks and love to my girlfriend Aimee Hayward for being by my side, and picking me up during stressful times.

# Contents

<b>Abstract</b>	<b>ii</b>
<b>Acknowledgements</b>	<b>iii</b>
<b>List of figures</b>	<b>v</b>
<b>List of tables</b>	<b>vii</b>
<b>1 Introduction</b>	<b>1</b>
1.1 History of Superoscillations . . . . .	3
1.2 Mathematics of Superoscillations . . . . .	3
1.3 Superoscillations and it's applications in optics . . . . .	6
<b>2 Background Reading</b>	<b>13</b>
2.1 Superoscillating Function . . . . .	13
2.2 Mathematical description of Superoscillations . . . . .	24
2.3 D dimensional Superoscillations . . . . .	33
2.4 Superoscillations in speckle patterns . . . . .	51
<b>3 Superoscillations in non-monochromatic waves in 2-Dimensions</b>	<b>62</b>
<b>4 Mathematics</b>	<b>89</b>
4.0.1 Laplace Method . . . . .	89
4.0.2 Volume of Hypersphere . . . . .	90
4.0.3 Gaussian Average . . . . .	92
4.0.4 Central limit Theorem . . . . .	93
4.0.5 Speckle Statistics . . . . .	93
4.0.6 Helmholtz equation . . . . .	96
<b>Bibliography</b>	<b>98</b>

# List of Figures

1.1	Superscillating function as given by equation (1.2.1) . . . . .	4
1.2	Superscillating function as given by equation (1.2.1).Showing the region of superscillations. . . . .	4
1.3	Intensity plot of the superscillating function as given by equation (1.2.1). . . . .	5
1.4	Intensity plot of the superscillating function as given by equation (1.2.1). Showing the region of superscillations. . . . .	5
1.5	Recreation of figure 5 in [6] and shows the intensity distribution for a superscillatory hot-spot. . . . .	7
1.6	c.f. From [6] figure (11) which is an adaptation from [7] figure(1). The figure shows the design for the quasicrystal array imaging technique. With the images of the point light sources taken as the source moves by delta y. . . . .	8
1.7	c.f. Figure 12 [6] (a) focal spot of $0.48\lambda$ produced from a 27-fold symmetry QNA. (b) Focal spot of $0.39\lambda$ produced by the 40-fold symmetric mask. (c)Focal spot of $0.23\lambda$ produced by the optimized binary ring mask. . . . .	9
1.8	c.f. Figure 2 [8] a $2.75\mu m \times 2.75\mu m$ SEM image of a cluster of nanoholes in a metal film. b, The image of the cluster is not resolved with a conventional lens of $NA = 1.4$ . c, The SOL image resolves all the main features of the cluster. Dashed circles map the positions of the holes. . . . .	9
1.9	c.f. Figure(16) in [6] Schematic for the setup of the superscillatory focusing using SLMs. The light from the fibre coupled laser is first collimated, expanded and polarised and the incident of an amplitude modulating SLM. The beam is then imaged onto a Phase modulating SLM using a 1:1 telescope with a polariser and demagnified onto the back focal plane of the microscopes objective using another telescope system. . . . .	10
1.10	c.f. Figure 1 from [9] Diagram of the polarisation contrast superscillatory microscope. . . . .	11
1.11	c.f. Figure(2) [10].Designs of lenses are given in a-c, while (d-f) are the scanning electron microscope SEM images. Images a and d are the superscillatory lense, b and e are the ONSOL with 20 micrometer opaque region. C-f are the control sample consisting of a 20 micrometer Au disk in a 70 micrometer transparent region. . .	12

2.1	track of the saddle $u_s$ using the wavenumber $k_5$ given by equation (2.1.31) . . . . .	18
2.2	Local wavenumber $q(\xi)$ with change in $\xi$ as given by equation (2.1.34)	19
2.3	Computations for the function in equation (2.1.35) and its saddle point approximations in equation (2.1.44). . . . .	22
2.4	The superoscillatory function (2.2.1) given that $N=20$ and $a=4$ . . .	26
2.5	Smooth curve showing the Gaussian approximation given in equation 2.2.37 . . . . .	31
2.6	Superoscillations given by the superposition of plane waves using equation (2.3.9) with $k_0 = 2\pi$ and $N = 10$ sources. . . . .	35
2.7	Contour plots of a two dimensional wavefunction sample's phases.	35
2.8	Plot of both the contour of several phases of the sample wave and the plot of the superoscillating surface of the two dimensional wave. (Figures 2.6 and 2.7) . . . . .	36
2.9	The relationship between the probability distribution against the ratio of the wavenumber $\frac{k}{k_0}$ . using equation (2.3.45) . . . . .	41
2.10	This is a sample wave given from equation (2.3.56) for 1 dimension, With the associated local wavenumber $k$ . . . . .	45
2.11	The resultant wave using equation (2.3.59). . . . .	47
2.12	Plot of the local wavenumber in 1D using expressions (2.3.64), (2.3.61) and (2.3.66) . . . . .	48
3.1	Relationship between bandwidth and average fraction of superoscillations. With $N=500$ waves and different $k_{min}$ values. . . . .	65
3.2	Fraction of superoscillations against bandwidth repeated for specific number of sources $N$ . Here the minimum wavenumber is given to be $k_{min} = 1\pi$ , and the number of sources are $N = 5, 6, 7, 8, 9, 10, 50$ .	66
3.3	Relationship between bandwidth and fraction of superoscillations repeated for a specific number of sources $N$ . Where $N = 5, 6, 7, 8, 9, 10, 50$ , and $k_{min} = 1\pi$ (zoomed in at bandwidth from 0 to $10\pi$ ). . . . .	66
3.4	Showing the average fraction against bandwidth for $k_{min} = 1\pi$ and $N=5, 6, 7, 8$ . The approximated curve is also given with the use of the expression given by (3.0.16) and (3.0.7). The points plotted are the average fraction superoscillating calculated. . . . .	68
3.5	Showing the average fraction against bandwidth for $k_{min} = 1\pi$ and $N=9, 10, 50, 500$ . The approximated curve is also given with the use of the expression given by (3.0.16) and (3.0.7). The points plotted are the average fraction superoscillating calculated for each bandwidth. . . . .	69
3.6	Figure of average fraction of superoscillations against bandwidth using the expression in (3.0.12). Using the expression (3.0.13) for delta and calculating the fraction using $k_{min} = 1\pi, 2\pi, 3\pi, 4\pi, 10\pi, 50\pi, 100\pi$ .	71
3.7	Average superoscillating fraction against bandwidth starting at $k_{min} = 1\pi$ for several values of sources $N = 5, 6, 7, 8, 9, 10, 50$ , for the special case where the bandwidth of every sample is fixed. . . . .	72
3.8	Zoomed figure of 3.4 at bandwidth 0 to $10\pi$ . . . . .	72

3.9	Average fraction of superoscillations with fixed bandwidth. (change in $k_{min}$ ) . . . . .	73
3.10	Relationship between $\Delta\lambda$ and $B$ (bandwidth) as given by (3.0.18). . . . .	74
3.11	Graph for the distribution of wavenumber $\frac{k}{k_{min}}$ for number of sources $N = 50$ and $k_{min} = 1\pi$ , with bandwidths given by $B = 0\pi, 2\pi, 50\pi$ . The bar chart is the probability distribution calculated, light blue line shows the theoretical prediction given by (2.4.37) using $k_2$ as given by (2.4.44). . . . .	75
3.12	Graph for the distribution of wavenumber $\frac{k}{k_{min}}$ for number of sources $N = 50$ and $k_{min} = 100\pi$ , with bandwidths given by $B = 0\pi, 2\pi, 50\pi$ . The bar chart is the probability distribution calculated, light blue line shows the theoretical prediction given by (2.4.37) using $k_2$ as given by (2.4.44). . . . .	76
3.13	Graph of distribution of the wavenumber $\frac{k}{k_{max}}$ for $N = 5$ and $N = 50$ , showing that $N = 5$ is higher overall. . . . .	77
3.14	Graph for the distribution of wavenumber $\frac{k}{k_{min}}$ for number of sources $N = 5$ and $k_{min} = 1\pi$ , with bandwidths given by $B = 0\pi, 2\pi, 50\pi$ . The bar chart is the probability distribution calculated, light blue line shows the theoretical prediction given by (2.4.37) using $k_2$ as given by (2.4.44). . . . .	78
3.15	Average fraction superoscillating for $N=10$ waves given $k_{min} = 1\pi, 2\pi$ for Random angles. . . . .	79
3.16	Superoscillatory region of a 2-D non-monochromatic sample wave with $k_{min} = 2\pi, N = 50$ and $B = 2\pi$ . . . . .	80
3.17	Superoscillatory region of a 2-D non-monochromatic sample wave with $k_{min} = 2\pi, N = 50$ and $B = 50\pi$ . . . . .	80
3.18	Superoscillatory region of a 2-D non-monochromatic sample wave with $k_{min} = 10\pi, N = 50$ and $B = 2\pi$ . . . . .	81
3.19	Superoscillatory region of a 2-D non-monochromatic sample wave with $k_{min} = 10\pi, N = 50$ and $B = 50\pi$ . . . . .	81
3.20	Comparison between intensity and superoscillatory regions, for 1 sample wave (Bandwidth=0). . . . .	82
3.21	Comparison between intensity and superoscillatory regions, for 1 sample wave (Bandwidth=2 $\pi$ ). . . . .	83
3.22	Comparison between intensity and superoscillatory regions, for 1 sample wave (Bandwidth=10 $\pi$ ). . . . .	83

# List of Tables

3.1	Table showing the value calculated analytically of the constant $a$ found in our expression in 3.0.9 for $N = 5, 6, 7, 8$ and $k_{min} = 1\pi, 2\pi, 3\pi, 4\pi, 10\pi, 50\pi, 100\pi$ . . . . .	87
3.2	Table showing the value calculated analytically of the constant $a$ found in our expression in 3.0.9 for $N = 10, 50, 500$ and $k_{min} = 1\pi, 2\pi, 3\pi, 4\pi, 10\pi, 50\pi, 100\pi$ , for the $N = 500$ . . . . .	88

# Chapter 1

## Introduction

---

The following thesis will be investigating specific properties of Superoscillations, which are an unusual phenomena caused by band-limited functions that oscillate faster than their fastest Fourier component. This seems almost paradoxical, however it is shown how such functions are found near regions of fine destructive interference between wave components where the function seems to vanish and the phase is large. It is known that functions can be constructed from their Fourier components, or rather, a superposition of waves of different frequencies. Superoscillations are then formed at specific points in the functions where the components interact with each other in such a way, as to produce a new wave that is oscillating faster than the band-limit. The main focus however is going to be the study of superoscillations in terms of waves constructed through the superposition of multiple wavefunctions. Regions where the phase of the wave tends to be undefined while the amplitude of the function is small (tends to 0), would correspond to superoscillations. The main focus of this thesis will be building on the works of Sir Michael Berry and Mark Dennis *Natural Superoscillations in Monochromatic Waves in D Dimensions*[3] as well as *Superoscillations in Speckle Patterns* [5] by Mark Dennis and will be the foundation of the work conducted here. An investigation is carried out into superoscillations formed through the superposition of non-monochromatic waves in 2 dimensions. The thesis will also analyse the effect of changing the bandwidth of wavenumbers and the number of waves on the fraction of superoscillations.

To begin with, a discussion will be made of a few examples of superoscillating functions as given by Sir Michael Berry's paper *Faster than Fourier* [1], where he provides an example of a superoscillating function and uses asymptotics; in particular the Saddle Point Method, to give an approximate solution to the integral of a specific function, and thus showing how such functions tend to be found in regions of complex saddles. In addition, the paper investigates the local wavenumber as an indication that the function is superoscillating. Following this, a brief analysis is made of the paper by M Berry and S Popescu *Evolution of Quantum Superoscillations and Optical Superresolution Without Evanescent Waves*[2], by looking at the example given in the paper for a superoscillatory function described as

the initial state of the wavefunction. The paper describes how such a function is superoscillatory and explores the regions where it exhibits this behaviour. In addition the evolution of the wavefunction over time is shown, though this will not be discussed in this thesis.

The second paper reviewed titled *Natural Superoscillations in Monochromatic Waves in D Dimensions* by Sir Michael Berry and Mark Dennis [3], describes superoscillations in naturally occurring monochromatic waves with D dimensions by analysing the local wavenumber of a function formed from the superposition of isotropic random waves in multiple dimensions, leading to a result showing that an increase in dimensions of the waves used corresponds to an increase in the fraction of superoscillations observed (regions where the local wavenumber is larger than maximum wavenumber in the spectrum). There is a focus on the one dimensional case here. The fractions are calculated by taking the probability distribution of all local wavenumber values relative to the maximum wavenumber. This paper makes the use of Gaussian statistics, which is given in the limit of a large number of independent random variables.

Following the study of [3], an in depth discussion is made of the results from a paper by M R Dennis titled *Superoscillations in Speckle Patterns* [5]. For this, 2-dimensional plane waves are superimposed, where the individual waves have a direction and phase that are independent of each other. The interference caused by the waves forms an intensity pattern referred to as speckle patterns. First a joint probability density function is found for both the intensity and the phase gradient of the wavefunction, and the correlation between both superoscillatory regions in intensity and phase gradient is described. Furthermore, the work by Mark Dennis and Jari Lindberg titled *Natural Superoscillation of Random Functions in One Or More Dimensions* [4] will be of great importance, as it expands the results in [5] including higher dimensions, and continues on with the specific case of one dimensional random waves.

For the work conducted in this thesis, an investigation will be carried out on how the superoscillating fraction of a 2-dimensional non-monochromatic wave, which is formed from the superposition of random waves, varies as the bandwidth of the individual waves changes. The wave in consideration is formed from the superposition of isotropic waves, each wave has an amplitude and phase component that are random and independent variables, but have the same underlying distribution. This is similar to what has been provided in [5] and [4], however specifically looking into the effects of changing the bandwidth from which the wavenumbers are selected. Furthermore, The effect of changing the maximum and minimum wavenumber (the largest and smallest wavenumber in the spectrum) on the fraction of superoscillations will also be examined, along side the change in the number of sources superimposing. A comparison is then made to the results found in [5] and [4], by analysing the probability density function of the local wavenumber, as this provides a clear indication of the superoscillatory regions. The computations here involves a large number of 2-dimensional wave samples in order to obtain an

average fraction of superoscillations. All the calculations here are conducted using MATLAB.

## 1.1 History of Superoscillations

Superoscillations have been known to exist through many observations and applications and some of which date back to around 1952 by Giuliano Toraldo di Francia [11], The microwave community were hard at work to find a way to beat the diffraction limit for directivity and this goes back to the theory of linear arrays proposed by Schelkunoff in 1943 [12]. Several studies have shown that super-directive antennas have the ability to beat the diffraction limit. This method involves an antenna array that creates an arbitrarily narrow beam through the interference of waves, which are created by various array elements [13]. However it was only until 1964-1988 that the works of Yakir Aharonov, Vaidman and Albert have brought to light the idea, through the results of weak measurements of post and pre quantum mechanical systems, which could lie outside of the allowed eigenstates, in particular it was a measurement of the spin  $\frac{1}{2}$  particle values [14].

Superoscillations since have been studied mathematically by many, for example in 2006 P.J.S.G. Ferreira and A Kempf [15] showed that an energy of a signal required increases exponentially as the number of oscillations required increases. This is a follow up to their previous work in 2002 [16] which investigates how superoscillations could be used to transmit information in low bandwidth channels. The paper also shows that it is possible to compress vast amount of information into a small segment of a signal with low bandwidth. In addition, the energy required increases with both the amount of compression and the size of the message. In 2006 [2] Sir M. Berry and Popescu S. describe the behaviour of a superoscillatory function, given as an initial state of a quantum wavefunction, when allowed to freely evolve with time. They demonstrate how sub-wavelength waves are formed beyond a diffraction grating and are also seen to be maintained for long distances. The study has been followed by a large number of applications in optics which we will discuss below.

## 1.2 Mathematics of Superoscillations

Superoscillations are known to be functions that oscillate faster than their fastest Fourier component, therefore a good way of expressing these functions is to start off with a simple 1 dimensional wave that is composed of six Fourier components as given by [17].

$$f(x) = \sum_{n=0}^5 a_n \cos(2\pi nx) \quad (1.2.1)$$

where  $a_n$  are the Fourier components and the phase of the waves are determined by  $2\pi n$ . Therefore the fastest Fourier components will have maximum wavenumber

of  $k_{max} = 10\pi$ . The values for  $a_n$  are given as  $a_0 = 1$ ,  $a_1 = 13295000$ ,  $a_2 = 30802818$ ,  $a_3 = 26581909$ ,  $a_4 = -10836909$  and  $a_5 = 1762818$  [17]. The following figures shows the resultant wave  $f(x)$  alongside the fastest Fourier component.

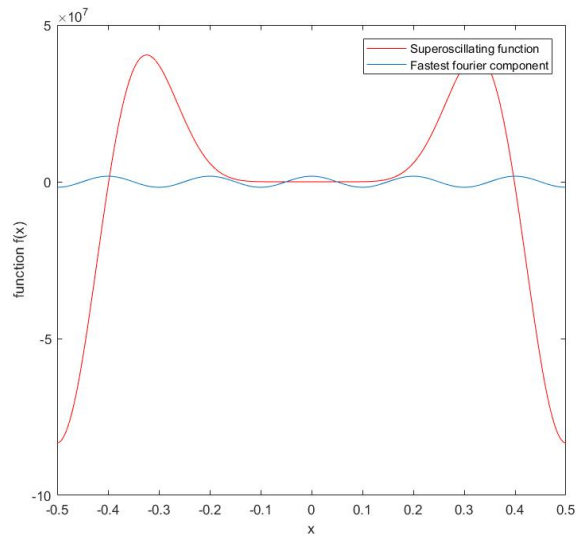


Figure 1.1: Superoscillating function as given by equation (1.2.1) alongside the fastest Fourier component.

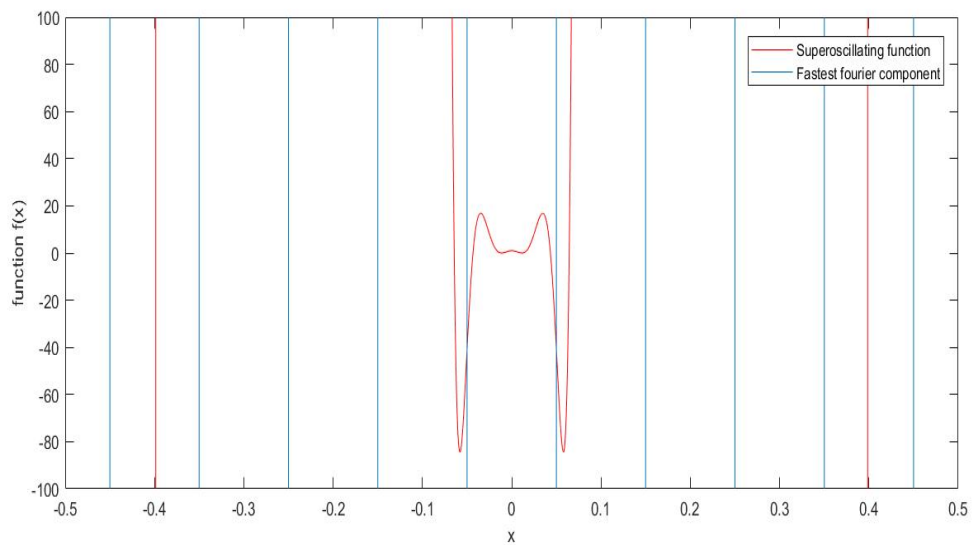


Figure 1.2: Superoscillating function as given by equation (1.2.1) alongside the fastest Fourier component. This is the same plot as figure 1.1 showing the region of superoscillations.

At first glance the function seems to oscillate slower than the fastest component, however at closer inspection when the value of  $x \approx 0$  then the function is seen to oscillate faster than the fastest Fourier component  $\cos(10.\pi)$ . The function can also be seen to exhibit superoscillatory behaviours in the region of low

intensity. The figure below shows the intensity plot of the function near  $x \approx 0$ , and is done by taking the modulus squared of the function,  $|f(x)|^2$ .

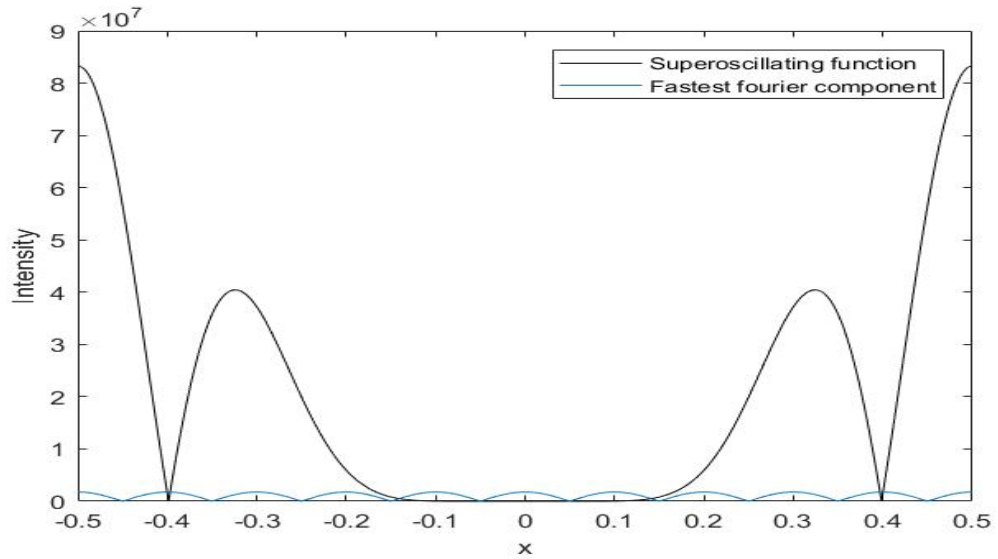


Figure 1.3: Intensity plot of the superoscillating function as given by equation (1.2.1) alongside the fastest Fourier component.

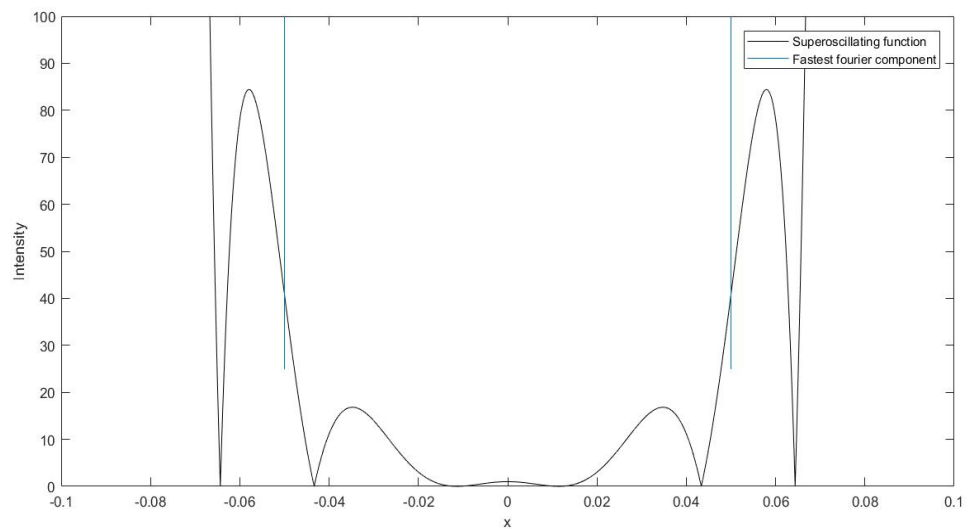


Figure 1.4: Intensity plot of the superoscillating function as given by equation (1.2.1) alongside the fastest Fourier component. This is as given in figure 1.3, showing the superoscillatory region.

Then from analysing the figures and equation (1.2.1) above, we can see that superoscillatory functions are generally found near regions of low intensity, and are caused by the delicate destructive interference of the waves. This idea is reinforced through the works of Mark R. Dennis, Alasdair C. Hamilton and Johannes

Courtial, where an analysis of random optical speckle patterns formed from the superposition of isotropic Gaussian waves, and by taking the joint probability density of both intensity and phase gradient [5]. The ideal way of representing superoscillations is by looking at the phase of the resultant function. That is by analysing the local wavenumber of the function, and so one can stipulate that at any point in the function where the local wavenumber of the function is larger than the wavenumber of the fastest Fourier component, then the function is said to be superoscillatory.

There are several other mathematical description of superoscillations, some of which are discussed in chapter 2 of the thesis. Here are some papers to consider [18] [19] where a mathematical description is provided along with the theory of weak measurements which lead to superoscillatory behaviour.[1] also describes this phenomena, and uses asymptotic analysis in order to gain a better understanding of them. A very fascinating paper by M. V. Berry and M. R. Dennis [20] titled *Phase Singularities in Isotropic Random Waves*, discusses a large number of statistical properties associated with dislocations that are formed through the superposition of isotropic but random Gaussian waves. The statistics are discussed for cases where the waves are not monochromatic and are not particularly isotropic. These Phase singularities would be of great interest since superoscillations are known to be found near these regions.

### 1.3 Superoscillations and it's applications in optics

In the recent years there has been many advances in optics that has changed the way we perceive the world around us and that has contributed to a wide range of scientific fields and discoveries. In spite of this, there is still much to be explored, specifically the use of the popular microscope as the standard imaging technique. Optical microscopes are limited in the resolution it can create and by the diffraction limit, which was first described by Ernest Abbe's equation  $d = \frac{\lambda}{2n \sin(\theta)}$ , here  $d$  is the Abbe diffraction limit and  $2n \sin(\theta)$  is the numerical aperture. However, there has been many attempts to beat this diffraction limit by using various methods, including the capture of evanescent waves in the near-field [21] [22] by the use of Near Field Scanning Microscope (SNOM), where a scanning tip collects light in the near-field of the surface. The resolution is dependent on the size of the aperture hole in which the light is collected through. The idea of capturing evanescent waves is found to date back to around 1928 [23].

Now we will look into the possibility of beating the diffraction limit using superoscillations. But first we will have to look at specific properties of "hot-spots" produced by superoscillations in order to understand superoscillatory lenses. As mentioned in [6] one of the main feature of the intensity pattern produced as shown in the figure 1.5 below is the hot-spot width which determines the resolution of the image. The side-bands usually degrades the image produced, and a good measure of the efficiency of the lens is by taking the ratio of the hot-spot to sideband intensities. The measure of the grass level, which is the residual low intensity found in the field of view, against the hot-spot intensity gives the noise of level of

the imaging apparatus.

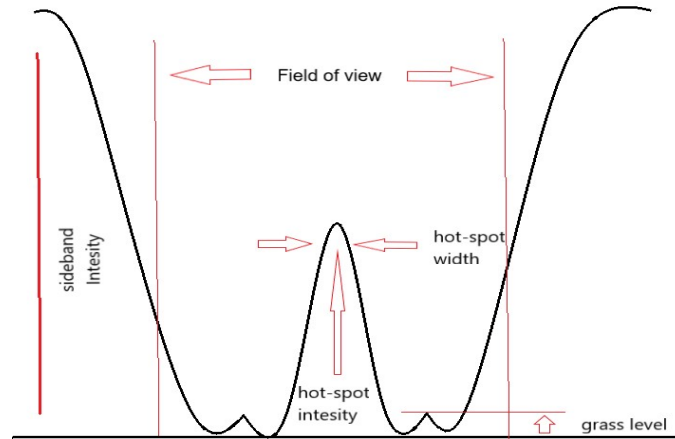


Figure 1.5: A recreation of figure (5) in [6] and shows the intensity distribution for a superoscillatory hot-spot. The figure shows important features such as the grass level, field of view and the sideband intensities

Now investigating the process of designing a superoscillatory mask that can create a hot-spot of light with arbitrary profile located at any distance from the mask, and outside the near-field. The paper [24] shows how designing such mask is possible and how it might be used as a super-resolution imaging tool. They show that there are two main steps in finding the algorithm for designing the mask, first, the required sub-wavelength hot spot is given as a series of prolate spheroidal wavefunctions [25]. Then the required complex mask transmission functions can be derived by using scalar angular spectrum description of light, from the mask, to the superoscillating feature.

In 2007 the first observation of optical superoscillations was made by Fu Min Huang, Nikolay Zheludev et al, in the papers [26] [7] where they illustrated how light can be focused to distances up to several tens of wavelengths from the screen, using a quasi-crystal array illuminated by a coherent light source. The array contained approximately 14000 holes with a diameter of 200nm each. In order to map the distribution created by the array a scanning near-field optical microscope was used as a point light source of wavelength 635nm, and the array acted as a superoscillatory lens that mapped the point like source to the other side. Figure 1.6, as shown in [6], below shows the schematic of such a setup.

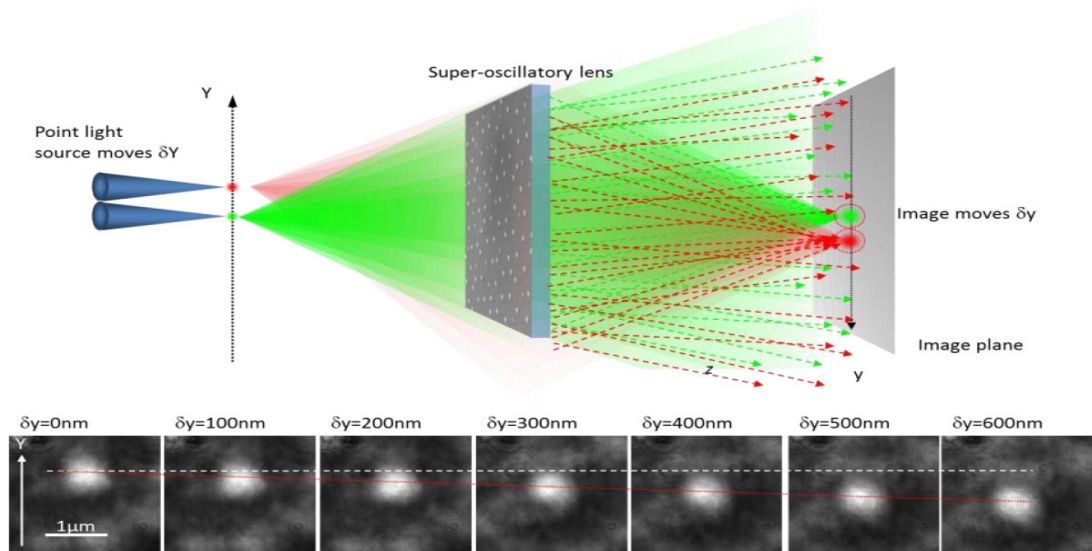


Figure 1.6: c.f. From [6] figure (11) which is an adaptation from [7] figure(1). The figure shows the design for the quasicrystal array imaging technique. With the images of the point light sources taken as the source moves by  $\delta y$ .

It was shown the point like source is imaged on the other side as a hot-spot, and when the point like source is moved, it was shown to have moved by the same amount on the opposite side. The hot-spots produced by the array was created using superoscillations. This array is also shown to have the property of magnification without the need to move the array closer or further from the source, but also multiple images of the observed object can be made on the same focal plane [27].

There has been several developments of superoscillatory binary lenses which stem from the previous work on the quasicrystal hole arrays. Here we will review some of these binary lenses as shown in [6]. First is a 27-fold symmetric quasicrystalline array, which is quasi periodic and is made by projecting a hypercubic lattice, which is 27 dimensional, to a plane. This comes from the works of [28], which provides a grid-projection method for creating quasiperiodic tilings. The second mask is a 40-fold symmetric mask, which is quasi-random. This randomness is achieved by using randomly placed holes on spiral arms, where the distance between each hole and the central point is random [29]. Following the works of [30] and [31], an optimized binary ring mask is created using the binary particle swarm optimization method.

It is shown in [6] figure 12 and given below by figure 1.7, the focal point produced by each of these binary masks has its own unique property. For example the 27-fold symmetry mask forms a focal spot of  $0.48\lambda$  with a field of view of  $90^\circ$ , but has very low sidebands this is given as figure 1.7 a . Whereas in figure 1.7 b representing the 40-fold symmetric mask, the focal spot is  $0.39\lambda$  but has a moderate amount of sideband intensity. Lastly the optimized binary ring mask is shown to give a focal spot of  $0.23\lambda$  but has the highest amount of sideband intensity. Though each of these masks show different focal point sizes, the applications of each could vary from one mask to the other. Note here that the wavelength used

is around 640nm and each mask is observed in different mediums. Where (a) is in a panel, (b) in air and (c) in immersion oil.

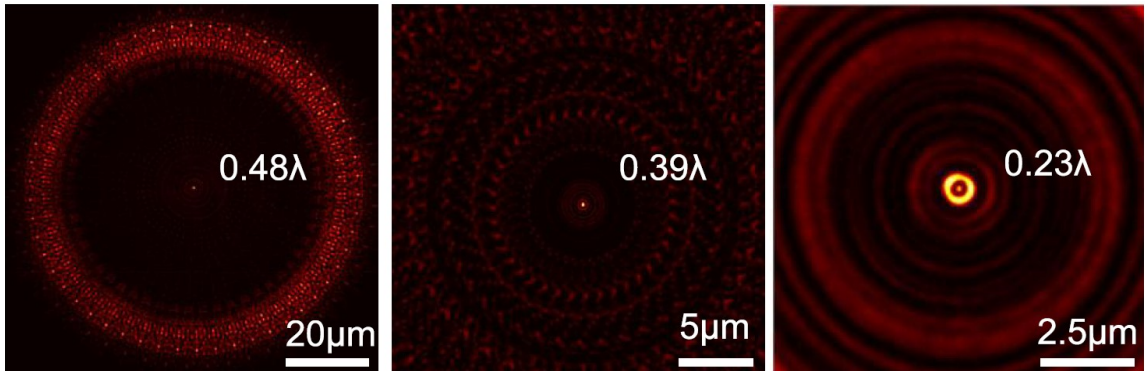


Figure 1.7: c.f. Figure 12 [6] (a) focal spot of  $0.48\lambda$  produced from a 27-fold symmetry QNA. (b) Focal spot of  $0.39\lambda$  produced by the 40-fold symmetric mask. (c) Focal spot of  $0.23\lambda$  produced by the optimized binary ring mask.

Using binary masks as an imaging technique is shown in the paper [8], instead of using a continuous mask, they have been able to develop a high-throughput binary superoscillatory lens. This lens is easy to manufacture and is consisted of several concentric rings of varying width and diameter. Here a particular scanning mode is used alongside the superoscillatory lens illumination, where a CCD detector is used to reconstruct the image from the signal. This allows the unwanted scattering created by the ‘halo’ to be removed. The construction of the binary lens here uses binary particle swarm optimization method as mentioned above. Using a fabricated cluster of nanoholes in a 100nm gold film, it can be shown that the superoscillatory lens surpasses the performance of the conventional lens, were a conventional lens has not identified the holes as clearly as the superoscillatory lens. This is shown in figure 1.8 below as given by figure 2 of [8]. The paper also reinforces this result by comparing the recorded images with ones simulated by computer modelling and shown good agreement with the resolution and shape.

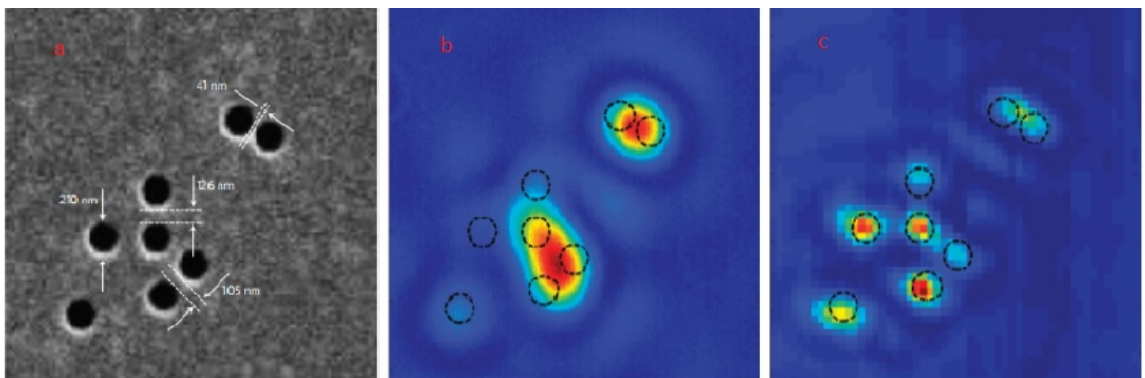


Figure 1.8: c.f. Figure 2 [8] a  $2.75\mu\text{m} \times 2.75\mu\text{m}$  SEM image of a cluster of nanoholes in a metal film. b, The image of the cluster is not resolved with a conventional lens of  $NA = 1.4$ . c, The SOL image resolves all the main features of the cluster. Dashed circles map the positions of the holes.

There are other ways in which superoscillation focusing is achieved, and can be done by the using waves with precise amplitude and phase, that interfere and create a beam that is directed using a spatial light modulator alongside a conventional microscope objective. These are called dynamic superoscillatory lenses and are designed with the works of [11] [32][33][34]. First a Laser beam is directed at an amplitude shaping SLM, then beam is then directed at a phase shaping SLM by using an imaging telescope. The beam is then demagnified and directed at the back focal plane of the microscope's objective. Here the field on the focal plane is shown to be related by Fourier Transform and therefore any field profile can be found. This is as described in [6] figure 16 and recreated here in figure 1.9 below.

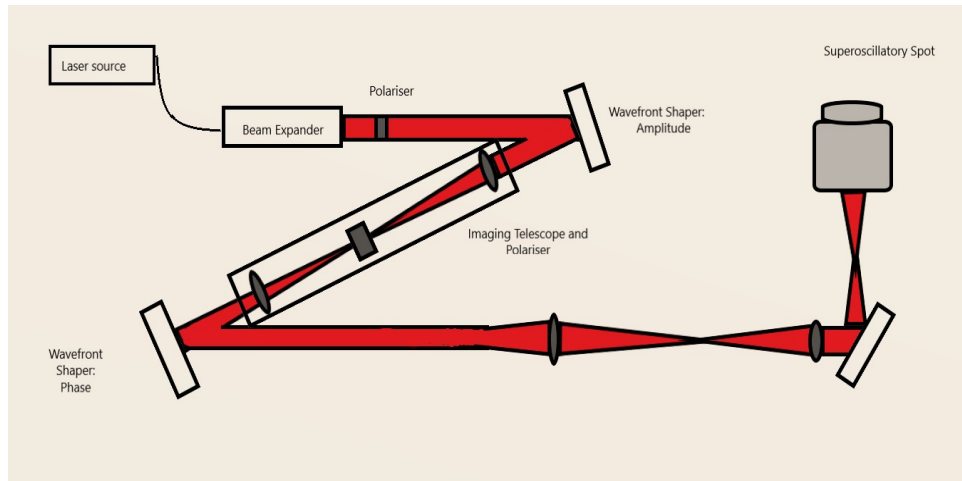


Figure 1.9: c.f. Figure(16) in [6] Schematic for the setup of the superoscillatory focusing using SLMs. The light from the fibre coupled laser is first collimated, expanded and polarised and the incident of an amplitude modulating SLM. The beam is then imaged onto a Phase modulating SLM using a 1:1 telescope with a polariser and demagnified onto the back focal plane of the microscopes objective using another telescope system.

In order to create a desired focal spots, a method called the eigenmode method [35] [36] is applied, here various test masks are used in order to probe the optical system's lenses, microscope objective and free space. The spot size and intensity matrix operators are found which in turn can given the eigenvalues for intensity and spot size from the eigenvectors and eigenmodes.

The use of superoscillatory lenses has been used in many applications and studies, for example in [9], demonstrates how superoscillations are used to probe unlabelled living cells using optical super-resolution imaging techniques without the need for fluorescent probes. In order to image unlabelled cells, a new system where a superoscillatory microscope is combined with a polarisation contrast imaging setup that contains spatial light modulators and a liquid crystal panel. Here the crystal panel controls the input polarization and the spatial light modulators directs the beam into the microscope. They have been able to capture four different super-resolved images of the sample with different incident polarisations, therefore can find the orientation angle and anisotropy of each pixel. The setup used for the polarisation-contrast superoscillatory microscope is shown in figure 1.10 as given in figure(1) from [9].

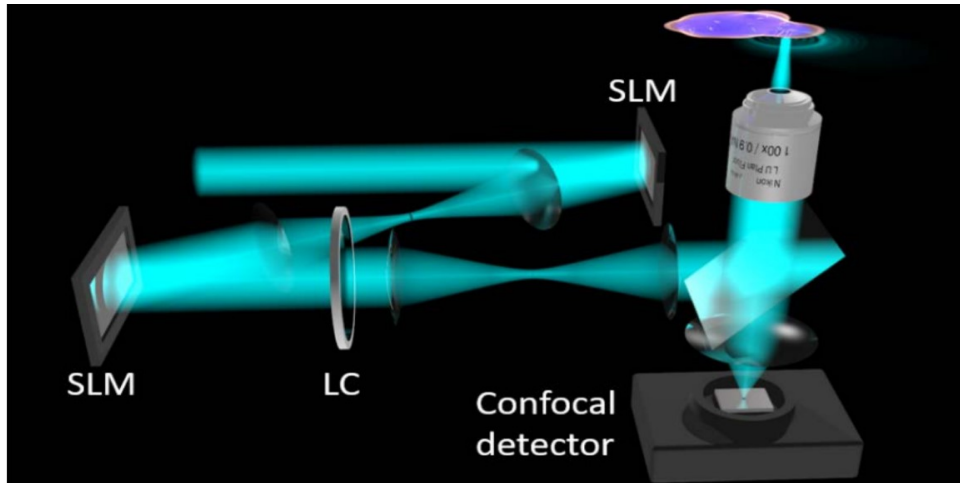


Figure 1.10: c.f. Figure 1 from [9] Diagram of the polarisation contrast superoscillatory microscope.

The result is the ability to highlight significant structures like cell membranes and actin-filaments to reveal new information about the biological structures. As an example in figure (2) of [9] it can be shown that a Osteosarcoma cell can be imaged with much higher resolution than using standard confocal microscopes.

Going back to Binary SOLs and superoscillatory focusing using SLM here are a few differences and advantages for each. To start, SLM setups are seen to have a more complex setup than Binary SOLs as they require more components, whereas the binary SOL only require one component. Furthermore, the SLM are more sensitive to aberrations. On the other hand, the working distance for a SLM is much larger than that of a binary setup, this is because the system can allow the focal spot to be directed at the microscope objectives' focus. This is said to give better results when imaging on thicker objects easier [6].

One of the main problems that SOL faces is the scattering caused by high intensity side bands that accompany the hot-spot generated. Therefore with smaller hot-spots, the sideband intensities increase relative to the hot-spot intensity. However there have been attempts to solve this, for example in [10], a new proposed class of superoscillatory lenses have been able to move the sidebands far from the focal point, and are called optical needle superoscillatory lenses (ONSOL for short). These lenses are shown to produce a focal spot that is extended in the axial direction as opposed to having many axially localised spots as given by SOLs. The main idea behind the design of the ONSOL is that the central region of the lens is concealed by a stop, this allows a shadow region to be formed around the focus. Figure 1.11 below as given by [10] figure (2), shows the design of the ONSOL lenses along with the standard SOL, these are made using focused ion beam milling of a gold film deposited on a silica substrate. Images a and d show the SOL, b and e show ONSOL. c and d show a simple disk with a transparent region behind it and is used as a control sample.

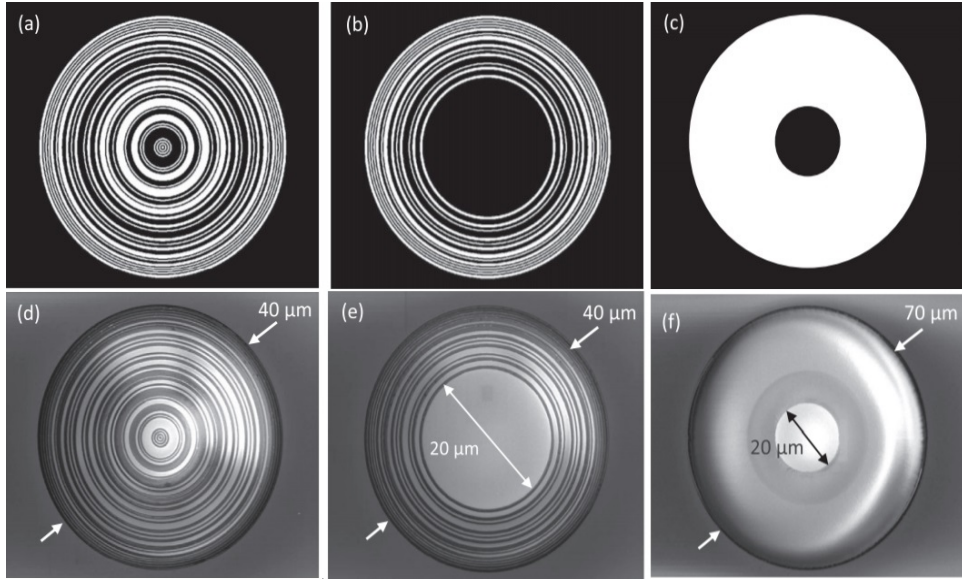


Figure 1.11: c.f. Figure(2) [10]. Designs of lenses are given in a-c, while (d-f) are the scanning electron microscope SEM images. Images a and d are the superoscillatory lens, b and e are the ONSOL with 20 micrometer opaque region. C-f are the control sample consisting of a 20 micrometer Au disk in a 70 micrometer transparent region.

The results in [10] show that when a beam of wavelength 640 nm is used, the ONSOL forms a long optical needle 4 micrometers from the lens, that is approximately 7 micrometers in length. While the SOL forms several focal spots at various distances from the lens. The size of the spot produced by ONSOL is found to be larger than that of the SOL, however it is isolated from any intense sidebands. The result of increasing the size of the blocked region in the ONSOL causes the needle to move away from the lens and the field of view around the needle also increases, this is though, at the expense of the intensity.

As seen, there are many applications of optical superoscillations in regards to imaging, but there are other areas of research where optical superoscillations are useful. As an example [37], shows the behaviour of a single photon and how the wavefunction can contain sub-diffraction properties, with length scale smaller than the wavevector eigenvalues. The method used here is quite similar to that of Young's double slit experiment, except here a superoscillatory pattern is observed using a one dimensional binary superoscillatory lens, through interference of multiple beams of specific phases and intensities. Then an analysis of the local momentum, spatial confinement and energy flow distribution is provided for the field which it created. The fantastic results shown in this paper, illustrates how superoscillations can be formed from the interaction of a single photon wavefunction with itself. In addition, the local momentum of the photon shows expectation values much higher than that of the largest Fourier component in the spectrum. This study may be a great path for applications in quantum physics. To conclude, superoscillations has been extensively researched by many, with a potential to be used in a wide range of applications.

# Chapter 2

## Background Reading

---

### 2.1 Superoscillating Function

#### Introduction

In the following section an in depth analysis of the paper *Faster than Fourier* [1] is made, as to obtain a better understanding of superoscillations. Here a mathematical model is written, which provides a clear description of superoscillating functions and uses asymptotics, in particular the saddle point method alongside numerics to describe specific aspects of such functions.

#### Example of Superoscillations

To begin with, a function  $f(x)$  that has a spectrum of frequencies that are band-limited by  $|K| \leq 1$  is required. Therefore the function should not oscillate faster than  $\cos(x)$ , however we want it to do so, for example by  $\cos(Kx)$ , where  $K$  is some large constant. An expression that exhibits this is provided in [1], and is given to be,

$$f(x, A, \delta) = \frac{1}{(\delta \cdot \sqrt{2\pi})} \int_{-\infty}^{\infty} e^{ixk(u)} \cdot e^{-\frac{1}{2\delta^2}(u-iA)^2} du. \quad (2.1.1)$$

$k(u)$  has to be even,  $k(0) = 1$  (for real  $u$ )  $|k| \leq 1$ ,  $\delta$  is very small and  $A$  is real and positive. Notice that the function in (2.1.1) could be described as the expectation value of  $e^{ixk(u)}$  with an underlying Gaussian probability density. The examples of  $k(u)$  listed in the paper are described as,

$$k_1(u) = \frac{1}{1 + \frac{1}{2}u^2}, \quad k_2(u) = \sec(u), \quad k_3(u) = e^{-\frac{1}{2}u^2}, \quad k_4(u) = \cos(u). \quad (2.1.2)$$

Looking at equation (2.1.1) if  $\delta$  is taken to be very small, it is clear that the second exponential would tend to disappear, and so would act as a complex delta function.

$$\delta(x) = \lim_{\sigma \rightarrow 0} e^{-\frac{x^2}{2\sigma^2}}. \quad (2.1.3)$$

This will lead to a projection of the first exponential at  $u = iA$  when integration is carried out, resulting in the function being expressed as,

$$f(x, A) \approx \int_{-\infty}^{\infty} e^{ixk(u)} \delta(u - iA) du \quad (2.1.4a)$$

$$f(x) \approx e^{iKx} \quad \text{where} \quad K = k(iA). \quad (2.1.4b)$$

Remembering the condition that  $|k| \leq 1$  for a function whose spectrum is band-limited, then through equation (2.1.4) if  $k(u) = \cos(u)$  for small  $\delta$  values,  $k$  can be described as follows,

$$k(u) = \cos(u) = \frac{e^{iu} + e^{-iu}}{2} \quad (2.1.5a)$$

$$k(iA) = \frac{e^{-A} + e^A}{2} = \cosh(A) \quad (2.1.5b)$$

$$k(iA) \approx \frac{e^A}{2} \quad \text{where } A \text{ is large.} \quad (2.1.5c)$$

Therefore seeing that the value for  $K > 1$  and it increases when moving up from  $u = 0$  to  $u = iA$  along the imaginary axis, and since it depends on  $A$ ,  $k$  can be arbitrarily large. These are described as regions where the function superoscillates. As can be seen if the values of  $u$  is taken to be imaginary, this causes the function to be superoscillatory, in this case.

## Asymptotics

This section looks into the asymptotics which will help explain some of the function's characteristics by looking into small  $\delta$  for the integral that represents the function (2.1.1), as this would be regions where the function superoscillates as described before. For a small  $\delta$  approximation to the integral, given that  $\xi$  is defined as,

$$\xi = \delta^2 x \quad (2.1.6)$$

$$f\left(\frac{\xi}{\delta^2}, A, \delta\right) = \frac{1}{\delta\sqrt{2\pi}} \int_{-\infty}^{\infty} e^{-\frac{1}{\delta^2} \phi(u, \xi, A)} du. \quad (2.1.7)$$

where,

$$\phi = \frac{1}{2}(u - iA)^2 - i\xi k(u). \quad (2.1.8)$$

When looking at small  $\delta$  of  $f$  in equation (2.1.7), the function can be approximated using a method called the saddle point method [38], which is described in the section that follows. Here a deformation of the integration path is taken, such that when integrating the function, it passes through the saddles given by  $u_s$ . Then a quadratic approximation can be taken near each saddle point  $u_s$  of the exponent  $\phi$  in equation (2.1.8).

## Saddle Point Method

This method deals with integrals of the form,

$$I = \int e^{\lambda f(z)} g(z) dz. \quad (2.1.9)$$

Certain integrals can be put into this form and then a deformation of the path of integration is made so that it contains all the saddle points where  $f'(z) = 0$ , and follow a path down the complex plane  $f(z)$ ; which is essentially complex for a specific set of saddles.  $z_0$  corresponds to the highest saddle point where  $f$  has its largest value. When  $\lambda$  tends to  $\infty$ ,  $z_0$  would be the main contribution to the integral along side the neighbourhood of  $z_0$ , given by  $z - z_0$ . If there were more saddle points then each have a weighted contribution, however in the case that they are of the same height, then the saddles would be of the same magnitude as each other.

If considering  $z_0$  as the only saddle point, near  $z_0$  we can expand through a Taylor series expansion,

$$f(z) = f(z_0) + a_2(z - z_0)^2 + a_3(z - z_0)^3 \dots \quad (2.1.10)$$

$$a_2 = \frac{1}{2} f''(z_0) \quad (2.1.11a)$$

$$a_3 = \frac{1}{3!} f'''(z_0). \quad (2.1.11b)$$

Replacing  $f(z)$  by its quadratic approximation near  $z_0$ ,

$$e^{\lambda f(z)} = e^{\lambda f(z_0) + \lambda a_2 (z - z_0)^2}. \quad (2.1.12)$$

The terms in equation (2.1.10) have an order of  $O(1), O(\nu^{-2}), O(\nu^{-3})$ . Note: when expanding the function in (2.1.10) the first derivative is zero at the saddle points so that a term  $a_1$  is not needed as shown in (2.1.10), furthermore terms of order  $O(\nu^{-3})$  or higher are neglected. Therefore the integral can now be written as,

$$I = g(z_0) e^{\lambda f(z_0)} \int e^{\lambda a_2 (z - z_0)^2} dz. \quad (2.1.13)$$

When selecting the path of integration,  $a_2$  is set to have a value of,

$$a_2 = A e^{i\alpha}. \quad (2.1.14)$$

If  $A > 0$  and  $z$  is taken to be expressed as,

$$z = z_0 + r e^{i\theta}. \quad (2.1.15)$$

Therefore,

$$a_2 (z - z_0)^2 = A r^2 e^{i(\alpha + 2\theta)}. \quad (2.1.16)$$

For  $\theta = \pm\frac{\pi}{2} - \frac{1}{2}\alpha$ , equation (2.1.16) is going to be negative. The path of integration goes through the saddle point and in the direction of steepest descent, therefore writing equation(2.1.13) as,

$$I = g(z_0)e^{\lambda f(z_0)} \int e^{-A\lambda r^2 + \frac{1}{2}i(\pi-\alpha)} dr. \quad (2.1.17)$$

Let,

$$u^2 = A\lambda r^2, \quad dr = \frac{1}{\sqrt{A\lambda}} du. \quad (2.1.18)$$

Then the integral will look like a Gaussian,

$$I = g(z_0)e^{\lambda f(z_0) - \frac{1}{2}i\alpha} e^{\frac{1}{2}i\pi} \frac{1}{\sqrt{A\lambda}} \int_{-\infty}^{\infty} e^{-u^2} du. \quad (2.1.19)$$

Knowing that  $\int_{-\infty}^{\infty} e^{-u^2} du = \sqrt{\pi}$

$$I = g(z_0)e^{\lambda f(z_0)} \left(\frac{-\pi}{A\lambda e^{i\alpha}}\right)^{\frac{1}{2}}. \quad (2.1.20)$$

Given that  $Ae^{i\alpha} = \frac{1}{2}f''(z_0)$ ,

$$I = g(z_0)e^{\lambda f(z_0)} \left(\frac{-2\pi}{\lambda f''(z_0)}\right)^{\frac{1}{2}}. \quad (2.1.21)$$

Equation (2.1.21) gives an asymptotic approximation to the integral of the form (2.1.9) for a function with just one saddle point. If more than one saddle point is present, each will contribute similarly.

## Application of S.P.M to the function $f(x, A, \delta)$

Using the Saddle Point Method here to find the approximation to the function  $f(x)$  with small  $\delta$ .

$$f\left(\frac{\xi}{\delta^2}, A, \delta\right) = \frac{1}{\delta\sqrt{2\pi}} \int_{-\infty}^{\infty} e^{-\frac{1}{\delta^2}\phi(u, \xi, A)} du. \quad (2.1.22)$$

Need to find saddle points which are found by,

$$\frac{d\phi}{du} = 0 \quad \frac{\partial\left(\frac{1}{2}(u - iA)^2 - i\xi k(u)\right)}{\partial u} = 0 \quad (2.1.23)$$

$$u_s = i(\xi k'_{u_s} + A). \quad (2.1.24)$$

Where we define our saddle point by  $u_s$ . Comparing the results shown in the saddle point method and the function, using equation (2.1.22) and (2.1.9),

$$g(z) = \frac{1}{\delta\sqrt{2\pi}}, \quad \lambda = \frac{-1}{\delta^2}, \quad f(z) = \phi(u, \xi, A). \quad (2.1.25)$$

Using equations (2.1.8) and (2.1.24),  $\phi$  is given by,

$$\phi(u_s, \xi, A) = \frac{1}{2}(u_s - iA)^2 - i\xi k(u_s). \quad (2.1.26)$$

Given the approximation of the integral from equation (2.1.21) it is clear that the second derivative of  $\phi(u, \xi, A)$  is required. Therefore,

$$\phi''(u_s) = \frac{\partial}{\partial u}(u_s - iA - i\xi k'(u_s)) = 1 - i\xi k''(u_s). \quad (2.1.27)$$

Now putting equations (2.1.27), (2.1.26) and (2.1.25) in the form of equation (2.1.21) which is the saddle point approximation, and returning it to the form  $f(x, A, \delta)$ , resulting in,

$$f\left(\frac{\xi}{\delta^2}, A, \delta\right) = \frac{1}{\delta\sqrt{2\pi}} e^{\frac{-1}{\delta^2}\left[\frac{1}{2}(u_s - iA)^2 - i\xi k(u_s)\right]} \left(\frac{2\pi}{\frac{1}{\delta^2}(1 - i\xi k''(u_s))}\right)^{\frac{1}{2}}. \quad (2.1.28)$$

$$f(x, A, \delta) = \frac{e^{ixk(u) - \frac{(u_s - iA)^2}{2\delta^2}}}{\sqrt{1 - ix\delta^2 k''(u_s)}} \quad (2.1.29)$$

Looking into the characteristics of the function found above (2.1.29) it can be seen how  $u_s$ , which is the main saddle, changes as  $\xi$  is altered. For instance, when we take  $\xi$  to be of a value smaller than 1;  $\xi \ll 1$ , that is  $x \ll \delta^{-2}$ , from equation (2.1.24) it is clear that the saddle point  $u_s \approx iA$  and so the function that was derived in (2.1.29) will result in the exponential to be equal to the function given in (2.1.4) as  $f(x) \approx e^{iKx}$ . This as described before, is the region of superoscillations.

Now looking at (2.1.26) when  $\xi \gg 1$ , that is  $x \gg \delta^{-2}$ ,  $u_s$  can be approximated to give  $u_s \approx i\xi k'(u_s)$ ; where the term  $i\xi k'(u_s) \gg iA$ . The saddle must

be found in the region where  $k'(u_s) = 0$ , that is if  $k$  had only one value for the maximum (2.1.2), which it does for the  $k$  examples given in the paper. as  $\xi \gg 1$  the function (2.1.29) then becomes,

$$f(x, A, \delta) \approx \frac{1}{\delta \sqrt{x k''(0)}} e^{i(x - \frac{\pi}{4})} e^{\frac{A^2}{2\delta^2}} \dots \quad (2.1.30)$$

This shows that the function  $f(x, A, \delta)$  has an order of  $O(e^{\frac{A^2}{2\delta^2}})$ , and so the term is much larger than that of the region that represents the superoscillations, with the amplification of these regions being exponential. Given  $k$  value below, then looking at how the saddle changes and behaves as we vary  $x$ ,

$$k_5(u) = 1 - \frac{1}{2}u^2. \quad (2.1.31)$$

using equation(2.1.24) and using the derivative of (2.1.31),

$$u_s = i(\xi k'(u_s) + A) \quad (2.1.32a)$$

$$u_s = i(\xi(-u_s) + A) \quad (2.1.32b)$$

$$u_s = \frac{iA}{1 + i\xi}. \quad (2.1.32c)$$

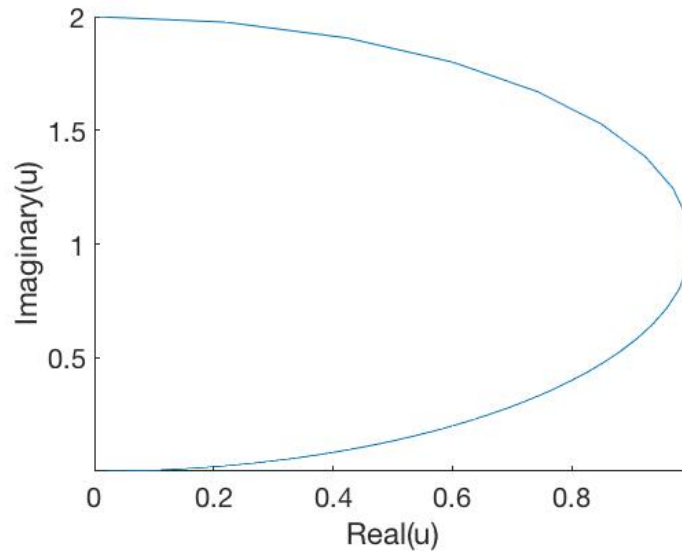


Figure 2.1: This figure shows the track of the saddle  $u_s$  as  $\xi$  is increased from 0 to  $\infty$  using the wavenumber  $k_5$  given by equation (2.1.31). Using the fact that  $A=2$ , the value of  $\xi$  when the real and imaginary part of the saddle are zero, is equal to  $\infty$ , but  $\xi = 0$  when the imaginary part reaches its maximum (regions of superoscillations). This is a recreation of figure 1 in [1].

Figure 2.1 shows the track of the leading saddle as  $x$  goes from  $iA$  to 0. There are several other curves and solutions, but they are much more complex. A second

way of looking into superoscillations is by taking the local wavenumber, this will be of great use in the later chapters to come, as it will be used to identify the superoscillatory regions. This is given by the function below,

$$q(\xi) = -\Im\left(\frac{\partial\phi(u_s(\xi), \xi, A)}{\partial\xi}\right) = \Re(k(u_s)). \quad (2.1.33)$$

Using the value for  $k$  given by equation (2.1.31) and the value for  $u_s$  given by equation (2.1.32), the value of the local wavenumber is provided below as well as a graph representing the function against  $\xi$ ,

$$q(\xi) = 1 + \frac{A^2(1 - \xi^2)}{2(1 + \xi^2)}. \quad (2.1.34)$$

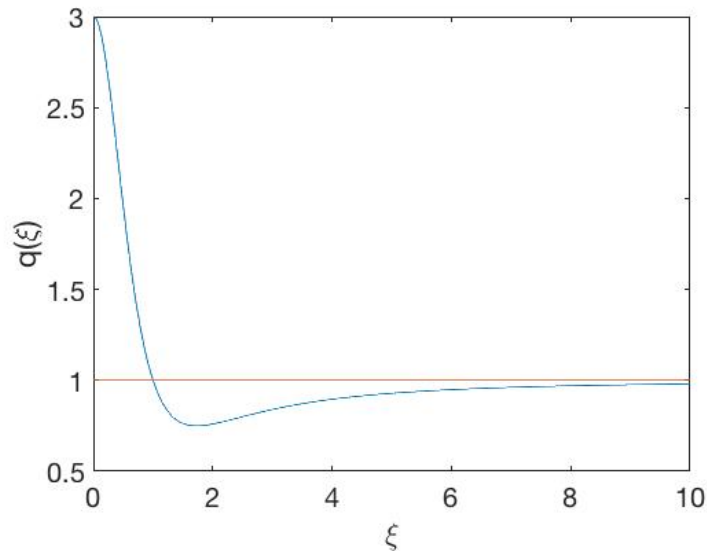


Figure 2.2: This figure is a recreation of figure 2 of [1] and shows the local wavenumber  $q(\xi)$  with change in  $\xi$  using  $A=2$ . As shown in equation (2.1.34).

Figure 2.2 shows that at the point where  $\xi = 0$  the local wavenumber will have the highest value and then rapidly decreases to a value smaller than 1. When  $q(\xi)$  is larger than 1 this is the region where the function is superoscillating, and when  $q(\xi)$  is a value lower than 1 then it would be the region where the function oscillates conventionally. If the function needed to be superoscillatory over a large domain of  $x$  then  $\delta$  has to be smaller in value so that  $\xi$  remains small. Notice that as mentioned before as  $\xi$  tends to decrease in value i.e.  $\xi \ll 1$  the function superoscillates.

Analysing equation (2.1.2) using different wavenumbers ( $k_1(u)$ ,  $k_2(u)$ ,  $k_3(u)$ ,  $k_4(u)$ ) as given in the paper, the resultant integral of  $f$  could not be evaluated using special functions. However if the function is taken to be of the form  $k_5(u) = 1 - \frac{1}{2}u^2$  from equation (2.1.31), it is possible to make it band-limited by letting  $|k| < 1$ . This is done by allowing  $u$  to take on values  $|u| \leq 2$  in equation (2.1.31). This will, in return, give a truncated integral of the form,

$$f(x, A, \delta) = \frac{1}{\delta\sqrt{2\pi}} \int_{-2}^2 e^{ix(1-\frac{1}{2}(u^2))} e^{\frac{-1}{2\delta^2}(u-iA)^2} du. \quad (2.1.35)$$

Which then becomes,

$$f(x, A, \delta) = \frac{1}{\delta\sqrt{2\pi}} \int_{-2}^2 e^{ix} e^{-ix\frac{1}{2}u^2} e^{-\frac{1}{2\delta^2}(u^2-2iAu-A^2)} du \quad (2.1.36a)$$

$$f(x, A, \delta) = \frac{1}{\delta\sqrt{2\pi}} e^{ix} e^{\frac{A^2}{2\delta^2}} \int_{-2}^2 e^{-u^2(\frac{1}{2}ix + \frac{1}{2\delta^2}) + \frac{iAu}{\delta^2}} du. \quad (2.1.36b)$$

Using,

$$K = \left(\frac{1}{2}ix + \frac{1}{2\delta^2}\right)^{\frac{1}{2}} \quad (2.1.37a)$$

$$D = \frac{iA}{2\delta^2\left(\frac{1}{2}ix + \frac{1}{2\delta^2}\right)^{\frac{1}{2}}}, \quad (2.1.37b)$$

substituting equation (2.1.37) into (2.1.36) we get,

$$f(x, A, \delta) = \frac{1}{\delta\sqrt{2\pi}} e^{ix} e^{\frac{A^2}{2\delta^2}} \int_{-2}^2 e^{-K^2u^2+2KD u} du \quad (2.1.38a)$$

$$f(x, A, \delta) = \frac{1}{\delta\sqrt{2\pi}} e^{ix} e^{\frac{A^2}{2\delta^2}} \int_{-2}^2 e^{-[(Ku-D)^2-D^2]} du. \quad (2.1.38b)$$

Now letting,

$$t = Ku - D \quad (2.1.39a)$$

$$dt = K du \quad (2.1.39b)$$

$$du = \frac{1}{K} dt \quad (2.1.39c)$$

and substituting in all the values from equation(2.1.39) will result with,

$$f(x, A, \delta) = \frac{1}{\delta\sqrt{2\pi}} e^{ix} e^{\frac{A^2}{2\delta^2}} e^{-D^2} \int_{-2K-D}^{2K-D} \frac{e^{-t^2}}{K} dt \quad (2.1.40a)$$

$$f(x, A, \delta) = \frac{1}{\delta\sqrt{2\pi}} e^{ix} e^{\frac{A^2}{2\delta^2}} e^{-D^2} \left[ \int_0^{2K-D} \frac{e^{-t^2}}{K} dt + \int_{-2K-D}^0 \frac{e^{-t^2}}{K} dt \right]. \quad (2.1.40b)$$

Now given that the error function is defined as,

$$\operatorname{erf}(z) = \frac{2}{\sqrt{\pi}} \int_0^z e^{-t^2} dt. \quad (2.1.41)$$

By this concept equation(2.1.40) can be written as,

$$f(x, A, \delta) = \frac{1}{2K\delta\sqrt{2}} e^{ix} e^{\frac{A^2}{2\delta^2}} e^{-D^2} (\operatorname{erf}(2K - D) - \operatorname{erf}(-2K - D)). \quad (2.1.42)$$

Now substituting back in the equations (2.1.37) gives,

$$f(x, A, \delta) = \frac{1}{2\sqrt{1+ix\delta^2}} e^{\frac{ix(2+A^2+2ix\delta^2)}{2(1+ix\delta^2)}} \left[ \operatorname{erf}\left(\frac{2+iA+2ix\delta^2}{\delta\sqrt{2+2ix\delta^2}}\right) + \operatorname{erf}\left(\frac{2-iA+2ix\delta^2}{\delta\sqrt{2+2ix\delta^2}}\right) \right] \quad (2.1.43)$$

Now to get superoscillations the wavenumber should be equal to  $k(u)$ , where  $u = iA$  therefore the wavenumber is,

$$k_5(iA) = 1 + \frac{1}{2}A^2. \quad (2.1.44)$$

Through the application of the saddle point method given in the previous sections the function can be approximated as,

$$f(x, A, \delta) \approx \frac{1}{\sqrt{1+ix\delta^2}} \exp\left(ix\left[1 + \frac{A^2}{2(1+x^2\delta^4)}\right]\right) \exp\left(\frac{A^2\delta^2x^2}{2(1+x^2\delta^4)}\right). \quad (2.1.45)$$

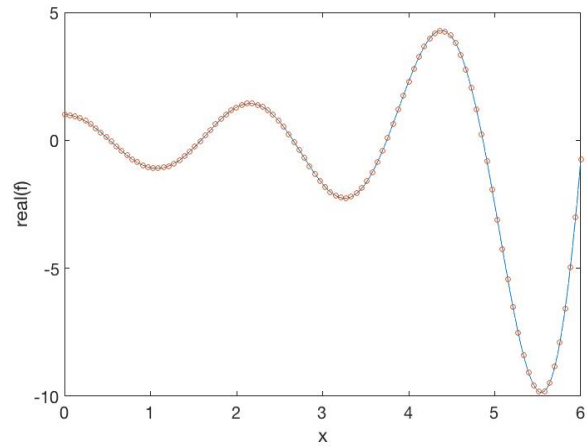
Note the integration is between the limits  $u = \pm 2$  and not  $\pm\infty$ , as it is considering the points at  $\pm 2$  as well as the saddle point  $u_s$ . Also the endpoints here are oscillating the slowest with a wavenumber equal to 1, these regions are of highest amplitude so to ensure that the regions of superoscillations doesn't get masked by the normally oscillating signal, it is a requirement that the absolute value for the Gaussian in equation (2.1.35),

$$\exp\left(\frac{A^2-4}{2\delta^2}\right) \leq 1. \quad (2.1.46)$$

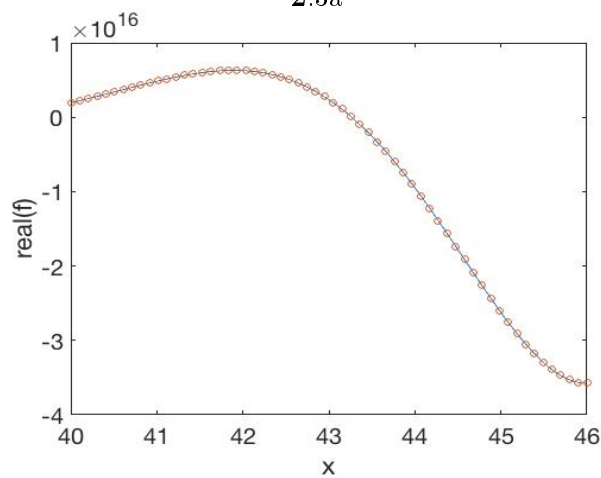
## Numerics

In this section a comparison is made between the exact results for the integral in equation (2.1.1), to the saddle point approximation in equation (2.1.29), using the wavenumber  $k_5$  in equation (2.1.31), the results will display the real part of the function against  $x$  with  $K = 3$   $A = 2$  and  $\delta = 0.2$ .

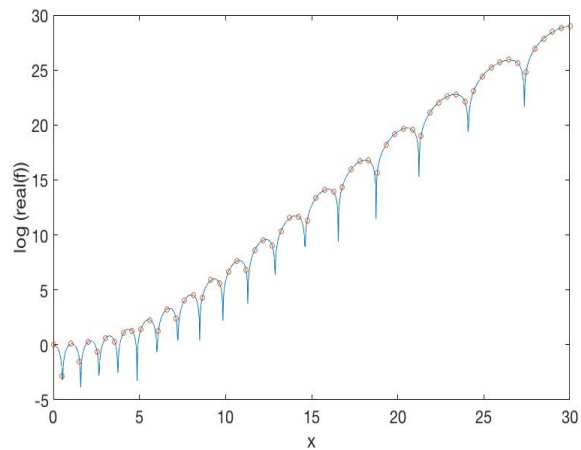
Figure 2.3 shows the comparison between the saddle point approximation in equation (2.1.45) and the exact expression in (2.1.35), which is similar to each other. Now for small  $x$  it can be seen that the local wavenumber  $q(\xi) \approx 3$  when  $x = 3$  using the expression in (2.1.6) and (2.1.34). In figure (2.3b) conventional oscillations are shown with  $x \approx 40$  giving a value for  $\xi \approx 1.6$ , and therefore a period that is almost 3 times slower than in the small  $x$  region.



2.3a



2.3b



2.3c

Figure 2.3: Shows the computations for the function in equation (2.1.35) as given in the form (2.1.43) and its saddle point approximations in equation (2.1.45), with  $A = 2$   $\delta = 0.2, 2$ . 2.3a showing regions of superoscillations where  $o$  is the calculation using the expression in (2.1.43) and the blue line is the Saddle point approximation, 2.3b conventional oscillations with large  $x$  between  $x = 40$  and  $x = 46$  and 2.3c shows the logarithm of the real part of the function and the associated Saddle point approximation. This is a recreation of figure 3 [1].

## Conclusion

The paper reviewed gives a description of what superoscillations are and some examples of such functions. It also highlights some mathematical methods used to analyse integral functions that diverge using an approximation called saddle point method. It shows how the regions of superoscillations can be explored by looking into the local wavenumber of the functions, in addition to the fact that the amplitude of the function where superoscillations are found is much smaller than that found where the function oscillates in a conventional way. This can be seen when trying to to extend the superoscillatory region ( $x$ ), causing the amplitude for conventional oscillations to increase by a large amount relative to the superoscillatory region. The method in which the local wavenumber is analysed will be used throughout the following chapters and will be fundamental in identifying regions where a given wave superoscillates.

## 2.2 Mathematical description of Superoscillations

### Introduction

This section follows the approach of the paper *Evolution of quantum Superoscillations and optical super-resolution without evanescent waves* written by Professor Sir Michael Berry and Sandu Popescu [2]. Our purpose is to explore the example given in paper [2] of the initial superoscillatory function, to give an in depth understanding of superoscillations, it also gives an example of how such functions are transpired. The paper looks into how a superoscillatory function that describes the initial state of a quantum wavefunction behaves when allowed to freely evolve with time. It also demonstrates how an evolving state can be described as waves propagating beyond a diffraction grating, and manages to illustrate how the grating can generate waves with much smaller wavelengths and thus achieving ‘super-resolution’. The paper *Mathematics of Superoscillations* [18] by Y.Aharonov *et al* was also of great importance throughout this chapter, as it provides a clear mathematical description of superoscillations. Here, however, we will not be concerned with the time evolution of superoscillations as shown in [2].

### Initial state of superoscillatory function $f(x)$

Starting with a function  $f(x)$  given by,

$$f(x) = (\cos(x) + ia \sin(x))^N \quad (a > 1, N \gg 1). \quad (2.2.1)$$

For any given value of  $a$ ,  $f(x)$  is periodic ( $2\pi$ ) if  $N$  is odd. If  $a = 1$ , then  $f(x)$  is a plane wave travelling to the right and can be expressed as  $f(x) = e^{iNx}$ . However the most interesting case is when  $a > 1$ , and taking in the limit that  $x = 0$ , here the function oscillates the fastest. Using small  $x$  approximations,

$$\cos(x) \approx 1 \quad \sin(x) \approx x. \quad (2.2.2)$$

From the approximation (2.2.2) an expression for  $f(x)$  in (2.2.1) is found,

$$f(x) \approx (1 + iax)^N = \exp(\ln[1 + iax]^N). \quad (2.2.3)$$

Using a Taylor series expansion of  $\log(1 + x) \approx x - \frac{x^2}{2} + \frac{x^3}{3}$  a final expression is given as,

$$f(x) \approx \exp(iaNx). \quad \text{where } x \ll 1 \quad (2.2.4)$$

It is essential now to prove that the function above is indeed superoscillatory. Therefore analysing the Fourier components of the function  $f(x)$  in (2.2.1) will be of great importance, since superoscillations are defined as functions that oscillate faster than their fastest Fourier component. The function in 2.2.1 can be expressed in the form,

$$f(x) = [\cos(x) + ia\sin(x)]^N = \frac{1}{2^N} (e^{ix} + e^{-ix} + ae^{ix} - ae^{-ix})^N \quad (2.2.5a)$$

$$= \frac{1}{2^N} [e^{ix}(1 + a) + e^{-ix}(1 - a)]^N. \quad (2.2.5b)$$

Expanding the function binomially gives,

$$f(x) = \frac{1}{2^N} \sum_{m=0}^N \frac{N!}{m!(N-m)!} [e^{ix}(1+a)]^{N-m} [e^{-ix}(1-a)]^m \quad (2.2.6a)$$

$$= \frac{1}{2^N} \sum_{m=0}^N \frac{N!}{m!(N-m)!} e^{ixN-2ixm} (1+a)^{N-m} (1-a)^m \quad (2.2.6b)$$

$$f(x) = \sum_{m=0}^N C_m \exp(iNk_mx). \quad (2.2.6c)$$

Where,

$$k_m = 1 - \frac{2m}{N} \quad C_m = \frac{N!}{2^N} (-1)^m \frac{(a^2 - 1)^{\frac{N}{2}} [(a+1)/(a-1)]^{\frac{Nk_m}{2}}}{[N(\frac{1+k_m}{2})!] [N(\frac{1-k_m}{2})!]}. \quad (2.2.7a)$$

The form for  $C_m$  has been found using the relations (2.2.10) shown below.

$$C_m = \frac{1}{2^N} (1-a)^m (1+a)^{N-m} \frac{N!}{(N-m)!m!} \quad (2.2.8a)$$

$$= \frac{(-1)^m}{2^N} (a-1)^m (1+a)^{N-m} \frac{N!}{(N-m)!m!}. \quad (2.2.8b)$$

$$(a-1)^m (1+a)^{N-m} = (a-1)^{\frac{N}{2}} (a-1)^{m-\frac{N}{2}} (a+1)^{\frac{N}{2}} (a+1)^{\frac{N}{2}-m} \quad (2.2.9a)$$

$$= (a^2 - 1)^{\frac{N}{2}} \left( \frac{a+1}{a-1} \right)^{\frac{N}{2}(1-\frac{2m}{N})}. \quad (2.2.9b)$$

$$\frac{N!}{(N-m)!m!} = \frac{N!}{(\frac{N}{2}(2-\frac{2m}{N}))! (N(1-1+\frac{m}{N}))!} \quad (2.2.10a)$$

$$= \frac{N!}{(\frac{N}{2}(1+k_m))! (N(1-1+\frac{2m}{N}))!} \quad (\text{using } k_m \text{ in equation 2.2.7}) \quad (2.2.10b)$$

$$= \frac{N!}{(\frac{N}{2}(1+k_m))! (\frac{N}{2}(1-k_m))!}. \quad (2.2.10c)$$

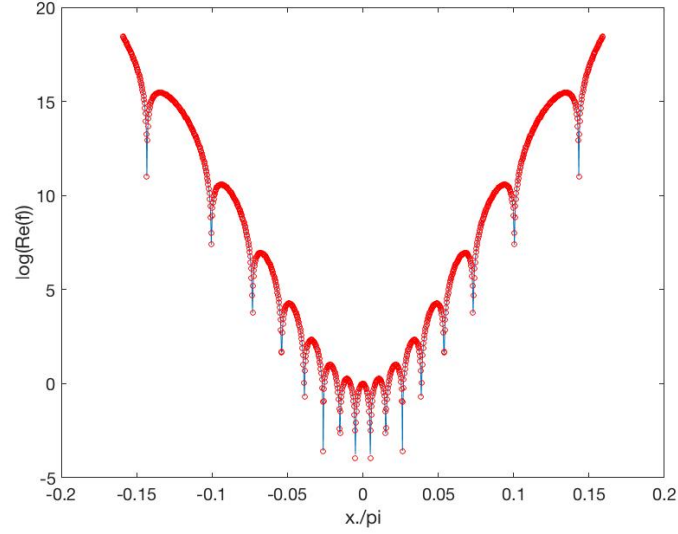


Figure 2.4: : The superoscillatory function (2.2.1) given that  $N=20$  and  $a=4$ , is plotted here as  $\log(\Re f)$  against  $\frac{x}{\pi}$ . Note that the blue line is the exact expression for  $f(x)$  and the red circles are the Fourier expression given by (2.2.6). Recreation of figure 1 [2].

By equation (2.2.7) the wavenumber is always  $|k_m| \leq 1$ , and therefore shows that the fastest contribution of the Fourier series is given by  $\exp(iNx)$ . However this is not the case when looking at (2.2.4), which shows that our function  $f(x) \approx \exp(iaNx)$  is superoscillatory, with degree of superoscillations given by the parameter  $a$ . Therefore it can be said that the Taylor series expansion of the function contains local information whilst the Fourier representation contains the global information. [18]

Next, converting  $f(x)$  to polar coordinates starting with the function (2.2.1).

$$r = \sqrt{f(x)f(x)^*} \quad (2.2.11)$$

$$\theta = \arctan \left| \frac{\Im f(x)}{\Re f(x)} \right| \quad (2.2.12)$$

Using  $f(x)$  from (2.2.1),

$$r = ([\cos(x) + ia \sin(x)]^N [\cos(x) - ia \sin(x)]^N)^{\frac{1}{2}} \quad (2.2.13a)$$

$$= [\cos^2(x) + a^2 \sin^2(x)]^{\frac{N}{2}} \quad (2.2.13b)$$

$$\theta = \arctan(a \tan(x)). \quad (2.2.13c)$$

Now writing the function in polar form,

$$f(x) = (\cos^2(x) + a^2 \sin^2(x))^{\frac{N}{2}} \exp[iN(\arctan(a \tan(x)))]. \quad (2.2.14)$$

Finding the derivative of the natural logarithm of  $f(x)$ ,

$$\ln f(x) = \ln[(\cos(x) + ia \sin(x))^N] \quad (2.2.15a)$$

$$\frac{d}{dx}(\ln f(x)) = N \frac{(-\sin(x) + ia \cos(x))}{\cos(x) + ia \sin(x)} \quad (2.2.15b)$$

$$= N \frac{((a-1)\sin(x)\cos(x) + ia)}{\cos^2(x) + a^2 \sin^2(x)}. \quad (2.2.15c)$$

From the equation above a description of the local wavenumber  $k(x)$  is provided, since it is defined as the imaginary part of equation (2.2.15)

$$k(x) = \frac{1}{N} \Im \left[ \frac{d}{dx}(\ln f(x)) \right] = \frac{a}{\cos^2(x) + a^2 \sin^2(x)}. \quad (2.2.16)$$

The term  $\frac{1}{N}$  in equation (2.2.16) is introduced here as to normalise the wavenumber  $k(x)$  to the maximum wavenumber of  $f(x)$ . Defining  $r$  as given in equation (2.2.13) as,

$$f(x) = \left( \frac{a}{k(x)} \right)^{\frac{N}{2}} \exp(iN \arctan(a \tan(x))) \quad (2.2.17)$$

$$r = (\cos^2(x) + a^2 \sin^2(x))^{\frac{N}{2}} = \left( \frac{a}{k(x)} \right)^{\frac{N}{2}}. \quad (2.2.18)$$

To help with understanding superoscillations, a new way of representing the function  $f(x)$  in (2.2.1) is required, using the integral

$$I = \int_0^x k(x') dx' = \int_0^x \frac{a}{\cos^2(x') + a^2 \sin^2(x')} dx' \quad (2.2.19a)$$

$$= \int_0^x \frac{a}{1 + (a^2 - 1) \sin^2(x')} dx'. \quad (2.2.19b)$$

Note now in equation (2.2.18),  $a > 1$  therefore  $(a^2 - 1 > 0)$ , using the standard integral

$$\int \frac{1}{a + b \sin^2(x)} dx = \frac{1}{\sqrt{a(a+b)}} \arctan \left( \sqrt{\frac{a+b}{a}} \tan(x) \right) \quad (2.2.20)$$

for  $\frac{b}{a} > 1$ . Now writing the integral in (2.2.19) as,

$$I = \int_0^x \frac{a}{(1 - (a^2 - 1) \sin^2(x'))} dx' \quad (2.2.21a)$$

$$= \arctan(a \tan(x)). \quad (2.2.21b)$$

Now the function  $f(x)$  can be expressed by,

$$f(x) = \left( \frac{a}{k(x)} \right)^{\frac{N}{2}} \exp(iN \int_0^x k(x') dx'). \quad (2.2.22)$$

The function  $k(x) = \frac{a}{\cos^2(x) + a^2 \sin^2(x)}$  above is the local wavenumber determined at every point in space  $x$ . Local wavenumbers describes the state of oscillation. Note here that when  $x = \frac{\pi}{2}$ ;  $k(\frac{\pi}{2}) = \frac{1}{a}$ , this is the region where the function oscillates the slowest since the term  $\cos(x)$  disappears. The state where  $x = 0$ ,  $k(0) = a$ , would be region in which superoscillations are observed. In addition the region where  $|k(x)| > 1$  in (2.2.16), is regions of superoscillations, since the largest band-limit is taken to be equal to 1 with the normalisation of  $k(x)$  as stated in equation (2.2.16).

$$\frac{a}{\cos^2(x) + a^2 \sin^2(x)} > 1 \quad (2.2.23a)$$

$$\frac{a}{\cos^2(x) + \sin^2(x) + (a^2 - 1) \sin^2(x)} > 1 \quad (2.2.23b)$$

$$\frac{a}{1 + (a^2 - 1) \sin^2(x)} > 1 \quad (2.2.23c)$$

$$\frac{a - 1}{(a^2 - 1)} > \sin^2(x) \quad (2.2.23d)$$

$$\frac{1}{a + 1} > \sin^2(x). \quad (2.2.23e)$$

In terms of  $\cos(x)$ ,

$$\frac{a}{a + 1} < \cos^2(x). \quad (2.2.24)$$

To find the condition for  $f(x)$  to be superoscillatory, the square root of both inequalities obtained are taken, providing the condition in  $x$  where superoscillations occur.

$$\sqrt{\frac{\frac{a}{a+1}}{\frac{1}{a+1}}} < \frac{\cos(x)}{\sin(x)} \quad (2.2.25a)$$

$$|x| < \operatorname{arccot}(\sqrt{a}). \quad (2.2.25b)$$

An expression is given below showing the number of oscillations in this region, equation (2.2.26).

$$\eta_{osc} = \frac{N}{2\pi} \int_{-\operatorname{arccot} \sqrt{a}}^{\operatorname{arccot} \sqrt{a}} k(x) dx \quad (2.2.26a)$$

$$= \frac{N}{2\pi} \int_{-\operatorname{arccot} \sqrt{a}}^{\operatorname{arccot} \sqrt{a}} \frac{a}{\cos^2(x) + a^2 \sin^2(x)} dx \quad (2.2.26b)$$

$$= \frac{N}{2\pi} [\arctan(a) \tan(x)]_{-\operatorname{arccot} \sqrt{a}}^{\operatorname{arccot} \sqrt{a}} \quad (2.2.26c)$$

$$\eta_{osc} = \frac{N}{\pi} (\arctan(a \tan(\operatorname{arccot} \sqrt{a}))) \quad (2.2.26d)$$

given  $\tan(-x) = -\tan(x)$ . Simplifying the expression above by considering the fact that  $\tan(\arctan(\frac{1}{\sqrt{a}})) = \frac{1}{\sqrt{a}}$ , and  $\arctan(\frac{1}{\sqrt{a}}) = \text{arccot}(\sqrt{a})$ , we can express the equation in (2.2.25) as,

$$\eta_{osc} = \frac{N}{\pi} \arctan(\sqrt{a}). \quad (2.2.27)$$

Looking back at equation (2.2.17), for regions of superoscillations,  $|f|$  is exponentially smaller than the normally oscillating region. The asymptotic parameter  $N$  determines the number of superoscillations as well as the exponential smallness of the function. Now Equation (2.2.4) shows the region of superoscillation where the amplitude is constant. For the meantime it shall be referred to as fast superoscillations. These fast superoscillations would be found in a region that is smaller than that derived before in equation (2.2.25). To investigate this further it is necessary to take the the function  $f(x)$  in equation (2.2.22) and expand it near  $x = 0$ . Starting with the expansion of the term  $\left(\frac{a}{k(x)}\right)^{\frac{N}{2}}$ ,

$$[\cos^2(x) + a^2 \sin^2(x)]^{\frac{N}{2}} = (1 + (a^2 - 1) \sin^2(x))^{\frac{N}{2}} \quad (2.2.28a)$$

$$\approx (1 + (a^2 - 1)x^2)^{\frac{N}{2}} \quad (2.2.28b)$$

$$(1 + (a^2 - 1)x^2)^{\frac{N}{2}} \approx (1 + \frac{1}{2}(a^2 - 1)x^2)^N. \quad (2.2.28c)$$

For small  $x$ , the exponential function is defined as,

$$e^x \approx 1 + x. \quad (2.2.29)$$

Expressing the function from (2.2.28) as,

$$(1 + \frac{1}{2}(a^2 - 1)x^2)^N \approx \exp[\frac{1}{2}N(a^2 - 1)x^2]. \quad (2.2.30)$$

Now finding an approximation to the integral  $\int k(x')dx'$  with small  $x$ , which will give the behaviour of the phase of the function  $f(x)$  in (2.2.22),

$$I = a \int_0^x \frac{1}{1 + (a^2 - 1)x'^2}. \quad (2.2.31)$$

Where the expression in equation (2.2.28) is applied with small  $x$  approximation. Using the approximation  $\frac{1}{1+x} \approx 1 - x$ ,

$$I \approx a \int_0^x 1 - (a^2 - 1)x'^2 dx \quad (2.2.32a)$$

$$I \approx a[x - \frac{a^2 - 1}{3}x'^3]_0^x \approx ax. \quad (2.2.32b)$$

Knowing that the function  $f(x)$  in (2.2.22) can be written as follows,

$$f(x) = \left( \frac{a}{\frac{a}{\cos^2(x) + a^2 \sin^2(x)}} \right)^{\frac{N}{2}} \exp(iN \int_0^x k(x') dx'). \quad (2.2.33)$$

Substituting in the values found in equations (2.2.30) and (2.2.32) gives the final result for small  $x$  approximations,

$$f(x) \approx \exp[iNax] \exp\left[\frac{1}{2}N(a^2 - 1)x^2\right]. \quad (2.2.34)$$

Notice that in the region of fast superoscillations the second exponential varies from 1 (at  $x = 0$ ) to a factor of  $e$  (at  $x = x_{fs}$ ). When  $x \ll 1$  the second exponential tends to 1 which in turn gives the expression found in (2.2.4). Now the region of fast superoscillations is given by,

$$|x| < x_{fs} = \frac{\sqrt{2}}{\sqrt{N(a^2 - 1)}}. \quad (2.2.35)$$

The number of oscillations in the region is given by  $\exp(iNax)$  where,

$$\exp[iNax] = \exp\left(iNa\sqrt{\frac{2}{N(a^2 - 1)}}\right) = \exp[2\pi\eta_{fs}] \quad (2.2.36a)$$

$$\eta_{fs} = a\frac{\sqrt{N}}{\pi\sqrt{2(a^2 - 1)}}. \quad (2.2.36b)$$

When taking the power density spectrum; which is the average power distributed over frequency, there will be no trace of any superoscillations. This is due to the delicate nature of superoscillations, which are caused by the fine interaction between the Fourier components of the function. So as given in the paper [2] the spectral density function is defined by

$$P(k) = \frac{Nc_m^2(m = (1 - k)N/2)}{2\sum_0^N c_m^2} \approx \frac{1}{\sigma\sqrt{2\pi}} \exp - \frac{(k - \langle k \rangle)^2}{2\sigma^2}. \quad (2.2.37)$$

Where  $c_m$  is the amplitude of the Fourier components, with

$$\langle k \rangle = \frac{1}{a}, \quad \sigma = \sqrt{(k - \langle k \rangle)^2} = \sqrt{\frac{a^2 - 1}{2Na^2}}. \quad (2.2.38)$$

A plot is provided below in figure 2.5, showing the relationship between spectral density and the local wavenumber, for the exact expression in equation (2.2.37) as well as the approximated expression given by the Gaussian expression.

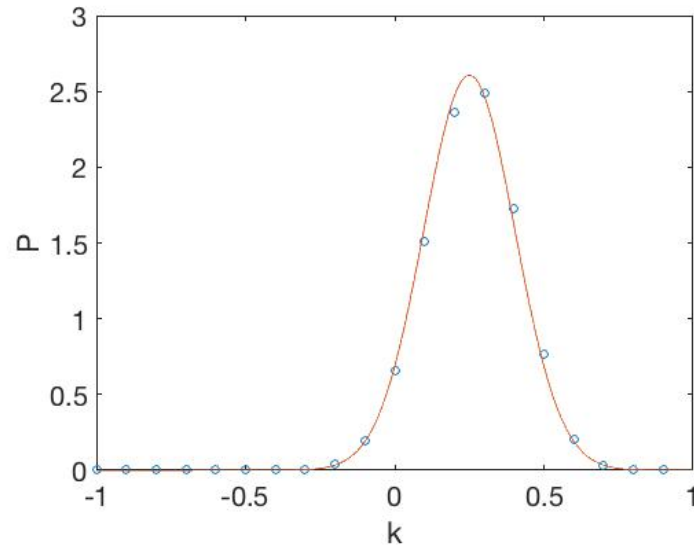


Figure 2.5: Smooth curve showing the Gaussian approximation given in equation (2.2.37) for the power density spectrum of the local wavenumber  $k$ , the circles indicate the exact spectrum (given by the first part of function 2.2.37) for  $f(x)$  with  $a=4$  and  $N=20$ . The smooth plot is the approximation given by the second part of equation (2.2.37). Recreation of figure 2 [2].

## Conclusion

The Chapter began with a clear example of a superoscillatory wavefunction given by equation (2.2.1). Through analysing the binomial expansion of the function, an expression was obtained for the Fourier components (2.2.6). A realization that the value for the largest wavenumber in the Fourier components cannot exceed 1 can be seen when looking at equation (2.2.7), this illustrates that the largest contribution in the series is given by  $\exp(iNx)$ . However when taking the  $x$  component in the function to be small, the function can be expressed as  $\exp(iaNx)$  as seen in (2.2.4). This indicates that our function oscillates, with a phase gradient that is much larger than the fastest Fourier component and so is shown to exhibit superoscillations. The parameter  $a$  is seen to govern the degree in which the function superoscillates. When looking specifically into the local wavenumber  $k(x)$  in (2.2.16), it is seen that the largest oscillations are found at  $k(0) = a$  where  $x = 0$  and the slowest variation is when  $k(\frac{n\pi}{2}) = \frac{1}{a}$ .

In addition, [2] also shows the region where superoscillations occur, through examining the values of  $x$  required for the function to exhibit these phenomena which is shown in equation (2.2.25). Using this known region, the number of oscillations has been found (2.2.26). Following these results, specific regions which are identified as fast superoscillations where the function is expressed as  $\exp(iaNx)$  are investigated, by taking the small  $x$  approximation of the function in equation (2.2.22). This resulted in the expression found in (2.2.34), which gives the region of fast superoscillations in (2.2.35). It is seen that the argument of the second exponential in (2.2.34) is constant for fast superoscillations. A final note is given about the power spectral density of the function, saying that there is no trace of superoscillations in the power spectrum, since the spectrum is taken from the distribution of individual Fourier components, and superoscillations are caused by a fine interaction between the components.

The example discussed in this section will be fundamental in the understanding and analysis of the chapters to come, as it illustrates how a band-limited function can oscillate faster than its Fourier components. This will be important when analysing the formation of superoscillations with the superposition of plane waves.

## 2.3 D dimensional Superoscillations

### Introduction

The following section is an in depth analysis of the paper *Natural Superoscillations in monochromatic waves in D dimensions* by M V Berry and M R Dennis [3]. Here monochromatic waves and their associated superoscillations, given by the calculation of the local wavenumber, is discussed for a wave formed from a superposition of many isotropic and monochromatic random waves in several dimensions ( $D$ ). The paper shows how the probability that a given wave function is superoscillating, increases with higher dimensions. A particular case is 2 dimensions, where the fraction of superoscillation is given by  $\frac{1}{3}$ . In addition the paper provides an in depth description of the special 1D case. The analysis given in this chapter in conjunction with the chapter 2.4, will form the foundation of the research conducted in this thesis, where an extension is made to the non-monochromatic case for two dimensional waves.

### D dimensional wave $\psi$

Given in previous work on superoscillations, it is well established that there are functions that can oscillate faster than their fastest Fourier component [1][2], given that the function is band limited. It is also understood that such superoscillations are found near regions of small amplitude. Paper [3] initially states functions of complex scalar waves that are monochromatic in multiple dimensions, which are also band-limited. These are described as

$$\psi(x) = u(x) + i\nu(x) \quad (2.3.1a)$$

$$\psi(x) = \rho(x)e^{i\chi(x)}. \quad (2.3.1b)$$

Let,

$$r = [x_1, x_2, x_3, \dots] \quad (2.3.2)$$

$$\psi(r) = u(r) + i\nu(r) = \rho(r) \exp[i\chi(r)]. \quad (2.3.3)$$

Here the time dependence is ignored. Looking into the fact that the wavefunction  $\psi$  must satisfy the Helmholtz equation, which presents the time-independent form of the wave equation

$$\nabla^2\psi + k_0^2\psi = 0 \quad (2.3.4)$$

Where  $k_0$  is the free space wavenumber. Superoscillations then, are when the wavefunction oscillates with a much higher wavenumber than that of the free space wavenumber, It's resultant wavelength is smaller than  $\frac{2\pi}{k_0}$ . In order to find how the function behaves at a given point, it is essential to measure the local wavenumber, which can be found by taking the rate at which the phase (given by  $\chi(r)$  in equation (2.3.3)) changes. This is shown through the function

$$k(r) = |\nabla\chi(r)| = \Im[\nabla \ln(\psi(r))]. \quad (2.3.5)$$

Therefore from the function in equation (2.3.1), this is calculated as

$$k(r) = \Im[\nabla(\ln(u(r) + i\nu(r)))] \quad (2.3.6a)$$

$$k(r) = \frac{|(\nabla\nu(r))u(r) - (\nabla u(r))\nu(r)|}{u^2(r) + \nu^2(r)}. \quad (2.3.6b)$$

Since the magnitude of the wave is  $\rho(r)$ , which is expressed as  $\rho(r) = \sqrt{u^2(r) + \nu^2(r)}$ ,

$$k(r) = \frac{|(\nabla\nu(r))u(r) - (\nabla u(r))\nu(r)|}{\rho^2(r)}. \quad (2.3.7)$$

There are two ways in which  $k(r)$  is greater than  $k_0$ , the first is given as an example in [3] which is a two dimensional case where

$$\psi(r) = e^{iKx} e^{-y\sqrt{K^2 - k_0^2}}. \quad (2.3.8)$$

Where  $K > k_0$ .

Here  $K = k(r)$ , there are some subwavelength oscillations which are transverse to the direction of decay specifically in the  $x$  direction, since  $K > k_0$ . Then the spectrum in the  $x$  direction is much larger than that in the  $y$  direction which decays exponentially. These represent fast variation which are present in the spectrum of  $\psi$  and are not superoscillatory. The main interest is in the real plane wave, then we can say that the region where  $k(r) > k_0$  is in fact the region of superoscillations. These are expected to be situated near regions of wave vortices, which are waves or superposition of waves where the phase is undefined, this is also known as phase singularities.[20] [39] (can be thought of as waves with a phase varying infinitely rapidly).

Now looking into constructing monochromatic waves, which occur naturally by the isotropic superposition of plane waves,

$$\psi(r) = \sum_{n=1}^N a_n \exp[ik_n \cdot r] \quad (2.3.9)$$

where  $N \gg 1$ , and  $|k_n| = k_0$ .

Here the amplitudes are given by  $a_n$  which are random complex numbers, and the wavevector direction given by  $\frac{k_n}{k_0}$  which is uniformly distributed. Figure 2.6 shows our calculation of the superoscillatory area formed from the superposition of many waves in  $D = 2$  given by equation (2.3.9), in addition to figure 2.7 which is a contour plot of the phase of the wave with the lines indicating wavefronts at a constant phase interval. Where the lines intersect is an indication of wave vortices, which are found in the region of superoscillations as shown in figure 2.8. Furthermore, regions of superoscillations are found to be where the phase gradient is large (where the lines are closer together). Here, a calculation of the fraction of surface superoscillating is given to be around  $\frac{1}{3}$ , this result is to be expected and is described later in this section through the derivation of superoscillatory probability for two dimensional mono-chromatic waves. Our figures 2.6 2.7 2.8 has been created using MATLAB and supports the results as found in Ref [3].

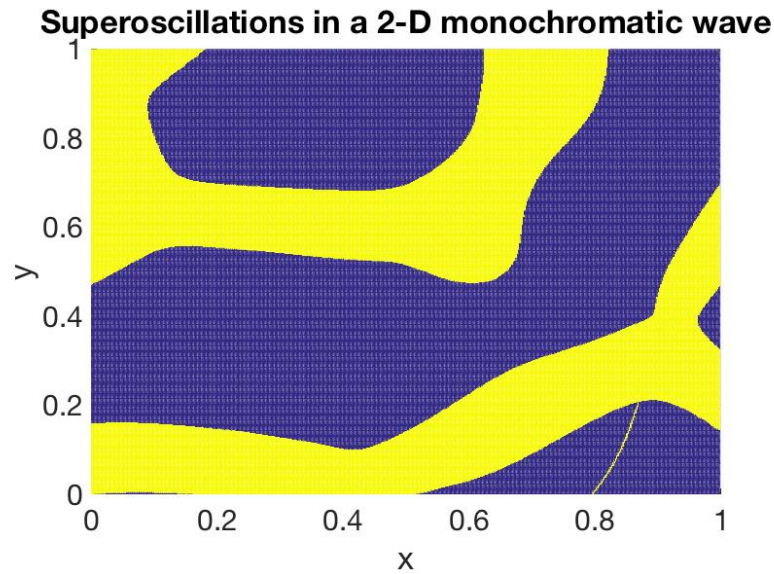


Figure 2.6: Our calculation of superoscillations given by the superposition of plane waves using equation (2.3.9) with  $k_0 = 2\pi$  and  $N = 10$  sources. This shows the superoscillatory region where  $k(r) > k_0$ , given by the yellow regions.

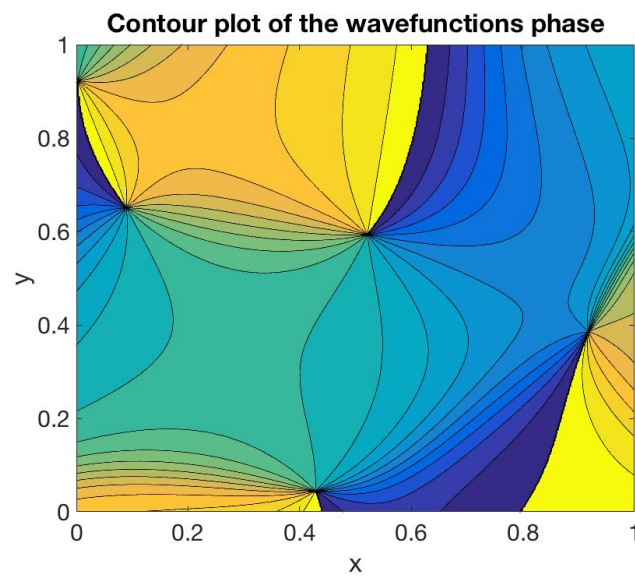


Figure 2.7: Shows the plot of 20 different phases (represented by the solid black lines) of a two dimensional sample wave as given by equation (2.3.9). The contour lines is seen to join in at the vortices.

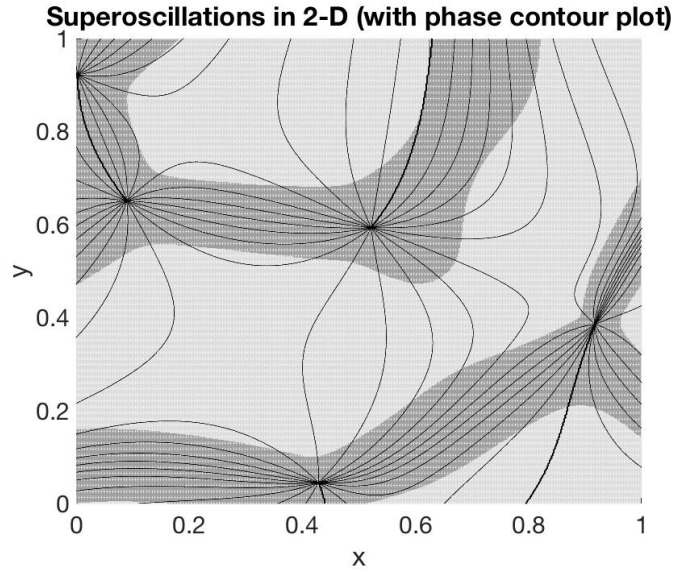


Figure 2.8: Plot of both the contour of several phases of the sample wave and the plot of the superoscillating surface of the two dimensional wave (Figures 2.6 and 2.7). Given that the dark regions are the regions of superoscillations. Each line shows the wavefront at a given phase.

## Probability of Superoscillations

For  $D$  dimensions it is essential to find a way of measuring the probability that local wavenumber exceeds the free space wavenumber;  $k(r) > k_0$ , at any given point  $r$ . This is done by using the fact that the functions are Gaussian and are isotropic. This is due to the central limit theorem which states that the sum of a large number of samples of an independent random variable will result in a normal distribution, that is if both the expected value and the variance is well defined (4.0.4). The waves described in equation (2.3.9) are Gaussian functions and are isotropic. The probability in a multiple  $D$  dimensions that the wave is Superoscillating through is shown to be

$$P_{Dsuper} = \int_{k_0}^{\infty} P_D(k) dk. \quad (2.3.10)$$

Where  $P_D(k)$  is the probability distribution in  $D$  dimensions for the local wavenumber  $k(r)$ . The aim is to find the probability distribution of  $k$  for a value of  $r$  in more than one dimension. This distribution can be described by

$$P_D(k) = \Omega_D k^{D-1} \left\langle \delta\left(k - \frac{u(\nabla\nu) - \nu(\nabla u)}{\rho^2}\right) \right\rangle. \quad (2.3.11)$$

Where  $\Omega_D = \frac{2\pi^{\frac{D}{2}}}{\Gamma(\frac{D}{2})}$  is the surface area of the unit sphere in multiple dimensions  $D$ . The unit sphere in multiple dimensions is explained fully in the mathematics section (4.0.2).

Essentially what equation (2.3.11) shows is that the function is superimposed on a unit sphere in  $D$  dimensions (hypersphere), so that at every point  $r$  on the

surface of the sphere,  $k$  has a value corresponding to the superposition of the isotropic, monochromatic waves at said point. The dirac delta function creates this distribution, so that when  $k = \frac{u(\nabla\nu) - \nu(\nabla u)}{\rho^2}$  the function contributes to the equation. Note that it is averaging over all values of  $u$ ,  $\nu$ ,  $\nabla u$  and  $\nabla\nu$ , that is averaging over all the wavefunctions at point  $r$ . Taking the Fourier inversion of the dirac delta function we obtain,

$$\delta(s) = \frac{1}{\sqrt{2\pi}} \int_{-\infty}^{\infty} e^{iks} \langle \delta(k - \frac{u(\nabla\nu) - \nu(\nabla u)}{\rho^2}) \rangle dk, \quad (2.3.12a)$$

$$\delta(s) = \frac{1}{\sqrt{2\pi}} \langle e^{is \frac{u(\nabla\nu) - \nu(\nabla u)}{\rho^2}} \rangle \quad (2.3.12b)$$

$$\delta(k) = \frac{1}{\sqrt{2\pi}} \int_{-\infty}^{\infty} \frac{1}{\sqrt{2\pi}} e^{-iks} \langle e^{\frac{is(u(\nabla\nu) - \nu(\nabla u))}{\rho^2}} \rangle d^D s \quad (2.3.12c)$$

$$\delta(k) = \frac{1}{(2\pi)^D} \int_{-\infty}^{\infty} e^{-iks} \langle e^{is \frac{u(\nabla\nu) - \nu(\nabla u)}{\rho^2}} \rangle . \quad (2.3.12d)$$

Then an expression of equation (2.3.11) is given as,

$$P_D(k) = \Omega_D k^{D-1} \frac{1}{(2\pi)^D} \int_{-\infty}^{\infty} e^{-isk} \langle e^{is[\frac{u(\nabla\nu) - \nu(\nabla u)}{\rho^2}]} \rangle d^D s. \quad (2.3.13)$$

Taking that in equation (2.3.13), the variables  $u$ ,  $\nu$ ,  $\nabla u$  and  $\nabla\nu$  are all independent of each other but have same distribution, also taking that  $\partial_i u$  is independent of  $\partial_j u$  for  $i \neq j$ .

$$\langle \exp[is \frac{u(\nabla\nu) - \nu(\nabla u)}{\rho^2}] \rangle = \langle \exp[-\frac{1}{2\rho^2} \langle (s(\cos\chi(\nabla\nu) - \sin\chi(\nabla u)))^2 \rangle_{\nabla u, \nabla\nu}] \rangle \quad (2.3.14)$$

The function (2.3.14) is found as follows, knowing that the expectation value of a given function is described as follows,

$$\langle e^{itx} \rangle = \frac{1}{\sigma\sqrt{2\pi}} \int_{-\infty}^{\infty} e^{-\frac{(x-\mu)^2}{2\sigma^2}} e^{itx} dx. \quad (2.3.15)$$

Where the variable  $x$  have a Gaussian distribution with a mean of  $\mu$  and a variance of  $\sigma^2$ . Making the substitution of

$$a = \frac{1}{\sigma\sqrt{2\pi}} \quad (2.3.16a)$$

$$c = \sqrt{2}\sigma. \quad (2.3.16b)$$

Now equation (2.3.15) becomes

$$\langle e^{itx} \rangle = a \int_{-\infty}^{\infty} e^{-\frac{(x-\mu)^2}{c^2}} e^{itx} dx. \quad (2.3.17)$$

Let

$$\alpha = x - \mu \quad (2.3.18)$$

$$\langle e^{itx} \rangle = a \int_{-\infty}^{\infty} e^{-\frac{\alpha^2}{c^2}} e^{it(\alpha+\mu)} d\alpha \quad (2.3.19a)$$

$$\langle e^{itx} \rangle = ae^{it\mu} \int_{-\infty}^{\infty} e^{-\frac{1}{c^2}(\alpha^2-itc^2\alpha)} d\alpha. \quad (2.3.19b)$$

Substitute  $c$  back in from the equation given in (2.3.16) into the brackets,

$$\langle e^{itx} \rangle = ae^{it\mu} \int_{-\infty}^{\infty} e^{-\frac{1}{c^2}(\alpha^2-i2t\sigma^2\alpha)} d\alpha \quad (2.3.20a)$$

$$= ae^{(it\mu-\frac{t^2\sigma^2}{2})} \int_{-\infty}^{\infty} e^{-\frac{(\alpha-it\sigma^2)^2}{c^2}} d\alpha. \quad (2.3.20b)$$

Using the substitution rule

$$\gamma = \alpha - it\sigma^2, \quad (2.3.21)$$

the equation becomes

$$\langle e^{itx} \rangle = ae^{(it\mu-\frac{t^2\sigma^2}{2})} \int_{-\infty}^{\infty} e^{-\frac{\gamma^2}{c^2}} d\gamma. \quad (2.3.22)$$

$$\phi = \frac{\gamma}{c} \quad (2.3.23a)$$

$$cd\phi = d\gamma \quad (2.3.23b)$$

$$\langle e^{itx} \rangle = ace^{(it\mu-\frac{t^2\sigma^2}{2})} \int_{-\infty}^{\infty} e^{-\phi^2} d\phi \quad (2.3.24a)$$

$$= ace^{(it\mu-\frac{t^2\sigma^2}{2})} \sqrt{\pi}. \quad (2.3.24b)$$

Substituting back in  $a$  and  $c$  from (2.3.16) into (2.3.24), yields the final relation:

$$\langle e^{itx} \rangle = e^{(it\mu-\frac{t^2\sigma^2}{2})}. \quad (2.3.25)$$

As have been previously described  $u$ ,  $\nu$ ,  $\nabla u$  and  $\nabla \nu$  are all independent from one another (i.e. each has its own probability distribution which is Gaussian), thus the average over  $\nabla u$  and  $\nabla \nu$  would tend to zero as it would be over  $\cos(\chi)$  and  $\sin(\chi)$ . This illustrates that  $\mu$  in the equation (2.3.14) is zero and the variance would be equal to  $\sigma^2 = \langle x^2 \rangle$ , therefore giving the relationship above (2.3.14) as,

$$\begin{aligned} (s[\cos \chi[\nabla \nu] - \sin \chi[\nabla u]])^2 &= |s|(\cos^2 \chi(\nabla \nu)^2 + \sin^2 \chi(\nabla u)^2 - 2 \sin \chi \cos \chi(\nabla \nu)(\nabla u)) \\ &= s_x^2[\cos^2 \chi(\frac{\partial \nu}{\partial x})^2 + \sin^2 \chi(\frac{\partial u}{\partial x})^2] \\ &+ s_y^2[\cos^2 \chi(\frac{\partial \nu}{\partial y})^2 + \sin^2 \chi(\frac{\partial u}{\partial y})^2] + s_z^2[\cos^2 \chi(\frac{\partial \nu}{\partial z})^2 + \sin^2 \chi(\frac{\partial u}{\partial z})^2]. \end{aligned} \quad (2.3.26a)$$

Given that the average of  $\langle \sin^2 \rangle = \langle \cos^2 \rangle = \frac{1}{2}$ ,  $\langle \frac{\partial u}{\partial x} \rangle = \langle \frac{\partial v}{\partial x} \rangle$ , it can be shown to be,

$$(s \cdot [\cos \chi \nabla v - \sin \chi \nabla u])^2 = s_x^2 \langle \left(\frac{\partial u}{\partial x}\right)^2 \rangle + s_y^2 \langle \left(\frac{\partial u}{\partial y}\right)^2 \rangle + s_z^2 \langle \left(\frac{\partial u}{\partial z}\right)^2 \rangle \quad (2.3.27a)$$

$$= 3s_x^2 \langle \left(\frac{\partial u}{\partial x}\right)^2 \rangle \quad (2.3.27b)$$

$$s_x^2 = \frac{1}{3}s^2 \quad (2.3.27c)$$

$$= s^2 \langle \left(\frac{\partial u}{\partial x}\right)^2 \rangle. \quad (2.3.27d)$$

From isotropy and monochromaticity, it can be seen that the value of

$$\langle \left(\frac{\partial u}{\partial x}\right)^2 \rangle = \frac{1}{D} \langle |\nabla u|^2 \rangle = \frac{k_0^2}{D} \langle u^2 \rangle. \quad (2.3.28)$$

Now substituting back in equations (2.3.27), (2.3.28) and (2.2.14) back into (2.3.13), yields

$$P_D(k) = \frac{\Omega_D k^{D-1}}{(2\pi)^D} \left[ \int e^{-iks} \langle e^{-\frac{1}{2\rho^2} s^2 \frac{k_0^2}{D} \langle u^2 \rangle} \rangle ds \right]^D. \quad (2.3.29)$$

Analysing the integral by completing the square,

$$y = \frac{1}{\sqrt{2\rho}} s \frac{k_0}{D^{\frac{1}{2}}} \langle u^2 \rangle^{\frac{1}{2}} + a \quad (2.3.30)$$

$$y^2 = \frac{1}{2\rho^2} s^2 \frac{k_0^2}{D} \langle u^2 \rangle + \frac{2}{\sqrt{2}} \frac{a}{\rho} \frac{k_0}{D^{\frac{1}{2}}} \langle u^2 \rangle^{\frac{1}{2}} + a^2. \quad (2.3.31)$$

Now comparing this with equation (2.3.29) gives

$$a = i \frac{k\rho D^{\frac{1}{2}}}{k_0 \langle u^2 \rangle^{\frac{1}{2}} \sqrt{2}}. \quad (2.3.32a)$$

Putting this back into the equation (2.3.31), results in

$$-y^2 = -\frac{1}{2\rho^2} s^2 k_0^2 \langle u^2 \rangle - iks + \frac{k^2 \rho^2 D}{k_0^2 \langle u^2 \rangle 2}. \quad (2.3.33)$$

Where  $dy = \frac{1}{\sqrt{2\rho}} \frac{k_0}{D^{\frac{1}{2}}} \langle u^2 \rangle^{\frac{1}{2}} ds$ .

$$P_D(k) = \frac{\Omega_d k^{D-1}}{(2\pi)^D} \left[ \langle \int e^{-y^2} e^{-\frac{k^2 \rho^2 D}{2k_0^2 \langle u^2 \rangle 2}} \left( \frac{\sqrt{2\rho} D^{\frac{1}{2}}}{\langle u^2 \rangle^{\frac{1}{2}} k_0} \right) dy \rangle \right]^D \quad (2.3.34a)$$

$$P_D(k) = \frac{\Omega_d k^{D-1}}{(2\pi)^D} \left[ \frac{\sqrt{2\rho} D^{\frac{1}{2}}}{\langle u^2 \rangle^{\frac{1}{2}} k_0} \right]^D \langle e^{-\frac{k^2 \rho^2 D}{2k_0^2 \langle u^2 \rangle}} \rangle \quad (2.3.34b)$$

$$P_D(k) = \frac{\Omega_D k^{D-1} D^{\frac{D}{2}}}{(2\pi)^{\frac{D}{2}} \langle u^2 \rangle^{\frac{D}{2}} k_0^D} \langle \rho^D e^{-\frac{k^2 \rho^2 D}{2k_0^2 \langle u^2 \rangle}} \rangle_{\rho, \chi}. \quad (2.3.34c)$$

Here the integral solution below is used,

$$\int_{-\infty}^{\infty} e^{-y^2} dy = \sqrt{\pi}. \quad (2.3.35)$$

First an expression of the probability density function is made so that the average is taken of the quantity in equation (2.3.34).

$$P_D(k) = \frac{\Omega_d k^{D-1} D^{\frac{D}{2}}}{(2\pi)^{\frac{D}{2}} \langle u^2 \rangle^{\frac{D}{2}} k_o^D} \int \rho^D e^{-\frac{k^2 \rho^2 D}{2k_o^2 \langle u^2 \rangle}} e^{-\frac{(u-\langle u \rangle)^2}{2\sigma_u^2}} e^{-\frac{(v-\langle v \rangle)^2}{2\sigma_v^2}} dudv \quad (2.3.36)$$

Now taking the polar form of the integral,

$$du dv = \rho d\rho d\chi \quad (2.3.37a)$$

$$u = \rho \cos \chi \quad (2.3.37b)$$

$$v = \rho \sin \chi. \quad (2.3.37c)$$

The expression for the probability density can be written as follows,

$$P_D(k) = \frac{\Omega_d k^{D-1} D^{\frac{D}{2}}}{(2\pi)^{\frac{D}{2}} \langle u^2 \rangle^{\frac{D}{2}} k_o^D} \int \rho^{D+1} e^{-\frac{k^2 \rho^2 D}{2k_o^2 \langle u^2 \rangle}} e^{-\frac{\rho^2}{2\langle u^2 \rangle}} d\rho d\chi. \quad (2.3.38)$$

In order to evaluate the average over  $\chi$ , an integral for 0 to  $2\pi$  divided by  $2/\pi$  is taken, meaning the average of the expression (2.3.38) is equal to 1. Also integrating over  $\rho$  from 0 to  $\infty$  will not give a useful answer because the end expression will give a non convergent result. Thus a Gaussian expression which is normalised is required, as given by,

$$\int_0^{\infty} A e^{-\frac{\rho^2}{2\langle u^2 \rangle}} \rho d\rho = 1 \quad (2.3.39a)$$

$$A = \frac{1}{\langle u^2 \rangle}. \quad (2.3.39b)$$

$$P_D(k) = \frac{\Omega_D k^{D-1} D^{\frac{D}{2}}}{(2\pi)^{\frac{D}{2}} k_o^D \langle u^2 \rangle^{\frac{D}{2}+1}} \int_0^{\infty} \rho^{D+1} e^{-\frac{\rho^2}{2\langle u^2 \rangle} (\frac{Dk^2}{k_o^2} + 1)} d\rho. \quad (2.3.40)$$

Let  $y = \rho^2$  and  $d\rho = \frac{1}{2\rho} dy$ , then equation (2.3.40) becomes

$$\int_0^{\infty} \frac{1}{2} y^{\frac{D}{2}} e^{-\frac{y}{2\langle u^2 \rangle} (\frac{Dk^2}{k_o^2} + 1)} dy. \quad (2.3.41)$$

From the relation given by the Gamma function,

$$\int_0^{\infty} t^b e^{-at} dt = \frac{\Gamma(b+1)}{a^{b+1}}, \quad (2.3.42)$$

equation (2.3.40) can be written as

$$P_D(k) = \frac{\Omega_D k^{D-1} D^{\frac{D}{2}}}{(2\pi)^{\frac{D}{2}} k_0^D \langle u^2 \rangle^{\frac{D}{2}+1}} \frac{1}{2} \Gamma\left(\frac{D}{2} + 1\right) \cdot \left[ \frac{1}{\frac{1}{2\langle u^2 \rangle} \left( \frac{Dk^2}{k_0^2} + 1 \right)} \right]^{\frac{D}{2}+1} \quad (2.3.43a)$$

$$P_D(k) = \frac{\Omega_D k^{D-1} D^{\frac{D}{2}}}{(2\pi)^{\frac{D}{2}} k_0^D \langle u^2 \rangle^{\frac{D}{2}+1}} \Gamma\left(\frac{D}{2} + 1\right) 2^{\frac{D}{2}} \cdot \frac{\langle u^2 \rangle^{\frac{D}{2}+1} k_0^{D+2}}{[Dk^2 + k_0^2]^{\frac{D}{2}+1}}. \quad (2.3.43b)$$

Knowing that the surface of the unit sphere  $\Omega_D$  is

$$\Omega_D = \frac{2(\pi)^{\frac{D}{2}}}{\Gamma\left(\frac{D}{2}\right)}, \quad (2.3.44)$$

and substituting (2.3.44) into (2.3.43) yields the final result of

$$P_D(k) = \frac{k^{D-1} k_0^2}{\left(k^2 + \frac{k_0^2}{D}\right)^{\frac{D}{2}+1}}. \quad (2.3.45)$$

Distributions for several values of D is given in figure 2.9 below:

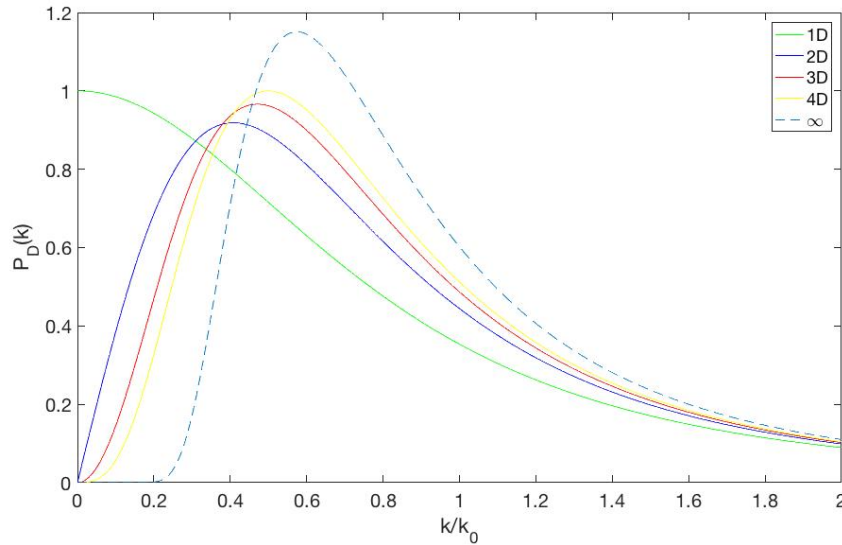


Figure 2.9:

Relationship between the probability distribution against the ratio of the wavenumber  $\frac{k}{k_0}$ . Using equation (2.3.45) for the probability distribution.  $D = 1, 2, 3, 4, 99$  where the green line is  $D = 1$  and the dashed line is  $D = 99$ . This figure is produced using MATLAB and supports the result in [3] figure 3.

Taking the equation in (2.3.45), and writing it in the form

$$P_D(k) = \frac{1}{\left(\frac{k^2+k_0^2/D}{k_0^{D+2}k^{D+2}}\right)^{\frac{D}{2}+1}} \quad (2.3.46a)$$

$$P_D(k) = \frac{1}{\left(\frac{k^{\frac{6}{D+2}}}{k_0^{D+2}} + \frac{k_0^{\frac{2D}{D+2}}/D}{k^{\frac{2D-2}{D+2}}}\right)^{\frac{D}{2}+1}} \quad (2.3.46b)$$

$$P_D(k) = \frac{1}{\frac{k^3}{k_0^2} \left(1 + \frac{k_0^{\frac{2D}{D+2}}/D}{k^{\frac{2D-2}{D+2}}} \frac{k_0^{\frac{4}{D+2}}}{k^{\frac{6}{D+2}}}\right)^{\frac{D}{2}+1}} \quad (2.3.46c)$$

$$P_D(k) = \frac{k_0^2}{k^3} \frac{1}{\left(1 + \frac{k_0^2/D}{k^2}\right)^{\frac{D}{2}+1}}. \quad (2.3.46d)$$

Expanding the term in equation (2.3.46)  $\left(1 + \frac{k_0^2/D}{k^2}\right)^{\frac{D}{2}+1}$  results in,

$$\left(1 + \frac{k_0^2/D}{k^2}\right)^{\frac{D}{2}+1} = 1 + \left(\frac{D}{2} + 1\right) \frac{k_0^2}{Dk^2} + \frac{1}{2!} \left(\frac{D}{2} + 1\right) \left(\frac{D}{2}\right) \frac{k_0^4}{D^2k^4} + \dots \quad (2.3.47a)$$

$$= 1 + \frac{k_0^2}{2k^2} + \frac{k_0^2}{Dk^2} + \frac{1}{2!} \frac{D^2}{4} \frac{k_0^4}{D^2k^4} + \frac{k_0^4}{2Dk^4} + \dots \quad (2.3.47b)$$

When  $D \rightarrow \infty$  it can be seen how the expanded term in (2.3.47) tends to an exponential, which gives the expression

$$P_\infty(k) = \frac{k_0^2}{k^3} e^{-\frac{k_0^2}{2k^2}}. \quad (2.3.48)$$

To calculate the probability for superoscillations, the first step is to express the probability density function as shown,

$$P_D(k) = \frac{k_0^2 k^{D-1}}{\left(k^2 + \frac{k_0^2}{D}\right)^{\frac{D}{2}+1}} \quad (2.3.49a)$$

$$= \frac{k_0^2 k^{D-1}}{k^{D+2} \left(1 + \frac{k_0^2}{Dk^2}\right)^{\frac{D}{2}+1}} \quad (2.3.49b)$$

$$= \frac{k_0^2}{k^3 \left(1 + \frac{k_0^2}{Dk^2}\right)^{\frac{D}{2}+1}}. \quad (2.3.49c)$$

Now calculating the probability of superoscillations as,

$$P_{Dsuper} = \int_{k_{max}}^{\infty} \frac{d}{dk} \left[1 + \frac{k_0^2}{Dk^2}\right]^{-\frac{D}{2}} dk \quad (2.3.50a)$$

$$= 1 - \frac{1}{\left(1 + \frac{1}{D}\right)^{\frac{D}{2}}}. \quad (2.3.50b)$$

Equation (2.3.50) above then, gives the probability of the wavefunction being superoscillatory at given  $D$  dimensions. For example at 1  $D$ , the probability is around 0.2928, while for two dimension i.e.  $D = 2$  the probability is  $\frac{1}{3}$ . As  $D$  increases the probability increases. The distribution in equation (2.3.49) diverges for orders 2 or higher of the term  $(1 + \frac{k_0^2/D}{k^2})^{\frac{D}{2}+1}$  (equation (2.3.47)) as  $k$  decays by a factor of  $k^{-3}$ , therefore the first moment; mean value of  $k(r)$ , is given by,

$$\langle k_D \rangle = \int_0^\infty k P_D(k) dk = \int_0^\infty \frac{k_0^2 k^D}{(k^2 + \frac{k_0^2}{D})^{\frac{1}{2}D+1}} dk. \quad (2.3.51)$$

The equation (2.3.51) can be expressed using the  $\beta$  function given below,

$$\beta(x, y) = \int_0^\infty \frac{t^{x-1}}{(1+t)^{x+y}} dt \quad (2.3.52a)$$

$$\beta(x, y) = 2 \int_0^\infty \frac{t^{2x-1}}{(1+t^2)^{x+y}} dt. \quad (2.3.52b)$$

Equation (2.3.51) can now be written as

$$\langle k_D \rangle = \frac{D^{\frac{1}{2}D+1}}{k_0^{D+2}} k_0^2 \int \frac{k^D}{(1 + \frac{k^2 D}{k_0^2})^{\frac{1}{2}D+1}} dk \quad (2.3.53)$$

Let  $t = \frac{k}{k_0} D^{\frac{1}{2}} \rightarrow \frac{k_0}{D^{\frac{1}{2}}} dt = dk$ .

$$\langle k_D \rangle = D \frac{k_0}{D^{\frac{1}{2}}} \int_0^\infty \frac{t^D}{(1+t^2)^{\frac{1}{2}D+1}} dt \quad (2.3.54a)$$

$$\langle k_D \rangle = D^{\frac{1}{2}} k_0 \frac{1}{2} \frac{\Gamma(\frac{D}{2} + \frac{1}{2}) \Gamma(\frac{1}{2})}{\Gamma(\frac{D}{2} + 1)} \quad (2.3.54b)$$

$$\langle k_D \rangle = k_0 \sqrt{\frac{\pi}{D}} \frac{\Gamma(\frac{1}{2}(\frac{D}{2} + 1))}{\Gamma(\frac{D}{2})}. \quad (2.3.54c)$$

In this section, a description of superoscillations is given for the superposition of a large number of waves which are Gaussian functions and isotropic (equation (2.3.9)). This was given by finding an expression for the probability distribution of the local wavenumber in  $D$  dimensions (given by equation (2.3.45)). Following this, an expression for the probability of the wavefunction being superoscillatory is shown in equation (2.3.50), which can be seen to be completely independent of the maximum wavenumber in the Fourier spectrum. Furthermore the probability of superoscillation was shown to increase with higher dimensions.

## Superoscillations In $D = 1$ Dimensions

This section looks at the special case of  $D = 1$ , where the probability of the function superoscillating was given to be around 0.293. A numerical and computational analysis of how such functions can superoscillate is provided, given that the plane wave and its components for a 1  $D$  wave would be concentrated at  $k_n = \pm k_0$  for a monochromatic wave. To start, allow  $k(x)$  to take on both negative and positive values (unlike before where the modulus was taken).

$$k(x) = \partial_x \chi(x) = \Im[\partial_x(\log \psi(x))]. \quad (2.3.55)$$

Then it is important that non-monochromatic waves are taken to be concentrated between the limits  $\pm k_0$ .

$$\psi(x) = \sum_{n=1}^N a_n \exp(ik_n x) \quad (2.3.56)$$

For  $1 \leq n \leq \frac{1}{2}N$ ,

$$-k_0 \leq k_n \leq -k_0(1 - \delta) \quad (2.3.57)$$

for  $\frac{1}{2}N + 1 \leq n \leq N$ ,

$$k_0(1 - \delta) \leq k_n \leq k_0. \quad (2.3.58)$$

Here  $N$  is given to be the number of waves superimposing and is given to be  $N \gg 1$ , also  $\delta$  is a parameter that gives the bandwidth of the waves, this is given to be  $\delta \ll 1$ , so that the waves are approximately monochromatic. When simulated through Matlab a good approximation is given for the wavefunction given by equation (2.3.56) repeated over  $10^5$  times. Giving a similar distribution for  $k$  values as predicted theoretically. The figures provided below in 2.10 is an example of one wavefunction.

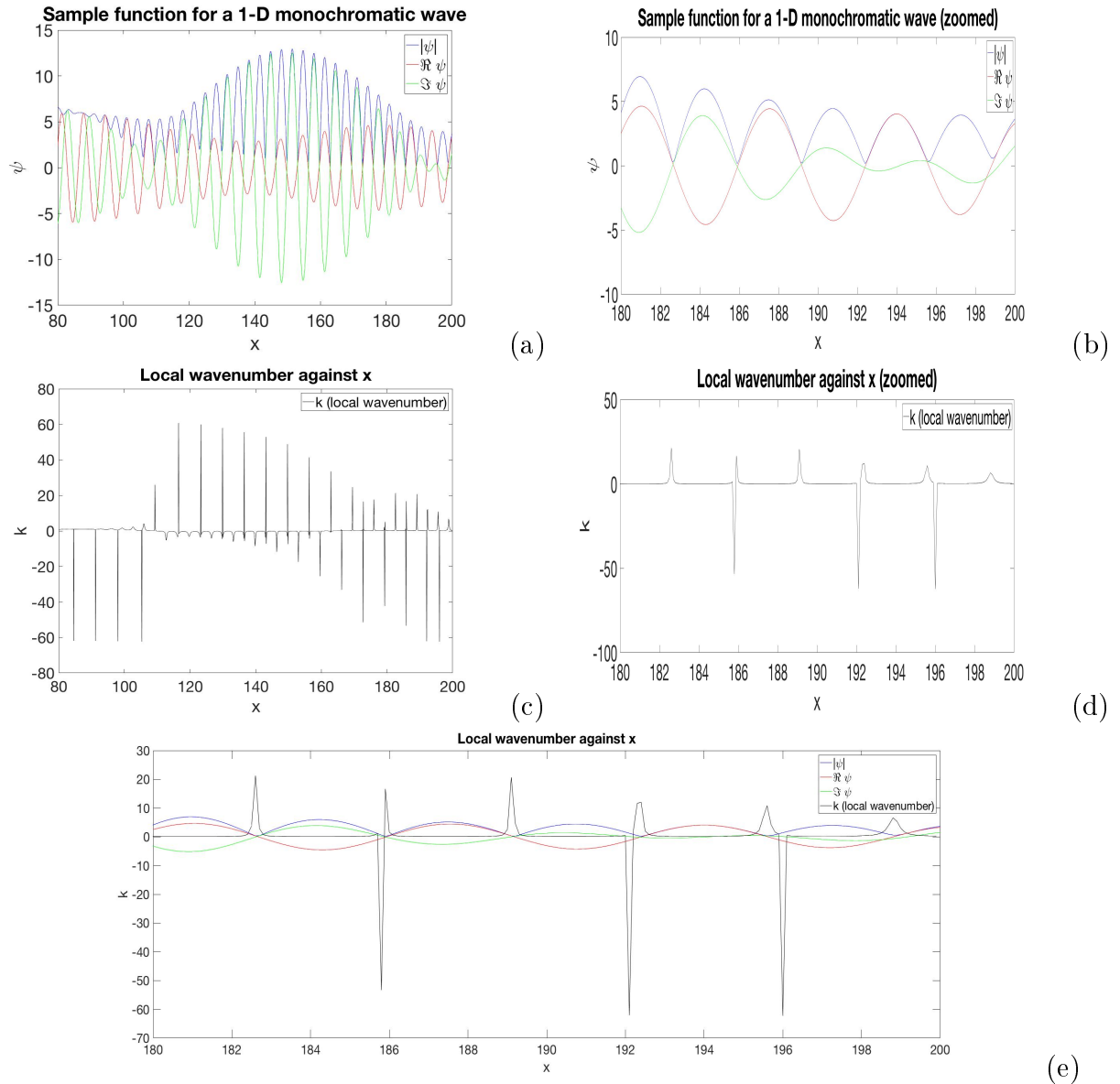


Figure 2.10: This is a sample wave given from equation (2.3.56) for 1 dimension, with  $N = 50$ ,  $k_0 = 1$ , and  $\delta = 0.1$  the red line shows  $\Re(\psi)$ , the green line shows  $\Im(\psi)$  and the blue line shows the  $|\psi|$ , (b) shows the magnification of (a). Plots (c) and (d) show the local wavenumber for (a) and (b) respectively as given by equation (2.3.55). Plot (e) shows the plot of both (b) and (d) on the same graph. Recreation of figure 5 in [3]

When looking at the graphs formed, the area where the wavenumber is a minimum, i.e. where  $|\psi(x)|$  is minimum, is the region where superoscillations occur, here large local wavenumbers are located as seen in figure 2.10e, which shows the plot of  $\psi$  and  $k$ . Therefore superoscillations are said to be found near regions of phase singularities (regions where the phase varies infinitely rapidly and functions tend to vanish).

To analyse how the asymptotic distribution is formed where  $P_\infty(k)$  tends to

$\frac{k_0^2}{k^3}$  for  $k \gg k_0$ , an example is given of a wave function given as,

$$\psi(x) = (1 + \epsilon)e^{ix} + e^{-ix}. \quad (2.3.59)$$

$\epsilon \ll 1$ , and is real. Now as before the local wavenumber is found using equation (2.3.55) this gives,

$$\psi(x) = \epsilon[\cos(x) + i \sin(x)] + 2 \cos(x) \quad (2.3.60a)$$

$$\nabla \ln \psi(x) = \frac{-(\epsilon + 2) \sin(x) + i\epsilon \cos(x)}{(\epsilon + 2) \cos(x) + i\epsilon \sin(x)} \quad (2.3.60b)$$

$$\Im[\nabla \ln \psi(x)] = \frac{(i\epsilon^2 + 2i\epsilon)}{\epsilon^2 + (\epsilon + 1)4 \cos^2(x)}. \quad (2.3.60c)$$

Now with  $\epsilon \ll 1$  the local wavenumber can be written as shown in (2.3.61), This is due to the fact that the terms at the denominator of the expression has  $\epsilon^2$  as the main contributor to the function, when  $\cos^2(x)$  has a small value or tends to zero. Therefore the term  $\epsilon^2$  cannot be ignored here, however the term  $4\epsilon \cos^2(x)$  can be disregarded as it has very little contribution to the function overall.

$$k(x) = \frac{\epsilon^2 + 2\epsilon}{\epsilon^2 + 4\cos^2(x)} \quad (2.3.61)$$

As shown in the figures computed below, the values for  $k(x)$  where it is a maximum with a magnitude of  $\frac{2}{\epsilon}$ , is at the same point where the wave  $|\psi(x)|$  is a minimum, which is equal to  $|\epsilon|$  at  $x = \frac{\pi}{2}$ . From equation (2.3.60) it is clear that  $\psi(x) = i\epsilon$  when  $x = \frac{\pi}{2}$ . Now an analysis is made for regions where the value for  $k$  is greatest (with the maximum  $k(\frac{\pi}{2})$ ), and where the wave  $|\psi(x)|$  disappears as the phase varies rapidly. Therefore taking the points for  $k(\frac{\pi}{2} + \xi)$  where  $\xi$  is small compared to  $\epsilon$ .

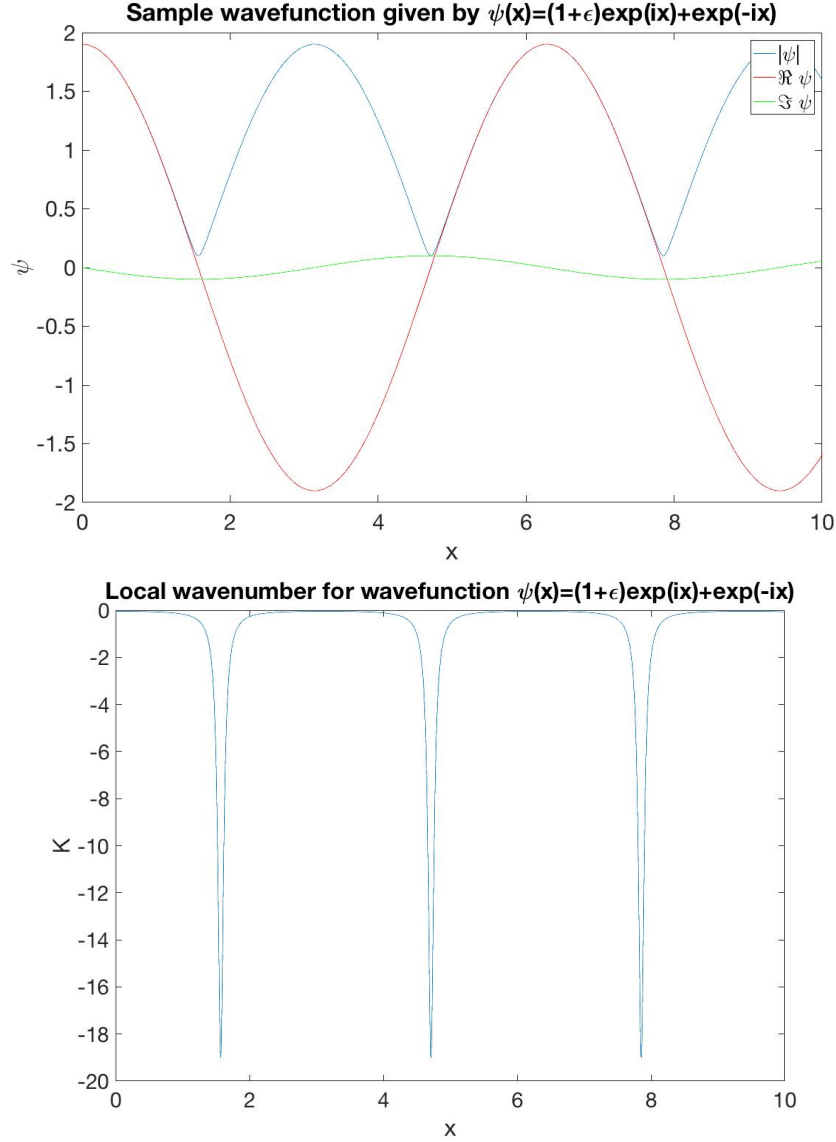


Figure 2.11: recreation of figure 6 in [3] and shows the resultant wave using equation (2.3.59) by plotting  $\text{Re}(\psi)$  (red curve), imaginary( $\psi$ ) (green) and  $|\psi|$  (blue). given  $\epsilon=-0.1$ . The figure also shows the plot of local wavenumber  $k(x)$  against  $x$ .

From equation (2.3.61),  $k(x)$  is given to be

$$k\left(\frac{\pi}{2} + \xi\right) = \frac{2\epsilon + \epsilon^2}{\epsilon^2 + 4\cos^2\left(\frac{\pi}{2} + \xi\right)} = \frac{2\epsilon + \epsilon^2}{\epsilon^2 + 4(\cos\left(\frac{\pi}{2}\right)\cos(\xi) - \sin\left(\frac{\pi}{2}\right)\sin(\xi))^2}. \quad (2.3.62)$$

If an assumption is made so that  $\xi \ll 1$ , then we can write (2.3.62) as,

$$\frac{2\epsilon + \epsilon^2}{\epsilon^2 + 4\sin^2\xi} = \frac{2\epsilon + \epsilon^2}{\epsilon^2 + 4\xi^2} \quad (2.3.63a)$$

$$= \frac{2\epsilon + \epsilon^2}{\epsilon^2} \left(1 + \frac{4\xi^2}{\epsilon^2}\right)^{-1}. \quad (2.3.63b)$$

Now we expand this through binomial expansion

$$k\left(\frac{\pi}{2} + \xi\right) = \left(\frac{2}{\epsilon} + 1\right) \left(1 - \frac{4\xi^2}{\epsilon^2} + \frac{16\xi^4}{\epsilon^4} + \dots\right) = \frac{2}{\epsilon} + 1 - \frac{8\xi^2}{\epsilon^3} - \frac{4\xi^2}{\epsilon^2}. \quad (2.3.64)$$

Here  $\epsilon$  is constant. If  $\xi \gg \epsilon$  then it can be seen that the series above diverges, giving an undefined value for  $k$ , however if  $\xi \ll \epsilon$  then it can be shown that the series converges. Expanding the expression with the factor  $\frac{2}{\epsilon}$  will always have the biggest contribution to the value of  $k$  if  $\epsilon \ll 1$  and  $\epsilon \ll \xi$ , therefore equation (2.3.64) can be approximated to that given in (2.3.66) as given in the paper [3].

Taking  $\xi \ll \epsilon$  would mean the series converges in (2.3.64). A calculation of the wavenumber in this case gives the result shown in (2.3.65), Comparing the two expressions in (2.3.65) and (2.3.66) the difference can be seen. The figure shown in 2.12, illustrates this.

$$k\left(\frac{\pi}{2} + \xi\right) \approx \frac{2}{\epsilon} - \frac{8\xi^2}{\epsilon^3} + 1 - \frac{4\xi^2}{\epsilon^2} \quad (2.3.65)$$

In [3] the local wavenumber was expressed as shown in equation (2.3.66), Here the approximation that  $\epsilon \ll 1$  is taken, yielding

$$k\left(\frac{\pi}{2} + \xi\right) \approx \frac{2}{\epsilon} - \frac{8\xi^2}{\epsilon^3}. \quad (2.3.66)$$

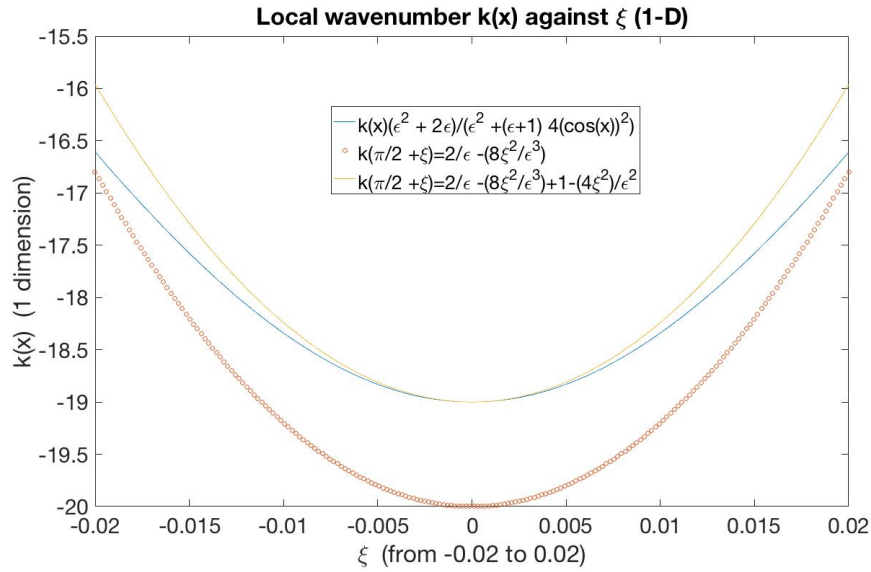


Figure 2.12: Here the figure shows the plots for the functions found for the local wavenumber of the expression (2.3.59), using the approximation of small  $\xi$  for  $k(\pi/2 + \xi)$ . The plots are given by the expression given in paper [3] given here by (2.3.66) shown in red, and the approximation calculated by us as (2.3.64) in orange. The exact local wavenumber is given by (2.3.61) in blue.  $\epsilon = -0.1$ ,  $-0.02 \leq \xi \leq 0.02$

Looking at the graph in figure (2.11) showing the relationship between the local wavenumber  $k(x)$  and  $x$  this gives a parabola shape distribution and so could be

approximated or expressed as a dirac delta function, with values of  $k = \frac{2}{\epsilon}$  and at  $k = 0$ . An average is taken of the dirac delta function over all values of  $\xi$  by integrating through all values of  $\xi$ , assuming that  $\epsilon$  is fixed. The integral is taken through all values of  $\xi$  because the distribution of  $\xi$  is known to be uniform, however it is not apparent what the underlying distribution is for the wavenumbers. Given that the probability distribution can be expressed as,

$$P(\epsilon, k) = \frac{2}{\epsilon} \int_0^{\frac{\epsilon}{2}} \delta \left( k - \left( \frac{2}{\epsilon} - \frac{8\xi^2}{\epsilon^3} \right) \right) d\xi \quad (2.3.67)$$

and changing the integral in terms of  $z$ , where  $z$  is defined as

$$z = \frac{2}{\epsilon} - \frac{8\xi^2}{\epsilon^3}. \quad (2.3.68)$$

$$\xi = \frac{\epsilon}{2} \sqrt{1 - \frac{z\epsilon}{2}} \quad (2.3.69a)$$

$$\frac{d\xi}{dz} = -\frac{\epsilon^2}{8} \left( 1 - \frac{z\epsilon}{2} \right)^{-\frac{1}{2}}. \quad (2.3.69b)$$

Substituting this back into equation (2.3.67) to find that

$$P(\epsilon, k) = \frac{2}{\epsilon} \int_{\frac{2}{\epsilon}}^0 -\frac{\epsilon^2}{8} \left( 1 - \frac{z\epsilon}{2} \right)^{-\frac{1}{2}} \delta(k - z) dz \quad (2.3.70a)$$

$$P(\epsilon, k) = \frac{2}{\epsilon} \int_{\frac{2}{\epsilon}}^0 -\frac{\epsilon^2}{8} \left( 1 - \frac{z\epsilon}{2} \right)^{-\frac{1}{2}} \delta(z - k) dz \quad (2.3.70b)$$

$$P(\epsilon, k) = -\frac{\epsilon}{4} \left( 1 - \frac{k\epsilon}{2} \right)^{\frac{1}{2}} \Theta \left( k - \frac{2}{\epsilon} \right) \quad (\Theta \text{ is a heaviside step function}). \quad (2.3.70c)$$

With the waves,  $\epsilon$  is not fixed so an estimate is taken of  $P_1(k)$  by averaging over  $\epsilon$ . Using the fact that the distribution of minimum values vanishes linearly as  $\epsilon$  tends to 0.

$$p_1(k) \approx \frac{1}{2} \int_0^2 \epsilon P(\epsilon, k) d\epsilon = \frac{1}{8} \int_0^2 \frac{\epsilon^2}{\sqrt{1 - \frac{k\epsilon}{2}}} \Theta \left( k - \frac{2}{\epsilon} \right) d\epsilon. \quad (2.3.71)$$

Now integrating the function (2.3.71) by parts twice yields the result

$$\frac{2}{15k^3} \left[ (3k^2 + 4k + 8)(1 - k)^{\frac{1}{2}} - 8 \right]. \quad (2.3.72)$$

Then when  $k > 1$  equation in (2.3.72), the variable  $(1 - k)^{\frac{1}{2}}$  becomes imaginary, therefore taking the real part giving the result

$$p_1(k) = -\frac{16}{15k^3}. \quad (2.3.73)$$

Using the expression of the wavenumber given in (2.3.65) the probability distribution  $P(\epsilon, k)$  is given to be,

$$P(\epsilon, k) = \frac{2}{\epsilon} \int_0^{\frac{\epsilon}{2}} \delta \left( k - \left( \frac{2}{\epsilon} - \frac{8\xi^2}{\epsilon^3} + 1 - \frac{4\xi^2}{\epsilon^2} \right) \right) d\xi \quad (2.3.74a)$$

$$P(\epsilon, k) = \frac{-\epsilon}{2 [(\epsilon + 2)^2 - k\epsilon(\epsilon + 2)]^{\frac{1}{2}}}. \quad (2.3.74b)$$

## Conclusion

The main aim of the paper analysed was to find a way of expressing superoscillations in monochromatic waves, specifically in several dimensions. As a result a large fraction of superoscillations is found in waves that are formed from the superposition of many monochromatic waves, where for 1 dimension the fraction was around 0.29, and increases to a  $\frac{1}{3}$  when dealing with 2 dimensions. In fact the fraction of superoscillations increases asymptotically to a value of 0.394 as  $D \rightarrow \infty$ . When analysing the superoscillatory region, the local wavenumber was compared to the free space wavenumber of the wave, since the local wavenumber gives a good description of the oscillatory state of the wave. If the local wavenumber was found to be greater than  $k_0$ , that is the largest wavenumber in the Fourier spectrum, then superoscillation is assumed. The paper also shows how the probability distribution of the local wavenumber  $k(r)$  decays as  $k^{-3}$  as given in equation (2.3.45). The special case where  $D = 1$  (1 dimensional case) has been analysed. Through an example given in equation (2.3.59) of a one dimensional wave, it has been proven through numerical calculations that the function does in fact superoscillate as given by equation (2.3.45), in addition the probability distribution is shown to decay proportionally to  $k^{-3}$  as predicted in (2.3.49). The ideas discussed in this section will form the foundation to the work conducted in the following chapters where the work is extended to non-monochromatic waves and specifically the two dimensional case.

## 2.4 Superoscillations in speckle patterns

### Introduction

The main purpose of this chapter is to study superoscillations in random optical speckle patterns. Speckle patterns are described as intensity patterns which are formed from the superposition of many random waves, and can be thought of as waves that were reflected or refracted from random rough surfaces. The focus here is to give an in depth description of the joint probability density function of the phase and intensity of a two dimensional wave. From this an accurate description of the superoscillations formed is provided. This section will be of great importance in understanding the special case of two dimensional superoscillations that is investigated in this thesis, as it provides a clear description of how the fraction of superoscillations changes with various wavenumber spectrums for a band-limited random function. This will be used in later chapters to analyse the effect of changing the bandwidth of the spectrum on the fraction of superoscillations. The following section is an analysis and discussion of the papers *Superoscillations in speckle patterns* by M R Dennis, A C Hamilton and J Courtial [5], as well as *Natural Superoscillation of random functions in one and more dimensions* by Mark Dennis and Jari Lindberg [4].

### Two dimensional Superoscillations

To start a wave is created from the superposition of many two dimensional waves, whose characteristics are defined as follows, the phase of the individual waves as well as their directions are taken to be independent of each other and are uniformly distributed random variables. Now a mathematical description can be shown for the condition of superoscillations in a two dimensional wave starting with a description of a wavefunction  $\psi$ ,

$$\psi = \rho e^{i\chi}, \quad (2.4.1)$$

where the intensity of the wave is characterized by  $I = \rho^2$  and the phase gradient given by  $\nabla\chi$ ; which can also be defined as the local wavenumber. Note here that  $\psi$  is dependent on position  $r = (x, y)$ . The superoscillatory condition can be given as,

$$|\chi|^2 - k_{max}^2 > 0. \quad (2.4.2)$$

Where  $k_{max}$  is the maximum wavenumber of the individual superimposed waves, or rather the maximum wavenumber in the Fourier spectrum of  $\psi$ . Since the main interest here is the superoscillations in random optical waves, it is important to investigate the regions where the wavefunction tends to zero, i.e. vanishes, and where the phase gradient of our wave is large. These are also known as optical vortices [5].

### Joint intensity and phase gradient probability

A requirement for the joint probability density function of both the intensity and the phase gradient of the wave is needed, for this Statistical Optics as well as

Gaussian statistics is used, which considers infinitely many random plane waves. The main statistical ideas used here are shown in *Statistical Optics* [40] and *Speckle Phenomena in optics* [41] by J W Goodman. A few terms need to be defined, the first is the relationship between the phase gradient and probability current of the wave. Probability current is described as the flow of probability per unit time per unit area, and is shown by the relation below (2.4.3), where  $J$  is the probability current,  $m$  is the mass and  $\nabla$  is the gradient operator,

$$J = \frac{\hbar}{2mi}(\psi^*\nabla\psi - \psi\nabla\psi^*). \quad (2.4.3)$$

The joint probability density of the intensity  $I$  and current  $J$  is going to be of great importance as it will further provide a description of the joint probability density of intensity  $I$  and the local wavenumber of  $\psi$ . Knowing  $\psi$  from equation (2.4.1) and taking  $m$ , as well as  $\hbar$  to be equal to 1 the expression can be rewritten as,

$$J = \frac{\hbar}{2mi}([\rho e^{-i\chi}(\nabla\rho e^{i\chi} + i\nabla\chi e^{i\chi})] - [\rho e^{i\chi}(\nabla\rho e^{-i\chi} - i\nabla\chi e^{-i\chi})]) \quad (2.4.4a)$$

$$= \frac{\hbar}{m}[\rho^2\nabla\chi] \quad (2.4.4b)$$

$$J = I\nabla\chi. \quad (2.4.4c)$$

It can also be shown that,

$$\psi^*\nabla\psi = a + ib \quad (2.4.5a)$$

$$\psi\nabla\psi^* = a - ib \quad (2.4.5b)$$

where  $a$  and  $b$  are arbitrary values. Therefore,

$$J = \Im[\psi^*\psi] \quad (2.4.6a)$$

$$J = \frac{[\psi^*\nabla\psi - \psi\nabla\psi^*]}{2}. \quad (2.4.6b)$$

## Random phasors

Now an analysis of the properties of random phasor sums [41] is given, these will be of great use when calculating the joint probability density function of phase and intensity. For isotropic random waves which are two dimensional, the components  $\psi$ ,  $\partial_x\psi$  and  $\partial_y\psi$ , have independent Gaussian probability density functions with variances given by equation (2.4.8) below. Note here that for every sample function  $\psi$  the amplitude of the individual waves are dependent of the wavenumber, so that each wavenumber is assigned an amplitude  $a_n$ . A wave can be expressed as,

$$\psi = \sum_n^N a_n e^{k_n r} \quad (2.4.7a)$$

$$\psi = \sum_n^N a_n (\cos\theta_n + i \sin\theta_n), \quad (2.4.7b)$$

where  $\theta$  is the phase, and  $k$  is the wavenumber. The amplitudes, which are defined as  $a_n$ , are described as complex circular Gaussian random variables. The phase of the amplitudes are given to be uniformly distributed, this will allow the wavefunction  $\psi$ , to be invariant to any translation [4]. In addition the random wave is said to be ergodic, meaning if a point  $r$  is taken and an average is found for all the amplitudes, this will be equivalent to averaging over all points  $r$ .

An important property to find would be the variance of the wave  $\psi$ , this is determined by,

$$\sigma_\psi^2 = \langle |\psi|^2 \rangle - \langle \psi \rangle^2. \quad (2.4.8a)$$

Now the average of the wavefunction is defined by,

$$\langle \psi \rangle = \langle \sum_n^N a_n [\cos \theta_n + i \sin \theta_n] \rangle. \quad (2.4.8b)$$

Taking the real part of  $\langle \psi \rangle$ ,

$$\Re \langle \psi \rangle = \langle \sum_n^N a_n \cos \theta_n \rangle = 0. \quad (2.4.8c)$$

It can be seen that the imaginary and real parts are equal to 0

$$\Im \langle \psi \rangle = \Im \langle \psi \rangle = 0. \quad (2.4.8d)$$

Now looking at the average of the absolute value of  $\psi$  which is described by,

$$\langle |\psi|^2 \rangle = \langle \sum_{n,m}^N a_n a_m^* (\cos \theta_n + i \sin \theta_n)(\cos \theta_m - i \sin \theta_m) \rangle. \quad (2.4.8e)$$

Therefore,

$$\langle |\psi|^2 \rangle = \langle \sum_{n,m}^N a_n a_m^* (\cos \theta_n \cos \theta_m - i \sin \theta_m \cos \theta_n + i \sin \theta_n \cos \theta_m + \sin \theta_n \sin \theta_m) \rangle. \quad (2.4.8f)$$

Where  $\Re$  is the real part and  $\Im$  is the imaginary part of the wave  $\psi$ . The brackets  $\langle \psi \rangle$  is the average of  $\psi$ .

Notice in equation (2.4.8), if  $n \neq m$ , then the function tends to zero as the average would be over  $\cos \theta$  and  $\sin \theta$ . Therefore only the  $n = m$  terms remain, resulting in the variance to be expressed as,

$$\langle |\psi|^2 \rangle = \langle \sum_n^N |a_n|^2 (\cos^2 \theta_n + \sin^2 \theta_n) \rangle \quad (2.4.9a)$$

$$\langle |\psi|^2 \rangle = \langle \sum_n^N |a_n|^2 \left( \left[ \frac{1}{2} + \frac{1}{2} \cos 2\theta_n \right] + \left[ \frac{1}{2} + \frac{1}{2} \sin 2\theta_n \right] \right) \rangle \quad (2.4.9b)$$

$$\langle |\psi|^2 \rangle = \sum_n^N \left\langle \frac{|a_n|^2}{2} \right\rangle + \sum_n^N \left\langle \frac{|a_n|^2}{2} \right\rangle. \quad (2.4.9c)$$

Now the mean intensity can be described by  $I_0$ ,

$$\langle |\psi|^2 \rangle = \sum_n^N \langle |a_n|^2 \rangle = I_0. \quad (2.4.9d)$$

In equation (2.4.9), it is possible to express the variance of the amplitudes by taking the power spectrum of the wave, this is defined as the distribution of power over the frequency. First taking a small infinitesimal region defined as  $\epsilon = dk$ , with a large number of wavenumbers  $k$ , the variance of the amplitude is described as,

$$\sum_{n \in \epsilon} \langle |a_n|^2 \rangle \approx S(k)dk \quad (2.4.10)$$

where  $S$  is the power spectrum of the wave  $\psi$ . The normalisation is shown to be,

$$\langle |\psi|^2 \rangle = \sum_{n,m} \langle a_n a_m^* \rangle e^{i(k_n - k_m) \cdot r} = \int S(k)dk = I_0. \quad (2.4.11)$$

Taking the derivative of the wavefunction  $\psi$  in equation (2.4.7), the variance is found to be,

$$\langle |\nabla\psi|^2 \rangle = \sum_{n,m} \langle a_n a_m^* \rangle k_n k_m e^{i(k_n - k_m) \cdot r} = \int k^2 S(k)dk \equiv k_2 I_0. \quad (2.4.12)$$

$k_2$  is the second moment of the spectrum and is normalized by the mean intensity  $I_0$  found in equation (2.4.11). If the wave function is expressed in terms of the real and imaginary part, considering that the real and imaginary part are independent random Gaussian functions which are isotropic and identically distributed, the variance of the real and imaginary part can be expressed as,

$$\psi(r) = \psi_1 + i\psi_2 \quad (2.4.13a)$$

$$\sigma_{\psi_1}^2 = \langle |\psi_1|^2 \rangle - \langle \psi_1 \rangle^2 \quad (2.4.13b)$$

$$\langle \psi_1 \rangle^2 = \langle \sum_n^N a_n \cos(\theta_n) \rangle^2 = 0 \quad (2.4.13c)$$

$$\langle \psi_1^2 \rangle = \langle \sum_{n,m}^N a_n a_m \cos(\theta_n) \cos(\theta_m) \rangle \quad (2.4.13d)$$

$$= \langle \sum_{n=m}^N a_n^2 \cos^2(\theta_n) \rangle \quad (2.4.13e)$$

$$= \langle \sum_{n=m}^N a_n^2 \left( \frac{1}{2} + \cos(2\theta) \right) \rangle \quad (2.4.13f)$$

$$\langle \psi_1^2 \rangle = \langle \psi_2^2 \rangle = \frac{I_0}{2}. \quad (2.4.13g)$$

Here the real part is expressed as  $\psi_1 = \sum_{n=m} a_n \cos_n(\theta)$  and the imaginary part  $\psi_2 = \sum_{n=m} a_n \sin_n(\theta)$ . Now taking the partial derivative of both the real and imaginary part, which are also independent Gaussian random variables,

$$\nabla\psi = \nabla[\sum_n^N a_n [\cos(\theta_n) + i \sin(\theta_n)]] \quad (2.4.14a)$$

$$= \sum_n^N a_n [-\sin(\theta_n) + i \cos(\theta_n)] \nabla\theta_n. \quad (2.4.14b)$$

Now finding the variance of both the real and imaginary part,

$$\sigma_{\Re}^2 = \langle |\Re \nabla \psi|^2 \rangle - \langle \Re \nabla \psi \rangle^2 \quad (2.4.15a)$$

$$\langle \Re \psi \rangle = 0 \quad (2.4.15b)$$

$$\langle |\Re \nabla \psi|^2 \rangle = \langle \sum_n^N \nabla \theta^2 a_n^2 \sin^2(\theta_n) \rangle \quad (2.4.15c)$$

$$= \frac{I_0 k_2}{2} = \langle |\Im \nabla \psi|^2 \rangle. \quad (2.4.15d)$$

Defining  $k_2$  as the second moment of  $k$  with respect to the power spectrum, given that  $k$  is defined as the gradient of the phase ( $\nabla \theta$ ).

## Calculations of joint probability density function in two dimensions of both the phase and intensity

The following will show the derivation of the joint intensity and phase gradient probability density function, for this we follow closely the derivations in Ref [4]. First a restatement that the real part and imaginary part of  $\psi$  are real independent random Gaussian functions, which are identically distributed and isotropic, and have variances given by (2.4.13). In addition the partial derivatives of the real part and imaginary part of  $\psi$  are also Gaussian random variables, with variances given by (2.4.15). Then an expression for the joint probability distribution for each component is given as follows,

$$p(\psi_1, \psi_2) = \frac{1}{\sqrt{2\pi\sigma_{\psi_1}^2}} \exp\left(-\frac{\psi_1^2}{2\sigma_{\psi_1}^2}\right) \cdot \frac{1}{\sqrt{2\pi\sigma_{\psi_2}^2}} \exp\left(-\frac{\psi_2^2}{2\sigma_{\psi_2}^2}\right) \quad (2.4.16a)$$

$$p(\psi_1, \psi_2) = \frac{1}{\pi I_0} \exp\left(-\frac{\psi_1^2 + \psi_2^2}{I_0}\right). \quad (2.4.16b)$$

Note the use of the expression for the variances of the real and imaginary part of our wave, from (2.4.13). Finding the expression for the probability density for the partial derivatives of the real and imaginary part can be seen to be,

$$p(\nabla \psi_1, \nabla \psi_2) = \frac{1}{\sqrt{2\pi\sigma_{\nabla \psi_1}^2}} \exp\left(-\frac{\nabla \psi_1^2}{2\sigma_{\nabla \psi_1}^2}\right) \cdot \frac{1}{\sqrt{2\pi\sigma_{\nabla \psi_2}^2}} \exp\left(-\frac{\nabla \psi_2^2}{2\sigma_{\nabla \psi_2}^2}\right) \quad (2.4.17a)$$

$$p(\nabla \psi_1, \nabla \psi_2) = \left(\frac{D}{\pi k_2 I_0}\right)^D \exp\left(-D \frac{\nabla \psi_1^2 + \nabla \psi_2^2}{k_2 I_0}\right). \quad (2.4.17b)$$

In equations (2.4.17),  $D$  is the number of dimensions in which the partial derivative is taken, so for the special case of two dimension,  $D = 2$  as shown in [4]. Now writing the joint probability distribution of (2.4.16) and (2.4.17), it is found that,

$$p(\psi_1, \psi_2, \nabla \psi_1, \nabla \psi_2) = p(\psi_1, \psi_2) \cdot p(\nabla \psi_1, \nabla \psi_2) \quad (2.4.18a)$$

$$p(\psi_1, \psi_2, \nabla \psi_1, \nabla \psi_2) = \frac{1}{\pi I_0} \left(\frac{D}{\pi k_2 I_0}\right)^D \exp\left(-\frac{\psi_1^2 + \psi_2^2}{I_0} - D \frac{\nabla \psi_1^2 + \nabla \psi_2^2}{k_2 I_0}\right). \quad (2.4.18b)$$

Given the expression for the distribution in (2.4.18), the density function for intensity and phase gradient is found by first taking the probability density of intensity and current density, then using the expression that  $J = I\nabla\chi$  in (2.4.4) and (2.4.6). The density function can be expressed as an average Dirac delta function.

$$P(I, J) = \langle \delta(I - (\psi_1^2 + \psi_2^2)) \rangle \cdot \langle \delta^D(J - (\psi_1\nabla\psi_2 - \psi_2\nabla\psi_1)) \rangle. \quad (2.4.19)$$

Analysing the expression (2.4.19), a value for  $I$  is found for each  $\psi_1$  and  $\psi_2$  random variables. Using Fourier inversion,

$$P(s) = \frac{1}{\sqrt{2\pi}} \int e^{-isI} \langle \delta(I - (\psi_1^2 + \psi_2^2)) \rangle dI \quad (2.4.20a)$$

$$P(I) = \frac{1}{2\pi} \int e^{isI} \langle e^{-is(\psi_1^2 + \psi_2^2)} \rangle ds \quad (2.4.20b)$$

$$P(t) = \left(\frac{1}{\sqrt{2\pi}}\right)^D \int e^{-itJ} \langle \delta(J - (\psi_1\nabla\psi_2 - \psi_2\nabla\psi_1)) \rangle d^D J \quad (2.4.21a)$$

$$P(J) = \left(\frac{1}{2\pi}\right)^D \int e^{itJ} \langle e^{-it(\psi_1\nabla\psi_2 - \psi_2\nabla\psi_1)} \rangle d^D t. \quad (2.4.21b)$$

$s$  and  $t$  here are arbitrary variables. Rewriting the joint probability density,

$$P(I, J) = \left(\frac{1}{2\pi}\right)^{D+1} \int e^{isI+itJ} \langle \exp(-is(\psi_1^2 + \psi_2^2) - it(\psi_1\nabla\psi_2 - \psi_2\nabla\psi_1)) \rangle d^D t. \quad (2.4.22)$$

It is known previously, that the Gaussian average with zero mean (2.3.25) is expressed as  $\langle \exp(-itx) \rangle = e^{-\frac{\sigma^2 t^2}{2}}$ , therefore the average in (2.4.22) is expressed as,

$$\langle e^{-it\psi_1\nabla\psi_2} \rangle = e^{-\frac{k_2 I_0}{2} \frac{t^2}{2} \psi_1} = e^{-\frac{k_2 I_0 t^2 \psi_1}{4}} \quad (2.4.23a)$$

$$\langle e^{it\psi_2\nabla\psi_1} \rangle = e^{-\frac{k_2 I_0}{2} \frac{t^2}{2} \psi_2} = e^{-\frac{k_2 I_0 t^2 \psi_2}{4}} \quad (2.4.23b)$$

$$\langle \exp(-it(\psi_1\nabla\psi_2 - \psi_2\nabla\psi_1)) \rangle = e^{-\frac{k_2 I_0 t^2}{4}(\psi_1 + \psi_2)}. \quad (2.4.23c)$$

Here an average is taken for  $\nabla\psi_1, \nabla\psi_2$  first. Then averaging over the real and imaginary parts  $\psi_1, \psi_2$ ,

$$\langle e^{-is(\psi_1^2) - \frac{k_2 I_0 t^2 \psi_1^2}{4D}} \rangle = \int_{-\infty}^{\infty} e^{-(is + \frac{I_0 k_2 t^2}{4D})\psi_1^2} \cdot \frac{1}{\sqrt{2\pi} \frac{I_0}{2}} e^{\frac{\psi_1^2}{I_0}} d\psi_1 \quad (2.4.24a)$$

$$= \int_{-\infty}^{\infty} \frac{1}{\sqrt{2\pi} \frac{I_0}{2}} e^{-(is + \frac{I_0 k_2 t^2}{4D} + \frac{1}{I_0})\psi_1} d\psi_1 \quad (2.4.24b)$$

$$= \frac{1}{\sqrt{I_0(is + \frac{I_0 k_2 t^2}{4D} + \frac{1}{I_0})}}. \quad (2.4.24c)$$

where the relation (2.4.25) shown below, is used.

$$\int_{-\infty}^{\infty} e^{-ax^2} = \sqrt{\frac{\pi}{a}}. \quad (2.4.25)$$

Now squaring the expression (2.4.24) to find the averages for both the real and imaginary parts which is substituted back into equation (2.4.22),

$$P(I, J) = \left(\frac{1}{2\pi}\right)^{D+1} \int_{-\infty}^{\infty} \frac{1}{1 + iI_0s + \frac{t^2 k_2 I_0^2}{4D}} e^{isI + itJ} ds d^D t. \quad (2.4.26)$$

The integral above can be solved by using the fact that there is a simple pole in  $s$ , first taking,

$$P(I) = \left(\frac{1}{2\pi}\right)^{D+1} \int_{-\infty}^{\infty} \frac{e^{isI + itJ}}{a + ibs} ds \quad (2.4.27a)$$

$$= \frac{1}{(2\pi)^{D+1} ib} \int \frac{e^{isI + itJ}}{\frac{a}{ib} + s} ds, \quad (2.4.27b)$$

where  $a$  and  $b$  are expressed as,

$$a = 1 + \frac{t^2 k_2 I_0^2}{4D} \quad (2.4.28a)$$

$$b = I_0. \quad (2.4.28b)$$

The function is seen to have a singularity at  $s = i\frac{a}{b}$ , therefore finding the residue and the integral,

$$R\left(i\frac{a}{b}\right) = \frac{1}{(2\pi)^{D+1} ib} \int e^{isI + itJ} ds \quad (2.4.29)$$

$$P(I) = \frac{2\pi i}{(2\pi)^{D+1} ib} \int e^{itJ + (-\frac{a}{b})I} d^D t. \quad (2.4.30)$$

Substituting back in the values for  $a$  and  $b$  from (2.4.28),

$$P(I, J) = \frac{1}{(2\pi)^D I_0} \int e^{-itJ - \frac{I}{I_0} \left(1 + \frac{t^2 k_2 I_0^2}{4D}\right)} d^D t. \quad (2.4.31)$$

Using the relation,

$$e^{-\frac{x^2}{2a}} = \sqrt{\frac{a}{2\pi}} \int_{-\infty}^{\infty} e^{ixy - y^2 \frac{a}{2}} dy \quad (2.4.32)$$

We can show that,

$$P(I, J) = \frac{1}{I_0} \left(\frac{D}{\pi k_2 I_0 I}\right)^{\frac{D}{2}} \exp\left(-\frac{I}{I_0} - \frac{DJ^2}{k_2 I_0 I}\right). \quad (2.4.33)$$

By isotropy of the random function,  $J$  is isotropically distributed in  $D$  dimensions. The joint probability distribution for  $I$  and  $j = |J|$  is found by integrating over all directions in  $D$  dimensions,

$$P(I, j) dI dj = P(I, J) \Omega_D j^{D-1} dI dJ. \quad (2.4.34)$$

Here  $\Omega = \frac{2\pi^{\frac{D}{2}}}{\Gamma(\frac{D}{2})}$ , as seen before in [3], which is the surface area of unit sphere in  $D$  dimensions.

$$P(I, j) = \frac{1}{I_0} \left( \frac{D}{\pi k_2 I_0 I} \right)^{\frac{D}{2}} e^{-\frac{I}{I_0} - \frac{D j^2}{k_2 I_0 I}} \frac{2\pi^{\frac{D}{2}}}{\Gamma(\frac{D}{2})} J^{D-1} \quad (2.4.35)$$

To find the probability density of the intensity  $I$  and the phase gradient  $\nabla\chi$ , first taking the Jacobian transformation of the function in (2.4.35) and specifically taking the result for  $D = 2$ , as this will be of great importance in the following chapters. This gives the result,

$$P(I, \nabla\chi) = \frac{I}{I_0} \left( \frac{2}{\pi k_2 I_0 I} \right) e^{-\frac{I}{I_0} - \frac{2I^2 \nabla\chi^2}{k_2 I_0 I}} 2\pi(I \nabla\chi). \quad (2.4.36)$$

Here the Jacobian transformation is used to obtain an expression in terms of  $I$  and  $\nabla\chi$ .

$$P(I, \nabla\chi) = \frac{4}{I_0^2 k_2} \nabla\chi I e^{-I \left( \frac{k_2 + 2\nabla\chi^2}{k_2 I_0} \right)} \quad (2.4.37a)$$

$$= \frac{4\nabla\chi}{I_0^2 k_2} \int_0^\infty I e^{-aI} dI \quad (2.4.37b)$$

$$= \frac{4\nabla\chi}{I_0^2 k_2} \left[ e^{-aI} \left( -\frac{I k_2 I_0}{k_2 + 2\nabla\chi^2} - \frac{k_2^2 I_0^2}{(k_2 + 2\nabla\chi^2)^2} \right) \right]_0^\infty \quad (2.4.37c)$$

$$= \frac{4k_2 \nabla\chi}{(k_2 + 2\nabla\chi^2)^2} \quad (2.4.37d)$$

$$P(\nabla\chi) = \frac{k_2 \nabla\chi}{\left( \frac{k_2}{2} + \nabla\chi^2 \right)^2}. \quad (2.4.37e)$$

Notice how equations (2.4.37) is of the same form as given in [3], shown here by equation 2.3.45, where  $k_2 = k_{max}^2 = k_0^2$  for the monochromatic case. However here  $k_2$  (spectral moment) is considered to have a distribution that depends on  $k_{max}$ , which is the maximum wavenumber in Fourier space. Now as before it can be shown that the fraction of superoscillations is given by,

$$f_{super} = \int_{k_{max}}^\infty P(\nabla\chi) d\nabla\chi \quad (2.4.38a)$$

$$= \int_{k_{max}}^\infty \frac{k_2 \nabla\chi}{\left( \nabla\chi^2 + \frac{k_2}{2} \right)^2} d\nabla\chi. \quad (2.4.38b)$$

Showing  $P(\nabla\chi)$  as,

$$P(\nabla\chi) = \frac{-k_2}{2} \frac{d\left( \nabla\chi^2 + \frac{k_2}{2} \right)^{-1}}{d\nabla\chi}. \quad (2.4.39)$$

Therefore for equation (2.4.38),

$$f_{super} = -\frac{k_2}{2} \left( \frac{1}{k_{max}^2 + \frac{k_2}{2}} \right) \quad (2.4.40a)$$

$$= -\frac{k_2}{2k_{max}^2 \left( 1 + \frac{k_2}{2k_{max}^2} \right)} \quad (2.4.40b)$$

$$= 1 - \frac{1}{1 + \frac{k_2}{2k_{max}^2}}. \quad (2.4.40c)$$

An expression for the probability density function can be provided for intensity as shown in [5] and [4], by integrating over all local wavevectors (phase gradients), the papers also discuss the relationship between the regions of intensity and phase gradient, however this will not be required for the remaining chapters. This expression is given by,

$$P(I) = \frac{\exp\left(\frac{-I}{I_0}\right)}{I_0}. \quad (2.4.41)$$

Usually it is possible to take a specific spectrum for a band-limited random function, for example a spectrum that is a ‘top hat’ spectrum with steps of 0 to  $k_{max}$ . The example given in paper [4] for a 1 dimensional random function, with  $k_2$  given as follows,

$$k_2 = \frac{1}{k_{max}} \int_0^{k_{max}} k^2 dk \quad (2.4.42a)$$

$$= \frac{k_{max}^2}{3}. \quad (2.4.42b)$$

However if the ‘top hat spectrum’ (disk spectrum for a two dimensional) is required then it is essential to change into polar coordinates, as shown below,

$$k_2 = \frac{1}{\pi k_{max}^2} \int_0^{k_{max}} \int_0^{2\pi} k \cdot k^2 dk d\theta \quad (2.4.43a)$$

$$k_2 = \frac{k_{max}^2}{2}. \quad (2.4.43b)$$

Looking at a different spectrum, and specifically of most importance for later discussions, is the annular spectrum. For this spectrum taking the limits to tend from  $k_{max}(1 - \delta)$  to an upper limit of  $k_{max}$ . Note here that  $0 \leq \delta \leq 1$ . If the specific case for the 2 dimensional function is taken as shown in [4], [5] then we

acquire,

$$k_2 = \frac{1}{\pi k_{max}^2 - \pi(k_{max}(1-\delta))^2} \int_0^{2\pi} \int_{k_{max}(1-\delta)}^{k_{max}} k \cdot k^2 dk d\theta \quad (2.4.44a)$$

$$= \frac{1}{2k_{max}^2(1-(1-\delta)^2)} (k_{max}^4 - k_{max}^4(1-\delta)^4) \quad (2.4.44b)$$

$$= \frac{k_{max}^2}{2(1-(1-\delta)^2)} [1 - (1-\delta)^4] \quad (2.4.44c)$$

$$= \frac{k_{max}^2}{2(1-(1-\delta)^2)} [4 - 6\delta^2 + 4\delta^3 - \delta^4] \quad (2.4.44d)$$

$$k_2 = \frac{k_{max}^2}{2} (2 - 2\delta + \delta^2). \quad (2.4.44e)$$

Now from the expression for the fraction of superoscillations in (2.4.40), the fraction is now given as,

$$f_{super} = 1 - \frac{1}{1 + \frac{k_2}{2k_{max}}} \quad (2.4.45a)$$

$$f_{super} = 1 - \frac{1}{1 + \frac{(2-2\delta+\delta^2)}{4}} \quad (2.4.45b)$$

$$f_{super} = 1 - \frac{4}{6 - 2\delta + \delta^2}. \quad (2.4.45c)$$

Notice that the expression in (2.4.45) for the fraction of superoscillation tends to  $\frac{1}{5}$  of the plane in the limit that  $\delta \rightarrow 1$ , therefore giving the disk spectrum that was found in (2.4.43). However as  $\delta \rightarrow 0$  a value of  $\frac{1}{3}$  is given, which is identical to the monochromatic case. The expression for the annular spectrum will be of great importance in the following chapter where a discussion will be made of the unusual result obtained from changing the band-limit of the spectrum for the individual superimposing waves.

## Conclusion

At the beginning of this section an analysis of the specific properties of superoscillations in speckle patterns was made, using Gaussian statistics and specific statistical optics. Through analysing the probability density of both intensity and probability current of two dimensional waves, a joint probability density was obtained for both intensity and the phase gradient (local wavenumber) of our wave as seen by equation (2.4.36). This in turn gave the probability density of the phase gradient (2.4.39). From there an expression for the fraction of superoscillations was given through the integration of the probability density function of local wavenumber over all values of  $k$  that are larger than the maximum wavenumber in the Fourier components  $k > k_{max}$ , giving rise to the function defined by equation (2.4.40). Following this an expression for the fraction of superoscillation was provided given that  $k_2$  (second moment  $k$  with respect to the power spectrum) has a 'top hat' spectrum (2.4.45). This finally provided the result that the fraction of superoscillations tends to  $\frac{1}{5}$  when taking a larger bandwidths, in other words when taking the value of  $\delta \rightarrow 1$  in equation (2.4.45). This is a rather interesting result that is discussed further in the following chapter, where an investigation into the effects of changing the band-limit on the fraction of superoscillations is conducted. The results found in the following chapters is compared to the theoretical values found in this section and previous sections, specifically the fraction of superoscillations for two dimensional non-monochromatic waves.

## Chapter 3

# Superoscillations in non-monochromatic waves in 2-Dimensions

---

### Introduction

The main purpose of this chapter is to further investigate the results obtained from [5], [4] and [3] which are discussed in the previous chapters. Specifically through analysing the effects of varying the bandwidth, as well as the number of sources which are superimposing, on the fractional area that exhibit superoscillatory behaviour. This will be done by numerically calculating the local wavenumber of our sample wave at every point in our region, which provides us with a good discription of the oscillatory nature of the wave. A comparison is then made with the maximum wavenumber of the individual waves in the Fourier spectrum.

A sample wavefunction  $\psi(x, y)$  here will be represented through the superposition of complex plane waves of a particular size  $N$ , where each individual wave is assigned a random amplitude  $a(n)$  and wavevector  $k(n)$ , both are independent random variables as shown in equation (3.0.1), below. The wavenumbers are given to be real and the amplitudes  $a(n)$  are described as complex circular random variables [4] [40], with their imaginary and real component also being independent of one another but have the same distribution. A specific bandwidth is chosen to start with, so that the maximum wavenumber contributing is given by  $k_{max}$ . In the following study two cases have been taken into consideration, the first is the analysis of the average fractional area; of a specified region, that is superoscillating given that a particular bandwidth is chosen with minimum and maximum wavenumbers given by  $k_{min}$  and  $k_{max}$  respectively. Now for one sample wave taken  $\psi(x, y)$ , the wavefunctions's components are randomly assigned a wavenumber  $k_n$  so that they can be be of any value within the band-limits provided. Then it can be seen that every sample function  $\psi(x, y)$  taken will vary in bandwidth such that the maximum and minimum wavenumber in the wave's spectrum will change from one sample function to another. The fraction of superoscillations for every sample wave  $\psi(x, y)$  is found by analysing the local wavenumber  $K$  at each point in a specific area given by  $x, y$ , and comparing it to the maximum wavenumber

in that sample function. Note here we define the local wavenumber as  $K$  in order to distinguish it from the Fourier components defined by  $k_n$  and the minimum and maximum wavenumbers ( $k_{min}$  and  $k_{max}$ ). If the local wavenumber is given to be larger than the maximum wavenumber in the wave's spectrum, then it is said that the wave exhibits superoscillations at that point. This is done for around  $10^5$  samples, then an average fraction of superoscillations is given. The effect of changing the bandwidth  $B$  and the number of sources  $N$  on the average fraction is also explored, this is done for several minimum wavenumbers  $k_{min}$ .

For the second case investigated here, the average fraction of superoscillations found for every sample wave is given as before, however the bandwidth is fixed for each sample wave  $\psi(x, y)$  and does not vary from one sample wave to another, so that the minimum wavenumber and maximum wavenumber of each sample wave is constant. Again the average fraction of superoscillations is found as before and a comparison between the two cases is provided. The main codes used can be found in Appendix A: MATLAB codes.

## Superoscillations in 2-Dimensional waves

First a definition for a wave is given as,

$$\psi(x, y) = \sum_{n=1}^N a_n \exp(ik_n \cdot r(x, y)) \quad (3.0.1)$$

where  $a_n$  is a random complex number that is independent of  $k$ , and can be described by,

$$a_n = \alpha e^{i\phi_n}. \quad (3.0.2)$$

Here  $\alpha$  is a random independent variable and is real. Now the phase  $\phi_n$  is taken to be a random independent variable and uniformly distributed between  $0 \leq \phi_n \leq 2\pi$ , such that the function  $\psi$  is statistically invariant to translation. Furthermore the number of sources  $N$  is taken to be  $N \gg 1$ . The expression (3.0.1) has wavenumbers in  $x$  and  $y$  given by,

$$k_{n_x} = k_n \cos((n-1)\theta) \quad (3.0.3a)$$

$$k_{n_y} = k_n \sin((n-1)\theta) \quad (3.0.3b)$$

where  $\theta = \frac{2\pi}{N}$ . this creates waves directed from different angles each with a wavenumber and amplitude that are chosen at random. This ensures that the waves are equally spaced and are of the same direction with each sample function. The expression (3.0.1) can then be written as,

$$\psi(x, y) = \sum_{n=1}^N a_n e^{i(k_{n_x} \cdot x + k_{n_y} \cdot y)}. \quad (3.0.4)$$

Now looking for regions where the wave oscillates faster than its Fourier components, a good measurement would be to analyse the local wavenumber of the function, as this gives the rate at which the function's phase is changing. Therefore

the local wavenumbers  $(K_x, K_y)$  is given by,

$$K_x = \Im\left[\frac{\partial \ln(\psi_{x,y})}{\partial x}\right] \quad (3.0.5a)$$

$$K_y = \Im\left[\frac{\partial \ln(\psi_{x,y})}{\partial y}\right] \quad (3.0.5b)$$

$$K = \sqrt{K_x^2 + K_y^2} \quad (3.0.5c)$$

where  $K$  is the local wavenumber of the function  $\psi(x, y)$ . The local wavenumber is calculated over all  $x$  and  $y$  values. The fraction of superoscillations is given by finding the points where  $|K| > k_{max}$ , which is the largest maximum wavenumber in the spectrum, this is done for every sample wave. A numerical computation of around  $1.10^5$  samples of the calculation is taken and an average of the fraction superoscillating is then given.

### First Case: Random Bandwidths

Provided in this section is a discussion of the effects of changing the minimum wavevector  $k_{min}$ , alongside the change in bandwidth  $B$  on the fraction of superoscillations, where  $B = k_{max} - k_{min}$ . The effect of increasing or decreasing the number of sources superimposing is also analysed and discussed. Noting as before that the wavenumber  $k_n$  of the individual waves are chosen at random so that the bandwidth for every sample function  $\psi$  in equation (3.0.1) is not fixed. This is closely related to what has been discussed in [5] for an annular spectrum, however the main focus here will be on the bandwidth rather than the scaled thickness delta as given by equation (2.4.45).

An interesting observation which will be discussed is that when the band-width  $B \ll 1$ , the average superoscillatory fraction tends to a third. This indicates that the closer the waves are in wavenumber the closer the resemblance is to that of the monochromatic case as seen in [3]. From intuition this result is plausible, however as the bandwidth gets larger, the number of superoscillations drops rapidly to a constant value, indicating that there is always a fraction of superoscillations present in the region taken. This is as discussed in paper [5] for a disk spectrum where the fraction of superoscillation is given to be around  $\frac{1}{5}$  in the limit that the bandwidth tends to increase. However a rather interesting observation given in the calculations below shows that the fraction of superoscillations is much lower than what was predicted. Graphs (3.1, 3.2) shows the relationship between the average fraction superoscillating and the bandwidth  $B$ .

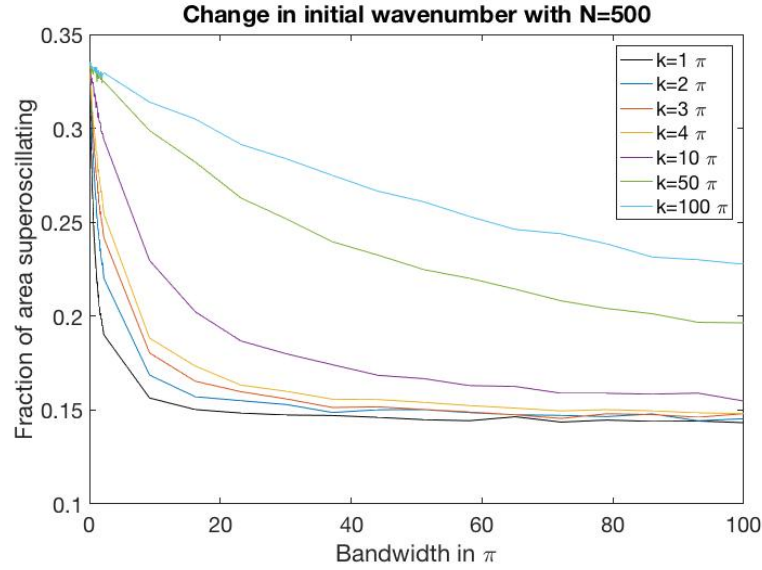


Figure 3.1: Relationship between bandwidth; measured in multiples of  $\pi$ , and average fraction of superoscillations. With  $N=500$  waves and  $k_{min} = 1\pi, 2\pi, 3\pi, 4\pi, 10\pi, 50\pi, 100\pi$ .  $k_{min} = 1\pi$  in black and  $k_{min} = 100\pi$  in cyan. This is done using samples of size  $10^5$ .

The first observation made when looking at Figure 3.1, is that for all  $k_{min}$  values the fraction of superoscillations is a  $\frac{1}{3}$  for bandwidth of  $0\pi$ , which is described as the monochromatic case. In addition, the fraction of superoscillations is shown to decrease with increase in bandwidth for all  $k_{min}$ , however it can be seen that increasing the minimum wavenumber  $k_{min}$  of our spectrum, causes the rate at which the fraction falls to decrease with every bandwidth. For example when the minimum wavenumber is set to  $k_{min} = 1\pi$  the fraction, at low bandwidths, falls at a much faster rate compared to a higher  $k_{min}$  value such as  $k_{min} = 100\pi$ , which decreases at the slowest rate compared to all other values. Furthermore, It is clear that all the values tends to the same constant fraction of superoscillations of approximately 0.15 of the plane, however it can be seen that for larger  $k_{min}$  values the average fraction of superoscillations asymptotically tend to this constant at much larger bandwidths. Then it can be said that the ratio between the bandwidth and the minimum wavenumber affects the average fraction of superoscillations present in our region. As an example if  $k_{min} \rightarrow \infty$  then it can be seen that the average fraction would be constant and of a value  $\approx \frac{1}{3}$ , then an increase in bandwidth of  $100\pi$  would be insignificant when compared to the value of  $k_{min}$ . This leads to interesting point made later in the chapter when analysing the relationship between the change in wavelength and the bandwidth. For these graphs it was of great importance that when calculating the local wavenumber the use of a small value for  $dx$  and  $dy$  in the expression (3.0.5) was taken in the code, as this ensures that all wavelengths are taken into consideration.

An investigation was also carried out in to the effects of changing the number of sources that are superimposing in every sample. Here a minimum wavevector

value  $k_{min} = 1\pi$  has been assigned, so that in every sample the smallest wavevector in the Fourier spectrum cannot have a value lower than this limit. Calculations for several  $N$  values where  $N = 5, 6, 7, 8, 9, 10, 50$  has been found. The results are shown in figure 3.2.

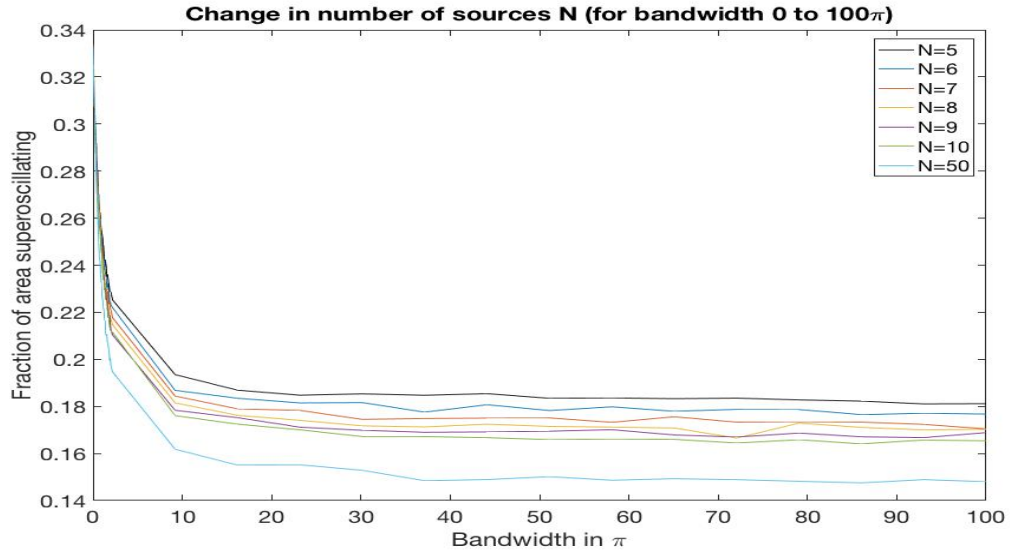


Figure 3.2: Showing the relationship between bandwidth and fraction of superoscillations, repeated for specific number of sources  $N$ . Here the minimum wavenumber is given to be  $k_{min} = 1\pi$ , and the number of sources are  $N = 5, 6, 7, 8, 9, 10, 50$ .

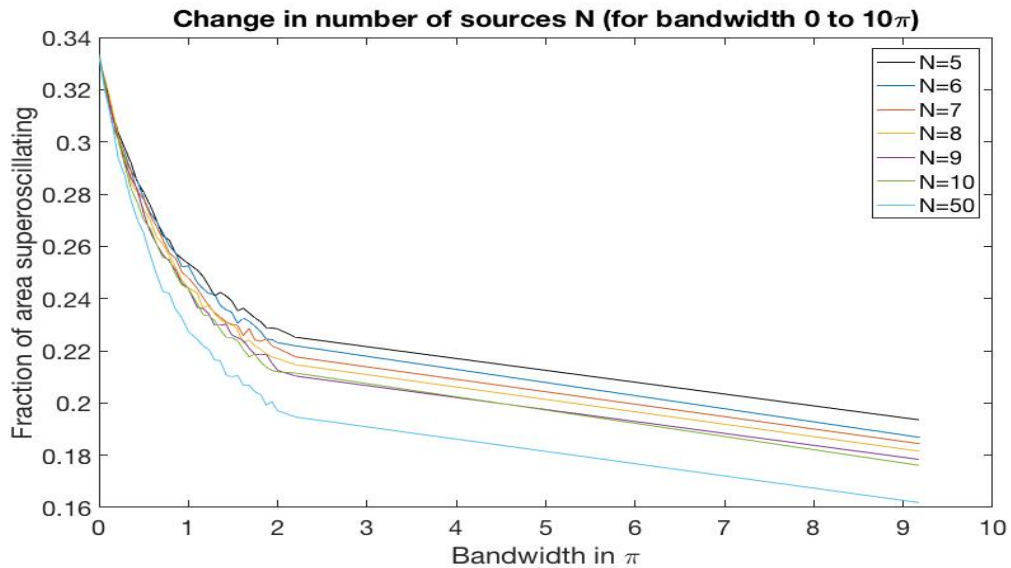


Figure 3.3: Showing the relationship between bandwidth and fraction of superoscillations repeated for a specific number of sources  $N$ . Where  $N = 5, 6, 7, 8, 9, 10, 50$  waves, and  $k_{min} = 1\pi$  (figure 3.2 zoomed in at bandwidth from 0 to  $10\pi$ ).

Through the analysis of figures 3.2 and 3.3, it can be seen that at very low bandwidths the fraction of superoscillation is a third for any value of  $N$ . However

as the bandwidth increases, and taking large number of sources the fraction tends to its lowest value. With  $N = 5$  the fraction of superoscillations tends to a constant value slightly smaller than  $\frac{1}{5}$  and is given to be approximately 0.18. Noticing that the results shown in both figures 3.2 and 3.3 contradict the results as given by [4] [5] in equation (2.4.45), where the effect of changing bandwidth on the fraction is illustrated by figure 3.6, as the average superoscillatory fraction shown is much smaller than  $\frac{1}{5}$  with large bandwidth. Now it is of great importance to find an expression for the probability density function of  $k(r)$  (local wavenumber), as this will provide a mathematical description of the fraction of superoscillations. Note the new notation for local wavenumber which is now given by  $k(r)$  For the specific case here the probability density is taken to be,

$$P(k) = \frac{\alpha^2 k_0^2 k}{\left(\frac{\alpha^2 k_0^2}{2} + k^2\right)^2}. \quad (3.0.6)$$

Here  $k_0$  is the maximum wavenumber in the bandwidth, and  $\alpha^2$  is a parameter to be found. This is done to get an approximate expression for the average fraction superoscillating that fits the results. It is seen that the expression in (3.0.6) is of the same form as (2.3.45) found in paper [3], but with an extra parameter  $\alpha$  multiplied by the maximum wavenumber  $k_0$ . As before to find the fraction superoscillating one might use the expression given by,

$$f_{super} = \int_{k_0}^{\infty} \frac{\alpha^2 k_0^2 k}{\left(\frac{\alpha^2 k_0^2}{2} + k^2\right)^2} dk \quad (3.0.7a)$$

$$= \int_{k_0}^{\infty} \frac{1}{2} \frac{1}{k^2 + \frac{\alpha^2 k_0^2}{2}} \frac{1}{dk} dk \quad (3.0.7b)$$

$$f_{super} = \frac{\alpha^2}{\alpha^2 + 2}. \quad (3.0.7c)$$

For the case of monochromatic waves  $\alpha^2 = 1$ , gives the superoscillatory region to be  $\frac{1}{3}$ . In the attempt to find an expression analytically for the results obtained in figures 3.1 and 3.2,  $\alpha^2$  is first defined as,

$$\alpha^2 \approx \exp\left(-a \frac{B}{k_{min} + B}\right). \quad (3.0.8)$$

As this expression of  $\alpha$  best fits the results found in figure 3.1, where  $B$  is the bandwidth,  $k_{min}$  smallest wavenumber allowed and  $a$  is a constant to be found. The following shows the results obtained by taking the expression of fraction to be (3.0.7), with alpha given by the expression (3.0.8) above,

$$f = \frac{e^{-a \frac{B}{B+k_{min}}}}{e^{-a \frac{B}{B+k_{min}}} + 2}. \quad (3.0.9)$$

The Plot for the average fraction superoscillating against bandwidth, with the best fit expression (3.0.9) is shown in figure 3.4 and 3.5, analysing the results

for several values of  $N$  ( $N = 5, 6, 7, 8, 9, 10, 50, 500$ ), the values for  $a$  has been calculated and shown in table 3.1 for several  $k_{min}$  values.

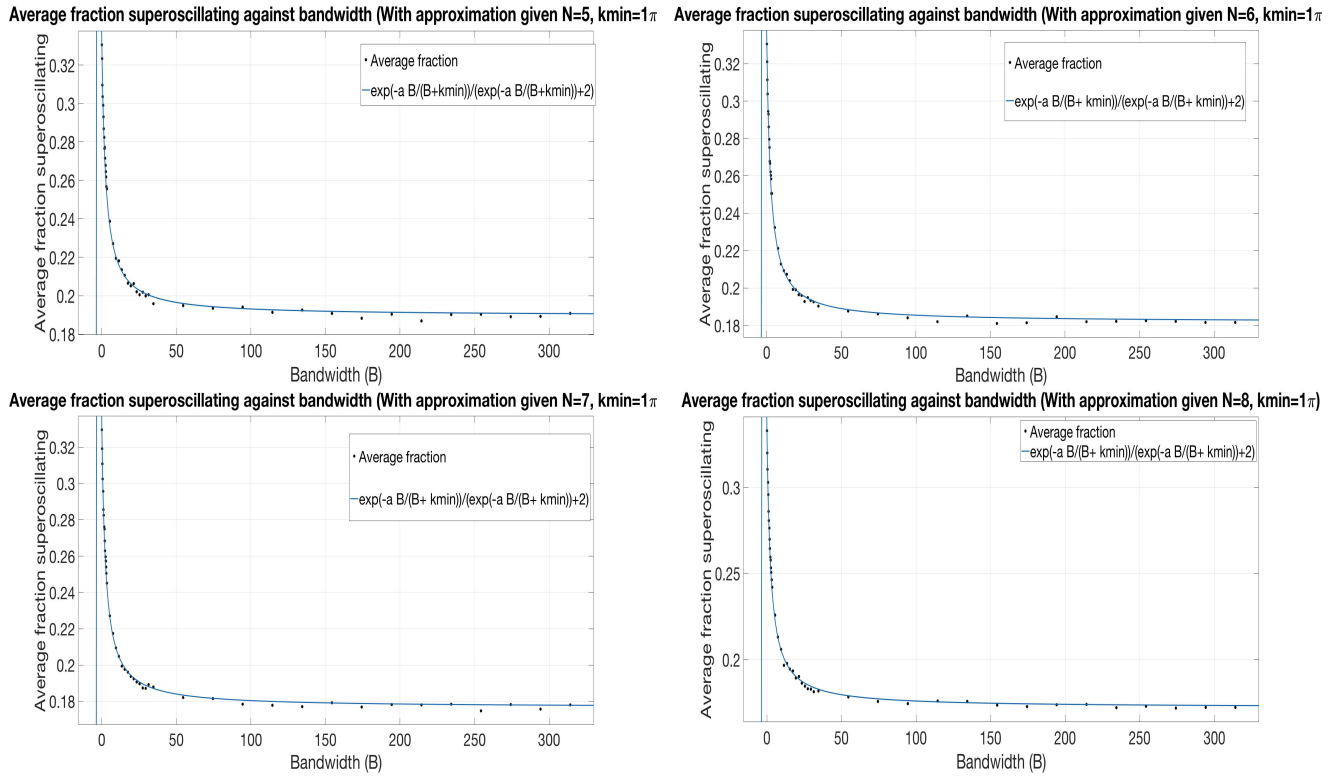


Figure 3.4: Showing the average fraction against bandwidth for  $k_{min} = 1\pi$  and  $N=5, 6, 7, 8$ . The approximated curve is also given with the use of the expression given by (3.0.16) and (3.0.7). The points plotted are the average fraction superoscillating calculated.

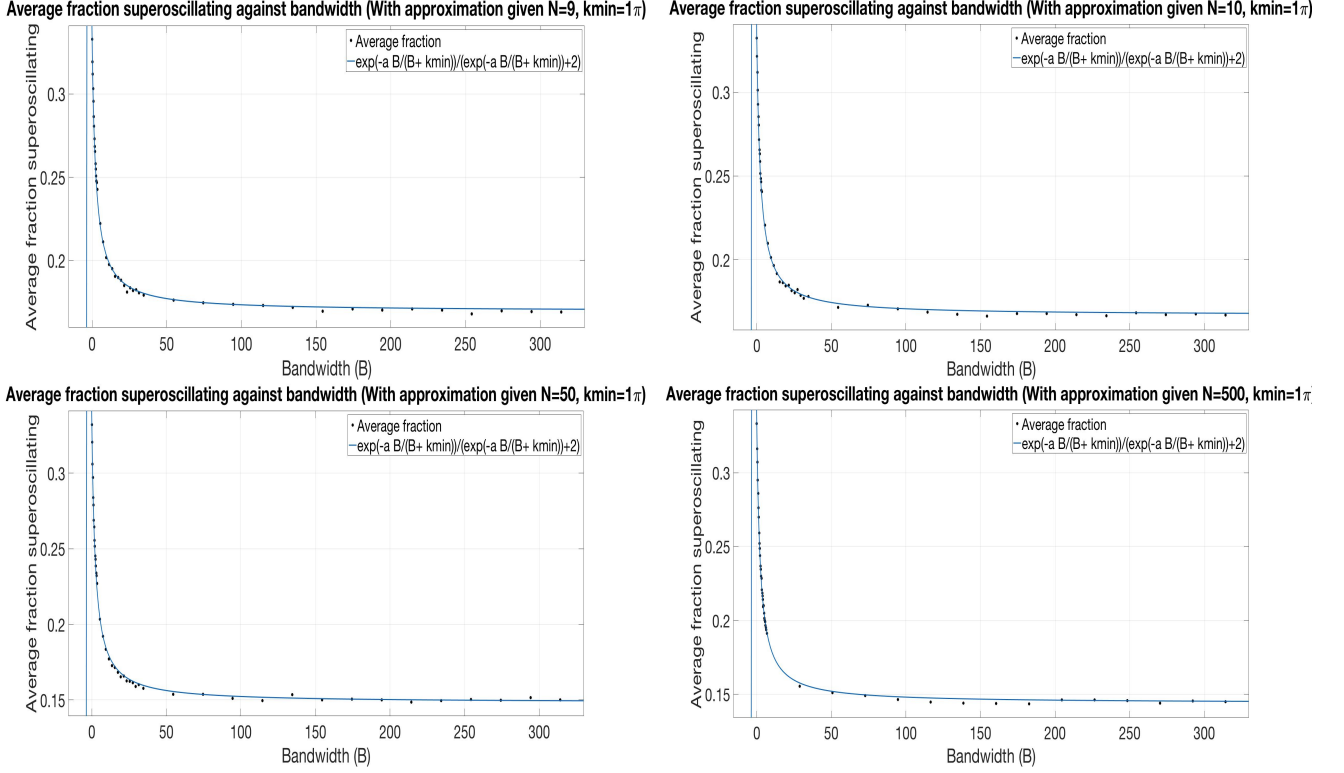


Figure 3.5: Showing the average fraction against bandwidth for  $k_{min} = 1\pi$  and  $N=9, 10, 50, 500$ . The approximated curve is also given with the use of the expression given by (3.0.16) and (3.0.7). The points plotted are the average fraction superoscillating calculated for each bandwidth.

Similar results are obtained to that of figure 3.4 and 3.5 when taking into account different values for  $k_{min}$ . It is shown that with larger values of  $N$  the fraction of superoscillations decreases, and can be seen to fall to a value of 0.15 for  $N = 500$  sources. An important observation would be the slight variation in the value for the constant  $a$  for each case. In addition, the effect of changing  $N$  on  $a$  is much larger than the effect of changing  $k_{min}$  as shown in table (3.1). The constant  $a$  is asymptotically tending to a value of approximately 1.09 as we increase the number of sources to  $N = 500$ . Then for large  $N$ , the expression in (3.0.9) can be approximated as follows,

$$f = \frac{e^{-1.09 \frac{B}{k_{max}}}}{e^{-1.09 \frac{B}{k_{max}}} + 2} \quad (3.0.10a)$$

$$\approx \frac{e^{\ln \frac{1}{3} \left( \frac{B}{k_{max}} \right)}}{e^{\ln \frac{1}{3} \left( \frac{B}{k_{max}} \right)} + 2}. \quad (3.0.10b)$$

Looking back at paper [5] (Superoscillations in speckle patterns), where a description of the probability density function of the wave is given by equation (2.4.37) in terms of the local phase gradient (local wavenumber) only. The relationship between  $k_2$  (second moment of the power spectrum) and the maximum wavenumber  $k_{max}$  in the spectrum here, determines the characteristics of superoscillations

[4], where  $k_{max}$  is upper limit of  $\sqrt{k_2}$ . The annular spectrum was given by,

$$k_{max}(1 - \delta) \leq k \leq k_{max}. \quad (3.0.11)$$

The fraction of superoscillation is given by,

$$f_{annulus} = 1 - \frac{4}{(6 - 2\delta + \delta^2)}. \quad (3.0.12)$$

Now for the case discussed here, the bandwidth is considered rather than a scaled thickness as in [5]. Therefore the bandwidth  $B$  can be described in terms of  $\delta$  as shown,

$$\delta = \frac{B}{k_{max}}. \quad (3.0.13)$$

Therefore equation (3.0.12) can be described in terms of bandwidth as,

$$f_{annulus} = 1 - \frac{4}{(6 - 2(\frac{B}{k_{max}}) + (\frac{B}{k_{max}})^2)}. \quad (3.0.14)$$

Equation (3.0.14) above is the expression as found in [5] and [4]. Now comparing the expression for the fraction of superoscillations in (3.0.7) and the fraction in (3.0.12),

$$f = \frac{\alpha^2}{\alpha^2 + 2} \quad (3.0.15a)$$

$$\alpha = \sqrt{\frac{2f}{1-f}}. \quad (3.0.15b)$$

Substituting (3.0.12) into (3.0.15), then taking  $\delta$  from (3.0.13),

$$\alpha = \sqrt{2 \frac{(\frac{4}{6-2\delta+\delta^2})}{(1 - \frac{4}{6-2\delta+\delta^2})}} \quad (3.0.16a)$$

$$\alpha = \sqrt{1 - \delta + \frac{\delta^2}{2}} \quad (3.0.16b)$$

$$\alpha = \sqrt{1 - \frac{B}{k_{max}} + \frac{B^2}{2k_{max}^2}}. \quad (3.0.16c)$$

Notice here if we computed the values for the fraction of superoscillations using alpha as found by equation (3.0.16) we get the result that as bandwidth tends to  $\infty$  our fraction of superoscillation tends to  $\frac{1}{5}$  as shown in figure 3.6, by the means of equation (3.0.12). On further inspection of the expression  $\alpha$  in 3.0.16, the resemblance to exponential function can be seen,

$$1 - \frac{B}{k_{max}} + \frac{B^2}{2k_{max}^2} \dots \approx e^{\frac{B}{k_{max}}} \quad (3.0.17a)$$

$$\sqrt{1 - \frac{B}{k_{max}} + \frac{B^2}{2k_{max}^2} \dots} \approx e^{\frac{B}{2k_{max}}} = \alpha. \quad (3.0.17b)$$

Therefore it can be said that the expression found analytically in (3.0.9) can be reduced down to the expression found in (3.0.16) when  $a = 1$  and  $\frac{B}{k_{max}} \ll 1$ . As seen in figure 3.6, the calculated fraction of superoscillations using the expression as given in (3.0.14) with different initial wavenumbers given by  $k_{min}$ , does not fall below  $\frac{1}{5}$ . Furthermore, the fraction changes with the initial wavenumber, this shows a similar trend to the results obtained analytically in 3.1 where the fraction of superoscillations increases as  $k_{min}$  increases.

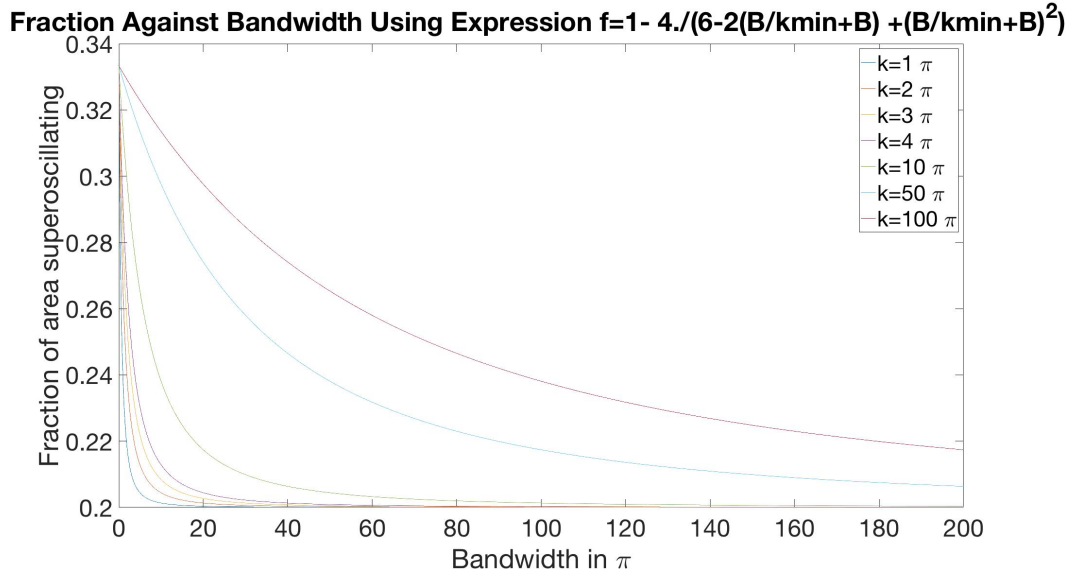


Figure 3.6: Figure of average fraction of superoscillations against bandwidth using the expression in (3.0.12). Using the expression (3.0.13) for delta and calculating the fraction using  $k_{min} = 1\pi, 2\pi, 3\pi, 4\pi, 10\pi, 50\pi, 100\pi$ .

## Second Case: Fixed Bandwidths

The second case investigated will consider a fixed bandwidth with every sample taken of our wave, this is done to analyse any changes that this might have to the results already obtained in the first case. The fraction of superoscillation is taken for a wave, given that there exists two components with wavenumbers assigned specific  $k_{min}$  and  $k_{max}$ , which are fixed for every sample. Here the amplitudes and the phase remains random and independent random variables as before. The fraction is taken for  $10^5$  samples and an average is calculated. This average is then plotted for multiple bandwidths ranging from 0 to  $100\pi$ . Furthermore the effects of changing the number of sources  $N$  and the initial wavenumber  $k_{min}$ , on the average fraction superoscillating is analysed, where  $N = 5, 10, 50, 100$  and  $k_{min} = 1\pi, 2\pi, 10\pi, 50\pi$ . The results are presented in figures (3.7, 3.8), showing similar trends to that of the first case where the wavenumbers are chosen at random from a given bandwidth. Still it can be seen that the value decreases to a

value much smaller than a fifth as the number of sources increases, and the rate at which the fraction varies with bandwidth decreases with an increase in  $k_{min}$ .

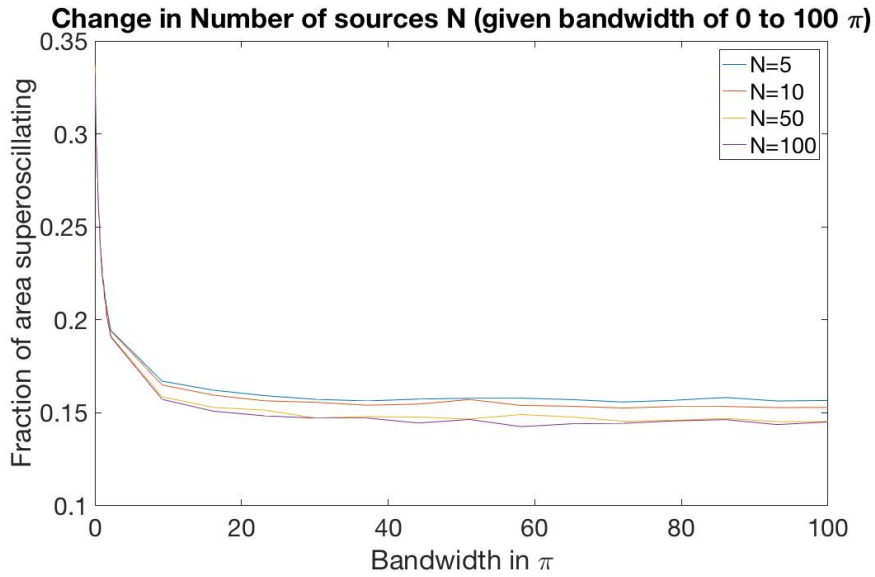


Figure 3.7: This figure shows the average superoscillating fraction against bandwidth starting at  $k_{min} = 1\pi$  for several values of sources  $N = 5, 10, 50, 500$ , for the special case where the bandwidth of every sample is fixed.

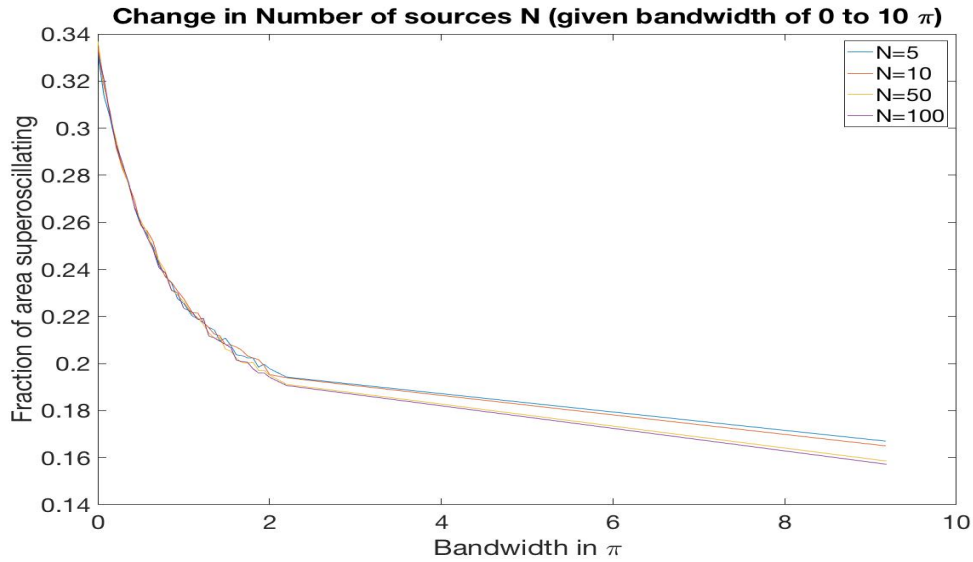


Figure 3.8: This figure shows the average superoscillating fraction against bandwidth starting at  $k_{min} = 1\pi$  for several values of sources  $N = 5, 10, 50, 500$ , for the special case where the bandwidth of every sample is fixed.(zoomed figure of 3.7 at bandwidth 0 to  $10\pi$  )

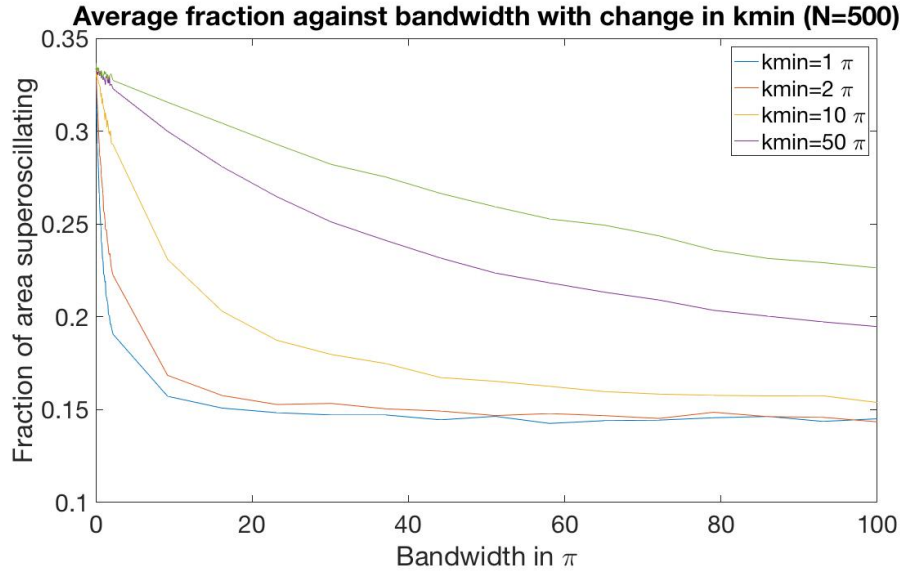


Figure 3.9: This figure shows the effect of changing bandwidth on the average superoscillating fractional area, with a fixed number of wave sources of  $N=500$ . This also shows the results for change in initial wavenumber  $k_{min} = 1\pi, 2\pi, 10\pi, 50\pi, 100\pi$ .

To understand why the fraction of superoscillations might change as seen by the graph 3.1, one might get a better understanding by looking into the difference in wavelength  $\Delta\lambda$  with every sample rather than the change in bandwidth. First, the bandwidth is expressed in terms of wavelength as follows:

$$B = k_{max} - k_{min} \quad (3.0.18a)$$

$$= \frac{2\pi}{\lambda_{min}} - \frac{2\pi}{\lambda_{max}} \quad (3.0.18b)$$

$$\Delta\lambda = \frac{\Delta k(\lambda_{min}\lambda_{max})}{2\pi} \quad (3.0.18c)$$

$B$ : bandwidth,  $\Delta\lambda$ :difference in wavelength.

Taking the bandwidth fixed in (3.0.18), then it is seen that with an increase in initial wavenumber the change in wavelength  $\Delta\lambda$  decreases with fixed bandwidth, this might explain some of the properties observed before from the relationship between the fraction of superoscillation and the change in the initial wavenumber. In addition the fraction is at its highest value when taking very large values for the initial wavenumber  $k_{min}$ , as seen in figures 3.2, 3.3 and 3.9. When analysed in terms of the difference in wavelengths, this would be where the difference in wavelength is at its lowest. To illustrate equation (3.0.18) we plot  $\Delta\lambda$  (change in wavelength) against  $B$  (bandwidth). Figure 3.10 shows this relationship. An interesting observation is that as bandwidth increases  $\Delta\lambda$  tends to a constant,

which might also be related to the result obtained for the average fraction of superoscillations where it tends to a constant value.

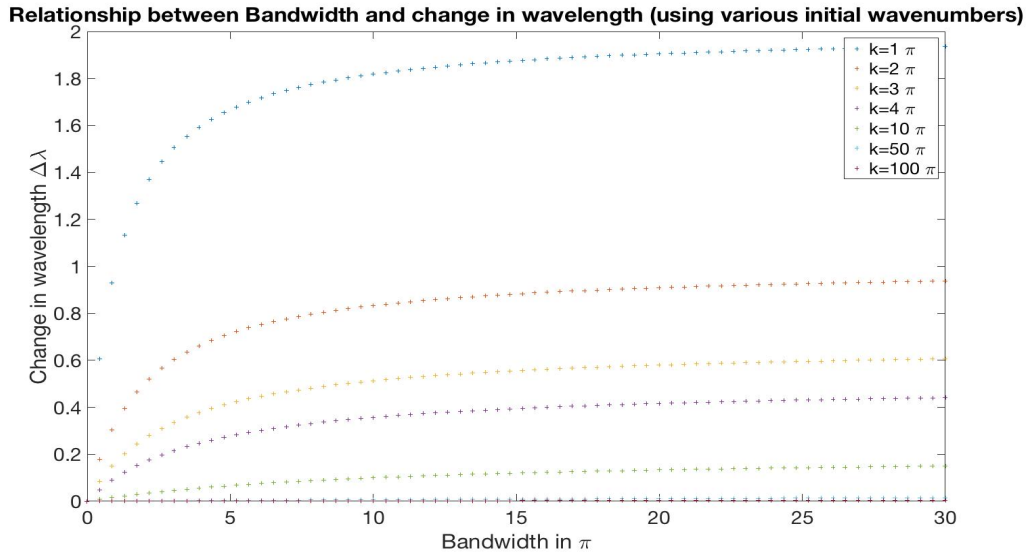


Figure 3.10: The following graph gives the relationship between bandwidth and change in wavelength for several initial wavenumbers as given by equation (3.0.18).  $k_{min} = 1\pi, 2\pi, 10\pi, 50\pi, 100\pi$ .

The plots for the distribution of the local wavenumber for each sample is shown in 3.11, 3.12 and 3.14. These plots show the distribution given for every  $\frac{k(r)}{k_0}$  (ratio of local wavenumber over the maximum wavenumber), calculated analytically alongside the theoretical equivalent as given by equation (2.4.37) shown in [5], using the fact that  $k_2$  is given by the expression in equation (2.4.44). Analysing the wavefunction's local wavenumber for number of sources  $N = 50$  in 3.11 and 3.12, as well as  $N = 5$  in figure 3.14 for several bandwidths given by  $B = 0\pi, 2\pi, 50\pi$  and minimum wavenumbers  $k_{min} = 1\pi, 100\pi$ . The distribution for the monochromatic case seems to agree with the theoretical calculation, as seen in the figures where  $B = 0$ , however the distribution seems to deviate from the theoretical expectation as the value of bandwidth increases. Note that the area under the graphs is the probability, and therefore any local wavenumber that gives a ratio  $\frac{k}{k_{max}}$  larger than 1 is an indication of superoscillation. Here we define  $k_0$  to be the maximum wavenumber  $k_{max}$ .

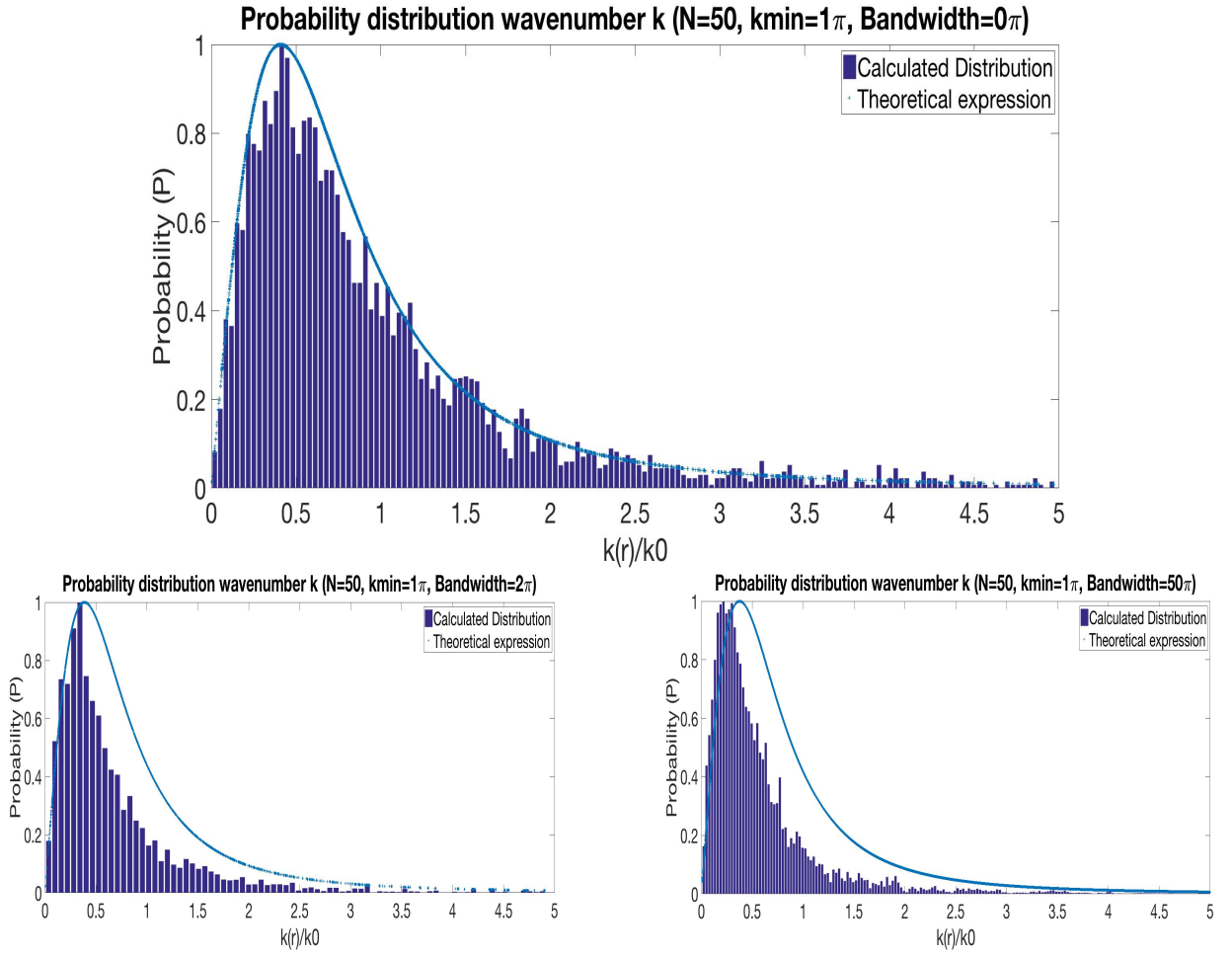


Figure 3.11: Graph for the distribution of wavenumber  $\frac{k}{k_{min}}$  for number of sources  $N = 50$  and  $k_{min} = 1\pi$ , with bandwidths given by  $B = 0\pi, 2\pi, 50\pi$ . The bar chart is the probability distribution calculated, light blue line shows the theoretical prediction given by (2.4.37) using  $k_2$  as given by (2.4.44).

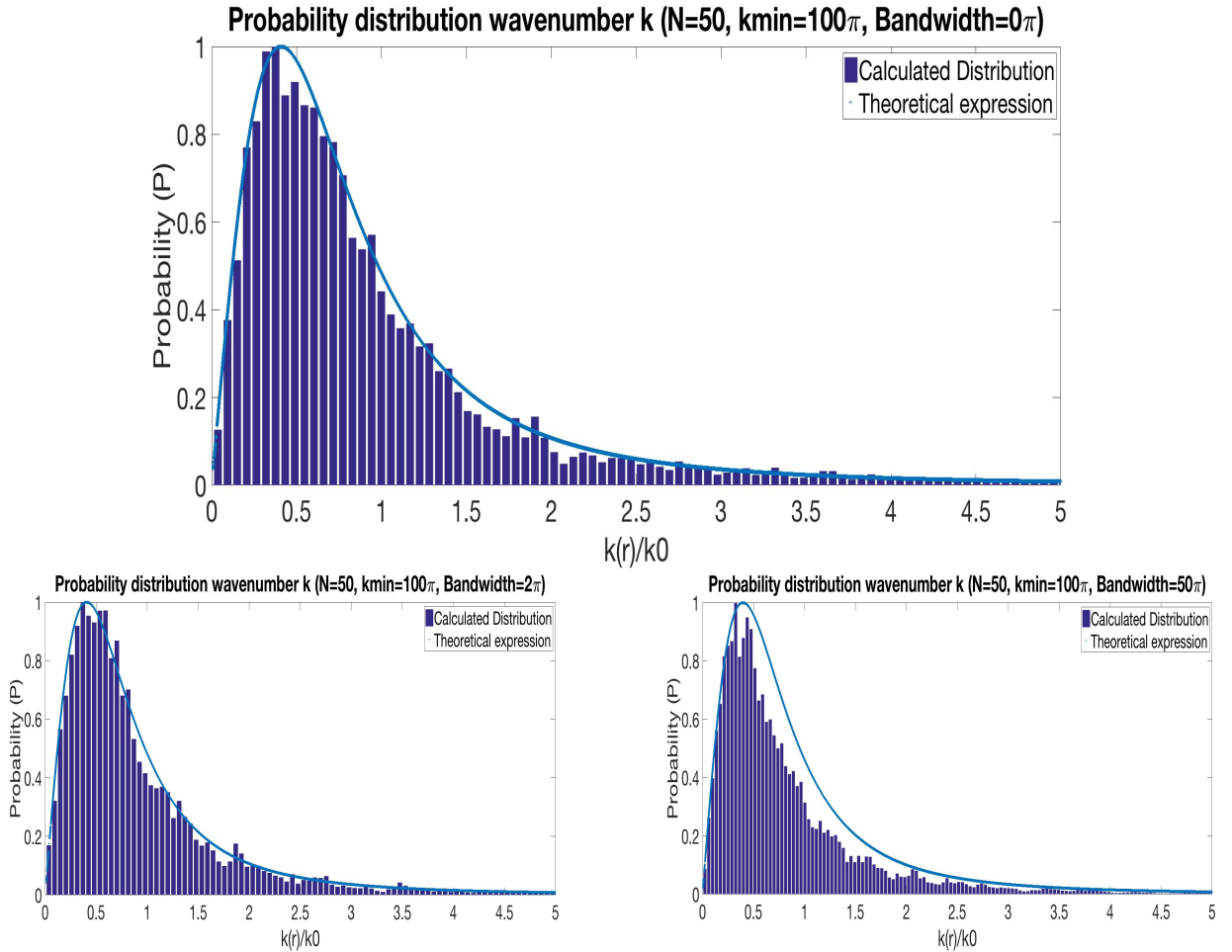


Figure 3.12: Graph for the distribution of wavenumber  $\frac{k}{k_{min}}$  for number of sources  $N = 50$  and  $k_{min} = 100\pi$ , with bandwidths given by  $B = 0\pi, 2\pi, 50\pi$ . The bar chart is the probability distribution calculated, light blue line shows the theoretical prediction given by (2.4.37) using  $k_2$  as given by (2.4.44).

There is a clear difference between figure 3.11 where the minimum wavenumber in the spectrum is given as  $k_{min} = 1\pi$  and 3.12 with wavenumber  $k_{min} = 100\pi$ . The first most notable difference is that the effect of changing the bandwidth  $B$  on the distribution of local wavenumbers for a larger  $k_{min}$ , is much smaller than that with a lower  $k_{min}$ . This is therefore in agreement to what has been observed in figure 3.1, which shows that the average fraction of superoscillation falls at a much smaller rate with higher initial wavenumbers  $k_{min}$ . Figure 3.12, shows that an increase of  $2\pi$  in bandwidth for large  $k_{min}$  has little effect to the overall distribution, and when looking into the change in wavelength as shown in figure 3.10, it is clear that the difference in wavelength is small. Therefore the waves could be approximated to that of the monochromatic case.

Knowing previously the relationship between the fraction of superoscillations and the number of sources taken, given by figure 3.7, the plot of the distribution in 3.14 reinforces the effect of changing the number of sources. Comparing the results to when the number of sources  $N = 50$ , a clear indication that the fraction of

superoscillations is higher overall for  $N = 5$ . This can be seen in figure 3.13 where the bandwidth  $B = 50\pi$  and  $k_{min} = 1\pi$ , here the probability of  $k(r)/k_0$  is seen to be larger in  $N = 5$  than  $N = 50$ . The difference between the two probability distributions can also be seen in figure 3.7 where the fraction of superoscillations for  $N = 5$  is  $\approx 0.16$  than that for  $N = 50$  which is  $\approx 0.15$ . This relationship still holds for large bandwidths.

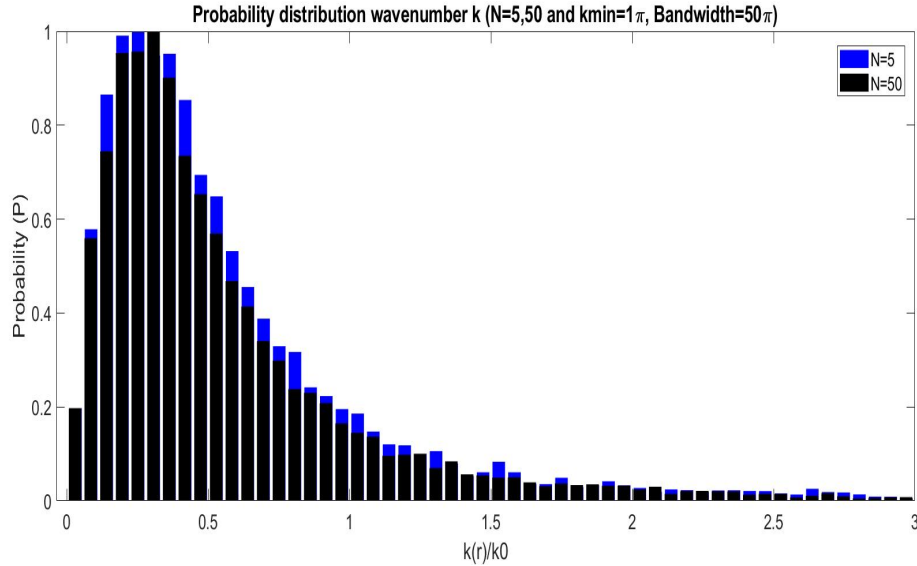


Figure 3.13: Graph of the distribution of wavenumber  $\frac{k}{k_{max}}$  for number of sources  $N = 5, 50$  with  $k_{min} = 1\pi$  and bandwidth  $B = 50\pi$ . The black bar shows the distribution for  $N = 50$  and the blue shows  $N = 5$ .

For the calculations in 3.11, 3.12 and 3.14 the number of samples taken had to be significantly decreased due to computational limitations. The number of samples taken for the wavefunction is given to be 4000 and the number of sources superimposing to form each wavefunction is given for both  $N = 5$  and  $N = 50$ . The local wavenumber  $k(r)$  is then found for all  $x$  and  $y$  values in our region chosen. The distribution is then plotted for all local wavenumbers relative to the associated  $k_{max}$  in each sample wave, This is done for several bandwidths and initial wavenumbers.

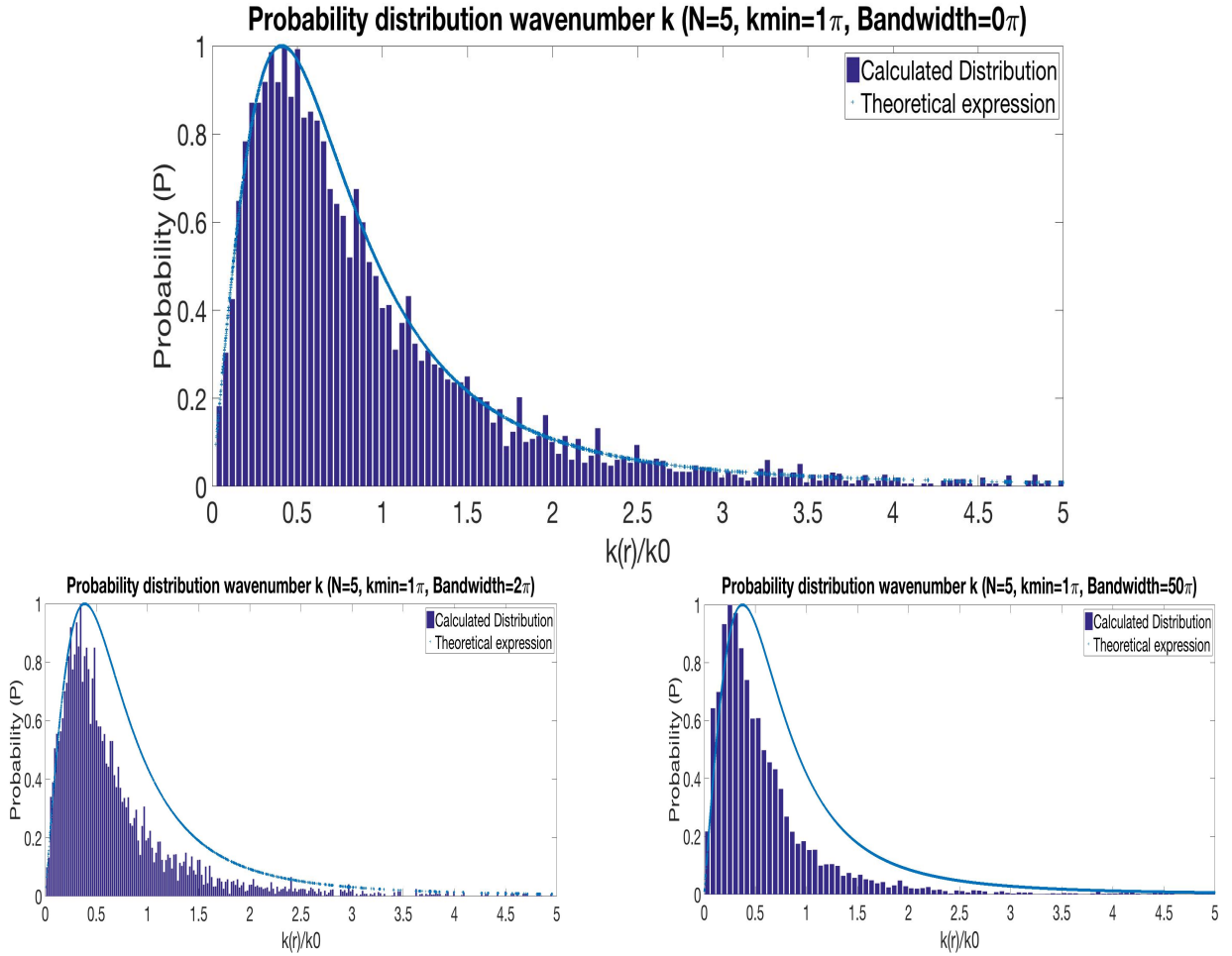


Figure 3.14: Graph for the distribution of wavenumber  $\frac{k}{k_{min}}$  for number of sources  $N = 5$  and  $k_{min} = 1\pi$ , with bandwidths given by  $B = 0\pi, 2\pi, 50\pi$ . The bar chart is the probability distribution calculated, light blue line shows the theoretical prediction given by (2.4.37) using  $k_2$  as given by (2.4.44).

preliminary evidence of changing the angles in equation (3.0.3) so that they are not equally spaced and are chosen at random, as well as having random  $k_n$  values has no significant effect on the results obtained here. Therefore, each sample wave is created by waves superimposing from random directions. This can be seen by figure 3.15 showing the superposition of  $N = 10$  waves for  $k_{min} = 1\pi, 2\pi$ . The code for this can be found in Appendix A: MATLAB codes.

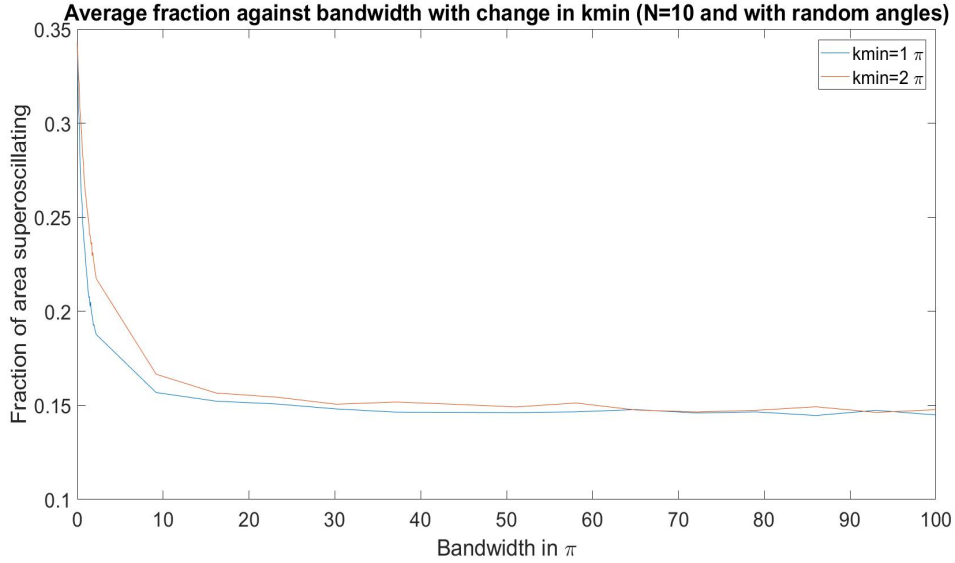


Figure 3.15: The following graph gives the relationship between the bandwidth and the average fraction of superoscillations observed for  $N = 10$  and  $k_{min} = 1\pi, 2\pi$ . This is done for wave samples created through superposition of waves from random directions (random angles in (3.0.3)).

Figures 3.16, 3.17, 3.18 and 3.19 are plots of the superoscillatory region (seen by the blue region) for several sample wavefunctions for a 2-D non-monochromatic wave formed through the superposition of  $N = 50$  waves as given by equation (3.0.1). The black lines are contour plots of several phases of the wave, the intersection of these lines are the phase singularities. It is clear that superoscillations are found near vortices and near regions where the phase gradient is high i.e. where the black lines shown in the figures are closer together. It is known from before that taking larger values for  $k_{min}$  the average fraction of superoscillations increases, this could be seen through the comparison between figure 3.16 and 3.18. However there is rather interesting observation that the number of wave vortices increases with larger  $k_{min}$  values and with larger bandwidths. This again might be due to the relationship between the bandwidth and the difference between the wavelengths of the waves superimposing as mentioned previously.

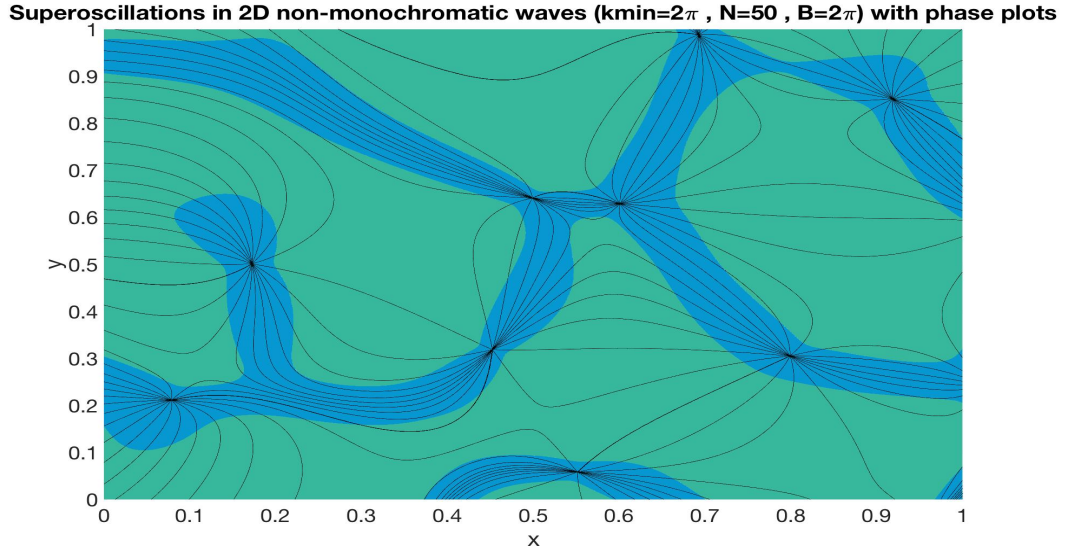


Figure 3.16: This figure shows a plot of the superoscillatory region of a sample wave formed through the superposition of  $N = 50$  waves, and is non-monochromatic with minimum wavenumber  $k_{min} = 2\pi$  and bandwidth of  $B = 2\pi$ . The black lines show the plot of multiple phases of the wave, intersecting at wave vortices found in the superoscillatory region.

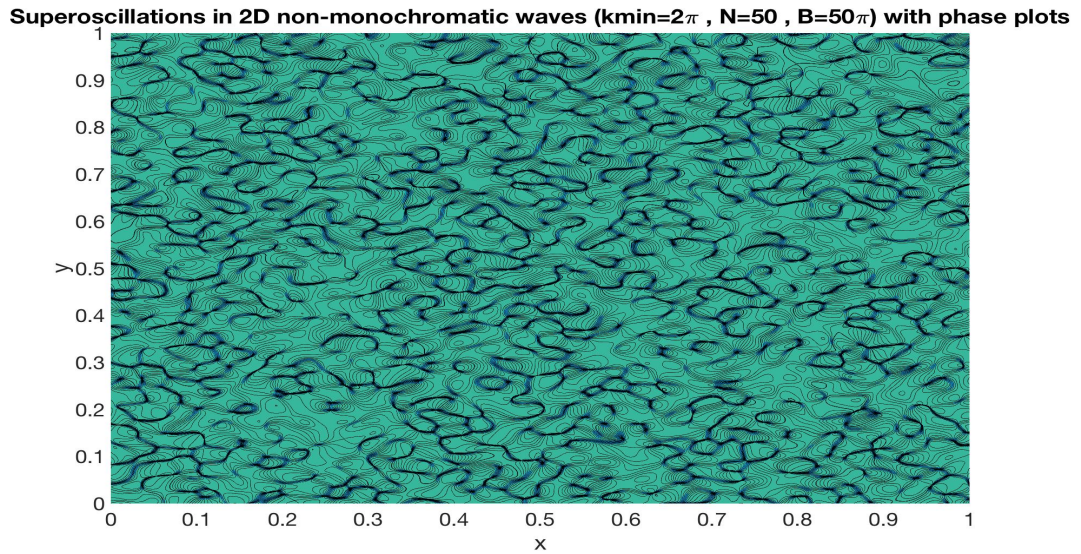


Figure 3.17: Figure showing a plot of the superoscillatory region of a sample wave formed through the superposition of  $N = 50$  waves, and is non-monochromatic with minimum wavenumber  $k_{min} = 2\pi$  and bandwidth of  $B = 50\pi$ . The black lines show the plot of multiple phases of the wave, intersecting at wave vortices found in the superoscillatory region.

**Superoscillations in 2D non-monochromatic waves ( $k_{min}=10\pi$  ,  $N=50$  ,  $B=2\pi$ ) with phase plots**

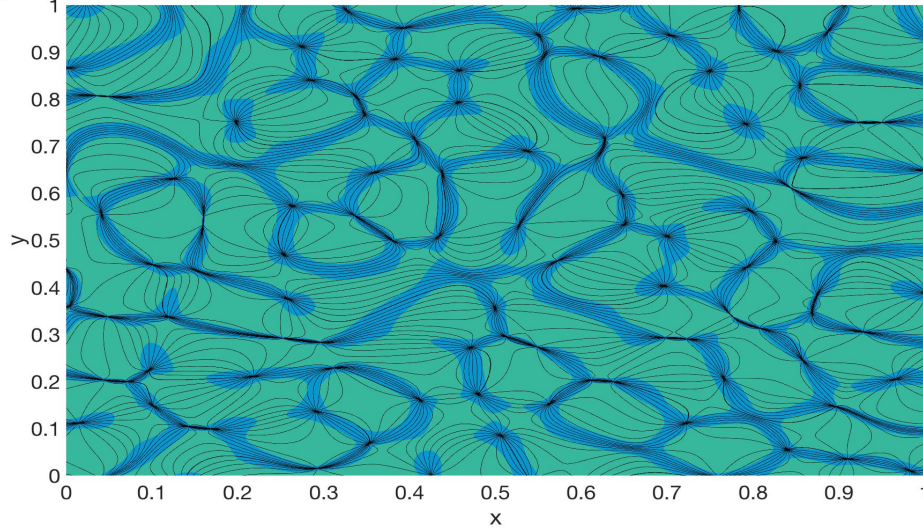


Figure 3.18: This figure shows a plot of the superoscillatory region of a sample wave formed through the superposition of  $N = 50$  waves, and is non-monochromatic with minimum wavenumber  $k_{min} = 10\pi$  and bandwidth of  $B = 2\pi$ . The black lines show the plot of multiple phases of the wave, intersecting at wave vortices found in the superoscillatory region.

**Superoscillations in 2D non-monochromatic waves ( $k_{min}=10\pi$  ,  $N=50$  ,  $B=50\pi$ ) with phase plots**

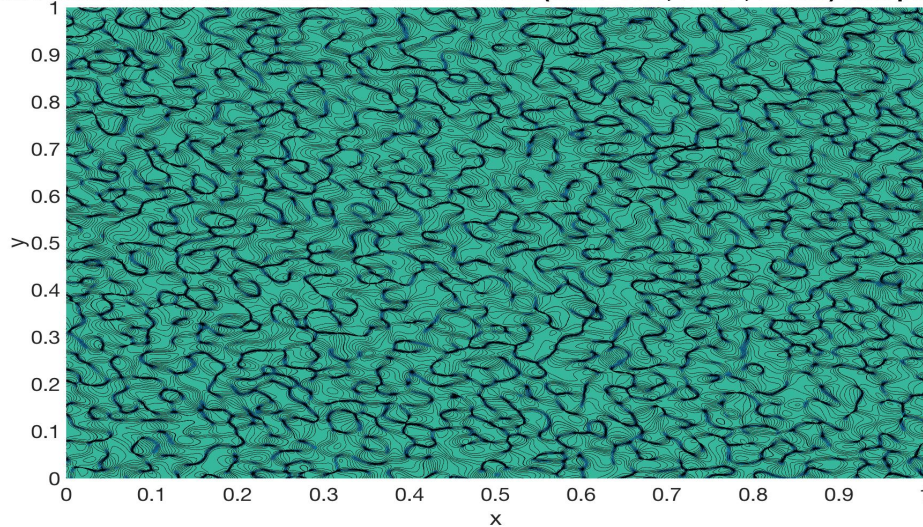


Figure 3.19: This figure shows a plot of the superoscillatory region of a sample wave formed through the superposition of  $N = 50$  waves, and is non-monochromatic with minimum wavenumber  $k_{min} = 10\pi$  and bandwidth of  $B = 50\pi$ . The black lines show the plot of multiple phases of the wave, intersecting at wave vortices found in the superoscillatory region.

A comparison between the intensity region and the superoscillatory region is shown in figures 3.20 , 3.21 and 3.22 for several bandwidths ( $B = 0\pi, 2\pi, 10\pi$ ) with  $k_{min} = 2\pi$ . The plots show how the superoscillatory region differs from

that of the lowest intensity region, however it does illustrate that superoscillations are found near regions of low intensities. The graphs produced are a plot of the intensity region shown by the coloured hues and lowest intensity region shown by the white line, for one sample wavefunction  $\psi$  which was formed from the superposition of  $N = 50$  waves. The lowest intensity region was found by taking the fraction of superoscillations calculated and taking the same fraction from the intensity pattern. The red lines encloses the superoscillatory regions. The results are similar to that found by paper [5].

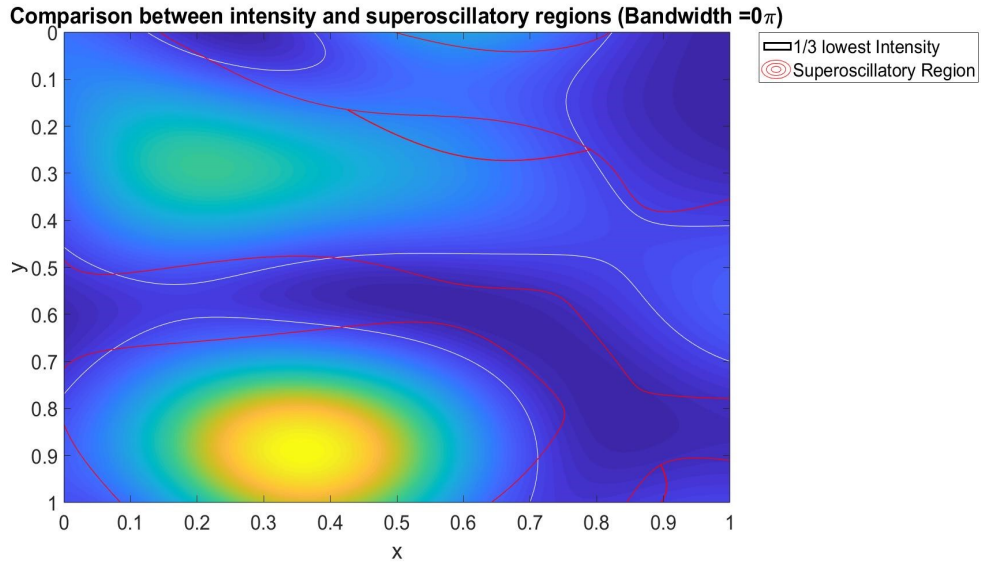


Figure 3.20: This is a plot of the intensity pattern shown as the coloured hue, along side the plot for the region superoscillating which is enclosed by the red lines, for 1 sample wavefunction given by the superposition of  $N = 50$  waves with  $k_{min} = 2\pi$ . The white lines shows the area of low intensities. Here the bandwidth is taken as  $B = 0\pi$ , so that the wave is considered to be monochromatic.

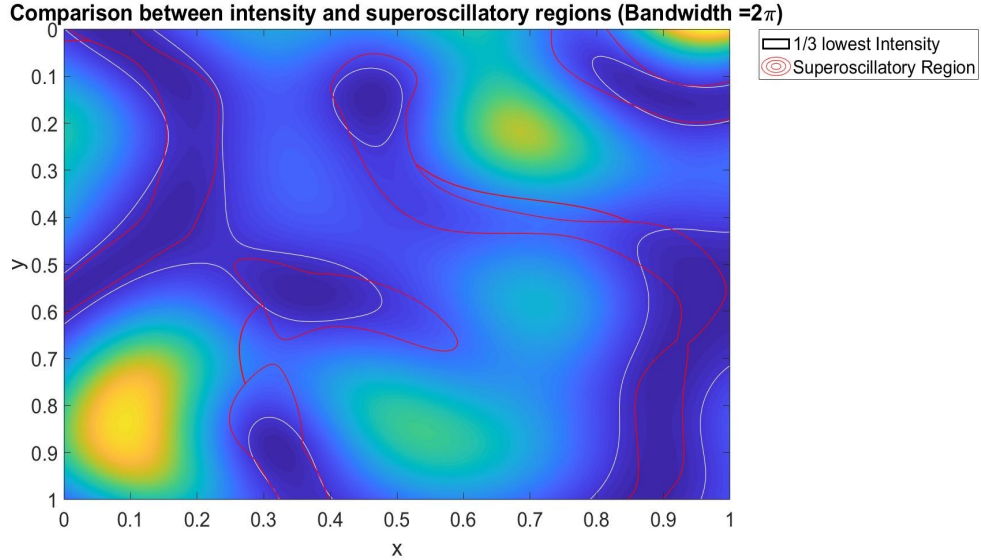


Figure 3.21: This is a plot of the intensity pattern shown as the coloured hue, along side the plot for the region superoscillating which is enclosed by the red lines, for 1 sample wavefunction given by the superposition of  $N = 50$  waves with  $k_{min} = 2\pi$ . The white lines shows the area of low intensities. Here the bandwidth is taken as  $B = 2\pi$ .

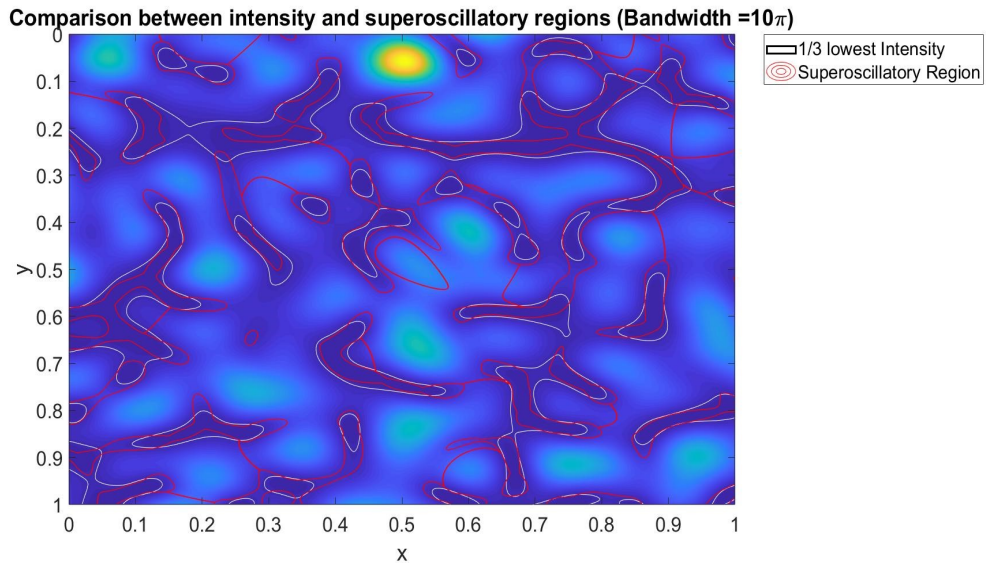


Figure 3.22: Similar plot to that of figures 3.20 and 3.21, however taking bandwidth  $B = 10\pi$ .

## Final Conclusion

The main body of this thesis covered a variety of different mathematical topics which were required to understand the nature and behaviour of superoscillatory function. One mathematical concept called the Saddle Point Method was essential in understanding paper [1], as it gives an approximation of a special kind of integral of the form shown in equation (2.1.21). Statistical optics along with Gaussian

statistics were also of great importance in the study of the papers [3], [5] and [4] and has been used throughout this thesis. The papers reviewed in the chapter Background Reading explain all the major physical concepts required, however the paper *Mathematics of Superoscillations* by Y. Aharonov *et al* [18] gives an in-depth mathematical analysis of superoscillations, which was of great use in understanding this fascinating phenomena.

The aims of the thesis was to give a clear description of superoscillations and how such functions behave. Expanding on the work conducted in [3], [5] as well as the [4], by studying the effect of changing the bandwidth of the individual superimposing waves, alongside the change in the number of sources on the average fraction of superoscillations observed in a fixed region of space. Furthermore, the effect of changing the smallest wavenumber in the spectrum is also analysed and observed.

A definition is given for a wave as before [3] [5], where a superposition of random waves is taken, each individual wave had components amplitude and phase, both of which were random independent variables, i.e the knowledge of one variable gives no indication of the behaviour of the other. The amplitudes are taken to be random complex circular Gaussian variables with a real and imaginary part that are also independent of each other. The expression for such a wave is given by (3.0.1).

The main idea was to find the region in the sample wavefunction (3.0.1) where the local wavenumber in the resultant wave exceeds that of the maximum wavenumber in the Fourier spectrum, as this indicates that the function is superoscillating. The fractional area of superoscillation is calculated for  $10^5$  sample waves. All the figures shown in chapter 3 were found computationally using MATLAB.

Two cases are taken into consideration as mentioned previously. The first creating sample waves by taking individual waves, where the wavenumber is chosen at random from a specified band-limit, so that the maximum wavenumber in the spectrum could vary from one sample to another. The second case is where the bandwidth is fixed for every sample function, which in turn means that there is always a wave that has maximum wavenumber  $k_{max}$  and a minimum  $k_{min}$ . Both cases here give similar results to one another, as shown in the graphs given by 3.1 and 3.9. This might be due to the high level of samples taken, since the average fraction of the area in which superoscillations is observed is taken for a vast number of sample waves. The main and most surprising result shown in figures 3.1, 3.2 and figures 3.7 to 3.9, is that for extremely large bandwidth the average fraction of superoscillations falls to a value of  $\approx 0.15$  with large number of sources. This contradicts the theoretical result in [4], as shown by equation (2.4.45), where a scaled thickness is used rather than bandwidth. Here the predicted value of a  $\frac{1}{5}$  is given for a ‘top hat’ spectrum, and the superoscillatory fraction against bandwidth is shown in figure 3.6. It can be seen that the fraction falls with bandwidth

to a fraction much larger than what was found numerically here. It was not clear what caused the fraction to fall below  $\frac{1}{5}$ , however a possibility might be the expression given to  $k_2$  which is the second moment of  $k$  with respect to the power spectrum, as shown in [4] and [5], this is shown in equation (2.4.42) to (2.4.44), other possibilities might be an approximation used in [5] [4] which has not been taken into consideration in the computation. Looking at equation (3.0.17), it can be seen that the expression for  $\alpha$  is similar to the expression obtained in (3.0.8), and can be considered as an approximation of it. Another interesting observation is made when comparing the fraction of superoscillation with the change in the minimum wavenumber  $k_{min}$ . It is seen through figures 3.8, 3.9, that as the minimum wavenumber decreases, the average fraction falls at a faster rate. This could be caused by the relationship between the change in wavelength and the bandwidth, the plot of  $\Delta\lambda$  against bandwidth  $B$  is given in figure 3.10 and this shows that with large initial wavenumber  $\Delta\lambda$  is almost constant with large bandwidths, however with small  $k_{min}$  the change is more significant with every step. The relationship between bandwidth and the change in wavelength is shown in equation (3.0.18). The plot for the theoretical result given by equation (2.4.45) is found in figure 3.6 and it shows that the fraction of superoscillation falls in the same manner as that found computationally however with the slight differences as mentioned earlier.

Looking back at the results, there is a clear correlation between the number of sources superimposing and the average fraction superoscillating. Surprisingly, the figures in 3.2, 3.7 show that as the number of sources increases the fraction tends to decrease, in the case of constant initial wavenumber. Since superoscillations are said to be found near regions where the functions tends to vanish and the phase is undefined. One possibility might be the underlying statistical link between the destructive interference of the waves and the number of sources, such that the probability for the waves to destructively interfere might decrease with the increase of the number of random waves superimposing.

From all the results found in chapter 3, It is essential to find an expression that fits the figures obtained in 3.1, 3.2 and 3.7 to 3.9 analytically and computationally. Initially the probability distribution for a monochromatic case is known to be of the form found in equation (2.3.45). Now a parameter  $\alpha$  in (3.0.6) is multiplied by the maximum wavenumber, this is done due to the fact that for a non-monochromatic case, the probability density function was shown to be expressed as (2.4.37), where  $k_2$  is the second moment of the power spectrum, which is dependent on the underlining distribution of the wavenumbers  $k$ . For the results obtained in chapter 3, an approximated fit is made using the expression given by equation (3.0.9), Where an expression for  $\alpha$  has been found as shown in (3.0.8). The approximated expression for the fraction of superoscillations was found to reduce down to the expression found in [4] and [5] as given by (3.0.14) with  $a = 1$  and  $\frac{b}{k_{max}} \ll 1$ .

Overall, superoscillations has been an interesting and exciting area to research

---

and study. It has shown to be an area that is growing rapidly and has been applied in a variety of different areas such as optical super-resolution. However there is still much to be explored in the field of superoscillations. If one were to further the work conducted here, they might consider expanding the  $2 - D$  case here into higher dimensions and analysing the statistics, as well as the effects of changing the number of sources on the superoscillatory fraction. Another possible area of research, would be explaining the reasoning behind the contradicting results obtained here for the theoretical description of the fraction of superoscillations, as shown in equation (2.4.45), and the results obtained from numerical computation of the fraction of superoscillations as provided in figures 3.1, 3.2, 3.7 and 3.9.

Effect of Change in $N$ , and $k_{min}$ on $a$			
Number of sources $N$	$k_{min}$	$a$	Root mean squared error
$N = 5$	$1\pi$	0.7599	0.0025
	$2\pi$	0.7561	0.0023
	$3\pi$	0.7579	0.0024
	$4\pi$	0.7616	0.0023
	$10\pi$	0.7513	0.0027
	$50\pi$	0.7244	0.0016
	$100\pi$	0.7135	0.0020
$N = 6$	$1\pi$	0.8119	0.0024
	$2\pi$	0.8081	0.0020
	$3\pi$	0.807	0.0021
	$4\pi$	0.8071	0.0024
	$10\pi$	0.7973	0.0021
	$50\pi$	0.7836	0.0020
	$100\pi$	0.7755	0.0022
$N = 7$	$1\pi$	0.8461	0.0023
	$2\pi$	0.8471	0.0021
	$3\pi$	0.8445	0.0024
	$4\pi$	0.8456	0.0023
	$10\pi$	0.8407	0.0024
	$50\pi$	0.8229	0.0017
	$100\pi$	0.8139	0.0017
$N = 8$	$1\pi$	0.877	0.0021
	$2\pi$	0.8747	0.0022
	$3\pi$	0.8734	0.0021
	$4\pi$	0.8688	0.0021
	$10\pi$	0.8653	0.0018
	$50\pi$	0.8437	0.0018
	$100\pi$	0.8354	0.0016

Table 3.1: Table showing the value calculated analytically of the constant  $a$  found in our expression in (3.0.9) for  $N = 5, 6, 7, 8$  and  $k_{min} = 1\pi, 2\pi, 3\pi, 4\pi, 10\pi, 50\pi, 100\pi$ . The root mean squared error has also been found using MATLAB, by finding the residuals which are the differences between the predicted and observed values of  $a$ . It is said to describe the sample standard deviation of the difference between the values found computationally and the predicted values.

Effect of Change in $N$ , and $k_{min}$ on $a$			
Number of sources $N$	$k_{min}$	$a$	Root mean squared error
$N = 10$	$1\pi$	0.9146	0.0021
	$2\pi$	0.9144	0.0025
	$3\pi$	0.911	0.0023
	$4\pi$	0.9138	0.0023
	$10\pi$	0.9086	0.0020
	$50\pi$	0.892	0.0015
	$100\pi$	0.8629	0.0015
$N = 50$	$1\pi$	1.055	0.0022
	$2\pi$	1.06	0.0021
	$3\pi$	1.06	0.0017
	$4\pi$	1.054	0.0021
	$10\pi$	1.055	0.0019
	$50\pi$	1.038	0.0018
	$100\pi$	1.015	0.0018
$N = 500$	$1\pi$	1.09	0.0020

Table 3.2: Table showing the value calculated analytically of the constant  $a$  found in our expression in (3.0.9) for  $N = 10, 50, 500$  and  $k_{min} = 1\pi, 2\pi, 3\pi, 4\pi, 10\pi, 50\pi, 100\pi$ , for the  $N = 500$  (we only found the value for  $k_{min} = 1\pi$  due to computational limitations). The root mean squared error has also been found using MATLAB, by finding the residuals which are the differences between the predicted and observed values of  $a$ . It is said to describe the sample standard deviation of the difference between the values found computationally and the predicted values.

# Chapter 4

## Mathematics

### 4.0.1 Laplace Method

The laplace method is used to find an estimation of integrals that are written in the form,

$$I = \int_a^b e^{-\phi f(x)} g(x) dx. \quad (4.0.1)$$

The values of  $a$  and  $b$  here can be either infinite or finite. It can be seen that the peak of the function given by  $e^{-\phi f(x)}$ , would be around the point  $x_0$ , and if  $\phi$  is taken to be very large then the peak is concentrated around the region  $(x - x_0)$ . Note that at the point  $x = x_0$ ,  $g(x_0)$  is a minimum.

For the moment taking that  $x_0 = a$  (some integer) and let  $f'(x_0) > 0$  and  $g(x_0) \neq 0$ . Then taking the Taylor series expansion of  $g(x)$  and  $f(x)$  near the point  $x = x_0$  obtains,

$$f(x) = f(x_0) + f'(x_0)(x - x_0) + \frac{1}{2}f''(x_0)(x - x_0)^2 + \dots + O(x - x_0)^3. \quad (4.0.2)$$

Returning back to equation (4.0.1) and let the limit  $b$ , which is the upper limit, be equal to infinite and replace the terms  $f(x)$  and  $g(x)$  with their expansions,

$$I = \int_a^\infty g(x_0) e^{-\phi(f(x_0) + f'(x_0)(x - x_0) + \dots)} dx \quad (4.0.3a)$$

$$= g(x_0) e^{-\phi f(x_0)} \left[ \frac{-1}{\phi f'(x_0)} \right]_a^\infty \quad (4.0.3b)$$

$$= g(x_0) \frac{e^{-\phi f(x_0)}}{\phi f'(a)} \quad (4.0.3c)$$

$$= g(a) \frac{e^{-\phi f(a)}}{\phi f'(a)}. \quad (4.0.3d)$$

Now considering a point  $x = x_0$  that is a minimum i.e. where  $f'(x) = 0$  and  $f''(x_0) > 0$ , then an expression of the integral in (4.0.3) is given as,

$$I = \int_a^b g(x_0) e^{-\phi(f(x_0) + \frac{1}{2}f''(x_0)(x - x_0)^2)} dx. \quad (4.0.4)$$

Replacing the limits  $a$  and  $b$  by  $\pm\infty$  respectively then,

$$I \approx g(x_0)e^{-\phi(f(x_0))} \int_{-\infty}^{\infty} e^{-\frac{\phi(x-x_0)^2}{2}} f''(x_0) dx. \quad (4.0.5)$$

Note that the integral in equation (4.0.5) is a Gaussian, then using the relation,

$$\int_{-\infty}^{\infty} e^{-ax^2} dx = \sqrt{\frac{\pi}{a}}, \quad (4.0.6)$$

Gives,

$$I \approx g(x_0)e^{-\phi f(x_0)} \sqrt{\frac{2\pi}{\phi f''(x_0)}}. \quad (4.0.7)$$

## 4.0.2 Volume of Hypersphere

First considering a hypersphere, which has a radius that will be denoted as  $R$ , and letting  $n$  be the number of dimensions of said sphere. Then a specific point can be defined on the  $n$  dimensional sphere in a euclidean space by  $(x_1, x_2, x_3, \dots, x_n)$ . The surface area of the hypersphere shall be denoted as  $A_{n-1}$  and can be described by the points,

$$R^2 \geq x_1^2 + x_2^2 + x_3^2 + \dots \quad (4.0.8)$$

Requiring the computation of the volume of the hypersphere  $V_n(R)$ . For this it can be described as,

$$V_n(R) \propto R^n \quad (4.0.9a)$$

$$V_n(R) = \int_{x_1^2+x_2^2+x_3^2+\dots+x_n^2} dx_1 dx_2 dx_3 \dots dx_n \quad (4.0.9b)$$

$$V_n(R) = B_n R^n. \quad (4.0.9c)$$

Since  $B_n$  is needed. A Construction of the volume is made by taking spherical shells that are infinitesimally thin of a radius ranging from  $0 < r < R$ , Therefore describing the volume as follows,

$$V_n(R) = \int_0^R A_{n-1}(r) dr. \quad (4.0.10)$$

It is also obvious that the surface area can also be expressed as,

$$A_{n-1}(R) = \frac{dV_n(R)}{dR} \quad (4.0.11a)$$

$$A_{n-1}(R) = nB_n R^{n-1}. \quad (4.0.11b)$$

Substituting in equation (4.0.11) into (4.0.10),

$$V_n(R) = nB_n \int_0^R r^{n-1} dr = \int_{x_1^2+x_2^2+x_3^2+\dots+x_n^2} dx_1 dx_2 dx_3 \dots dx_n. \quad (4.0.12)$$

To find  $B_n$ . Changing the integral to be of a hyper-spherical coordinate system where,

$$dx_1 dx_2 dx_3 \dots = r^{n-1} dr d\Omega_{n-1}. \quad (4.0.13)$$

Here  $\Omega_1 = d\theta$  for  $n = 2$ ,  $\Omega_2 = \sin(\theta)d\theta d\phi$  for  $n = 3$  and so on for multiple dimensions. Using the equation (4.0.13) and (4.0.12), it can be seen that,

$$\int d\Omega_{n-1} = nC_n. \quad (4.0.14)$$

A specific way of calculating  $B_n$ , by considering the function  $f(x)$

$$f(x_1, x_2, x_3, \dots, x_n) = \exp[-(x_1^2 + x_2^2 + \dots, x_n^2)] = \exp(-r^2). \quad (4.0.15)$$

If an integral is taken of the function  $f(x)$  in the hyper spherical coordinate system over all n dimensions,

$$\int_{-\infty}^{\infty} e^{-(x_1^2+x_2^2+x_3^2+\dots x_n^2)} dx_1 \dots dx_n = \int_0^{\infty} r^{n-1} e^{-r^2} dr d\Omega_{n-1}. \quad (4.0.16)$$

Using the relation in equation (4.0.14) gives,

$$\int_{-\infty}^{\infty} e^{-x_1^2} dx_1 \int_{-\infty}^{\infty} e^{-x_2^2} dx_2 \dots = nB_n \int_0^{\infty} r^{n-1} e^{-r^2} dr \quad (4.0.17)$$

The integrals shown above can be found by,

$$\int_{-\infty}^{\infty} e^{-x^2} dx = \sqrt{\pi} \quad (4.0.18a)$$

$$\int_0^{\infty} r^{n-1} e^{-r^2} dr = \frac{1}{2} \Gamma\left(\frac{n}{2}\right). \quad (4.0.18b)$$

Therefore, seeing now that the equation (4.0.17) is given by,

$$\pi^{\frac{n}{2}} = \Gamma\left(\frac{n}{2}\right) \frac{n}{2} B_n = \Gamma\left(1 + \frac{n}{2}\right) B_n. \quad (4.0.19)$$

Where the relation,  $x\Gamma(x) = \Gamma(x + 1)$  is used. Now a solution to  $B_n$  is found and is characterized as,

$$B_n = \frac{\pi^{\frac{n}{2}}}{\Gamma\left(1 + \frac{n}{2}\right)}. \quad (4.0.20)$$

The surface area and volume of an n dimensional hypersphere is thus given as,

$$V_n(R) = \frac{\pi^{\frac{n}{2}} R^n}{\Gamma\left(1 + \frac{n}{2}\right)} \quad (4.0.21a)$$

$$S_{n-1}(R) = \frac{n\pi^{\frac{n}{2}} R^{n-1}}{\Gamma\left(1 + \frac{n}{2}\right)} \quad (4.0.21b)$$

$$S_{n-1}(R) = \frac{2\pi^{\frac{n}{2}} R^{n-1}}{\Gamma\left(\frac{n}{2}\right)}. \quad (4.0.21c)$$

### 4.0.3 Gaussian Average

$$\langle e^{itx} \rangle = \frac{1}{\sigma\sqrt{2\pi}} \int_{-\infty}^{\infty} e^{-\frac{(x-\mu)^2}{2\sigma^2}} e^{itx} dx \quad (4.0.22)$$

Where the variable  $x$  has a Gaussian distribution with a mean of  $\mu$  and a variance of  $\sigma^2$ . Making the substitution of,

$$a = \frac{1}{\sigma\sqrt{2\pi}} \quad (4.0.23a)$$

$$c = \sqrt{2}\sigma. \quad (4.0.23b)$$

Now the equation (4.0.22) becomes,

$$\langle e^{itx} \rangle = a \int_{-\infty}^{\infty} e^{-\frac{(x-\mu)^2}{2\sigma^2}} dx. \quad (4.0.24)$$

let,

$$\alpha = x - \mu \quad (4.0.25a)$$

$$\frac{d\alpha}{dx} = 1 \quad (4.0.25b)$$

$$\langle e^{itx} \rangle = a \int_{-\infty}^{\infty} e^{-\frac{\alpha^2}{c^2}} e^{it(\alpha+\mu)} d\alpha \quad (4.0.26a)$$

$$\langle e^{itx} \rangle = ae^{it\mu} \int_{-\infty}^{\infty} e^{-\frac{\alpha^2}{c^2}} e^{it\alpha} d\alpha \quad (4.0.26b)$$

$$\langle e^{itx} \rangle = ae^{it\mu} \int_{-\infty}^{\infty} e^{-\frac{1}{c^2}(\alpha^2 - itc^2\alpha)} d\alpha. \quad (4.0.26c)$$

Substitute  $c$  back in from the equation given in (4.0.23) into the brackets,

$$\langle e^{itx} \rangle = ae^{it\mu} \int_{-\infty}^{\infty} e^{-\frac{1}{2}(\alpha^2 - i2t\sigma^2\alpha)} d\alpha \quad (4.0.27a)$$

$$= ae^{(it\mu - \frac{t^2\sigma^2}{2})} \int_{-\infty}^{\infty} e^{-\frac{(\alpha - it\sigma^2)^2}{c^2}} d\alpha. \quad (4.0.27b)$$

Using the substitution rule,

$$\gamma = \alpha - it\sigma^2 \quad \frac{d\gamma}{d\alpha} = 1 \quad (4.0.28a)$$

now the equation becomes,

$$\langle e^{itx} \rangle = ae^{(it\mu - \frac{t^2\sigma^2}{2})} \int_{-\infty}^{\infty} e^{-\frac{\gamma^2}{c^2}} d\gamma. \quad (4.0.29)$$

$$\phi = \frac{\gamma}{c} \quad (4.0.30a)$$

$$\frac{d\phi}{d\gamma} = \frac{1}{c} \quad (4.0.30b)$$

$$cd\phi = d\gamma. \quad (4.0.30c)$$

$$\langle e^{itx} \rangle = ace^{(it\mu - \frac{t^2\sigma^2}{2})} \int_{-\infty}^{\infty} e^{-\phi^2} d\phi \quad (4.0.31a)$$

$$= ace^{(it\mu - \frac{t^2\sigma^2}{2})} \sqrt{\pi}. \quad (4.0.31b)$$

Substituting back in  $a$  and  $c$  from (4.0.23) into (4.0.32) to get the final relation,

$$\langle e^{itx} \rangle = e^{(it\mu - \frac{t^2\sigma^2}{2})}. \quad (4.0.32)$$

#### 4.0.4 Central limit Theorem

Central limit theorem states that the sums of a large number of independent random variables tends towards a normal distribution and this does not depend on the original distribution of the variables. First take the independent random variables to be  $x_1, x_2, x_3, \dots, x_n$  with probability distributions that are not necessarily the same. Also expressing their mean as  $\bar{x}_1, \bar{x}_2, \bar{x}_3, \dots, \bar{x}_n$ , as well as the variance  $\sigma_1^2, \sigma_2^2, \sigma_3^2, \dots, \sigma_n^2$ . [40]

Then if,

$$Y = \frac{1}{\sqrt{n}} \sum_{i=1}^n \frac{x_i - \bar{x}_1}{\sigma_1}, \quad (4.0.33)$$

take that in the limit  $n$  tends to infinity the probability density function of  $y$  ( $p(y)$ ) approaches a Gaussian density.

$$\lim_{n \rightarrow \infty} p_Y(y) = \frac{1}{\sqrt{2\pi}} e^{-\frac{y^2}{2}}. \quad (4.0.34)$$

This also works for sums of samples. If a large number of samples of size  $n$  is taken then the distribution of the sums in  $n$  tends to be normally distributed.

#### 4.0.5 Speckle Statistics

The following information was deduced from the work of J.W. Goodman, *Statistical Optics* as well as *Speckle Phenomena in Optics* [40] [41], and includes specific relevant information required for the work conducted in this thesis. A definition of a speckle is given as , the intensity pattern usually formed by the interference of waves, and in a specific case when a number of independent phased components which are complex are added together to form a signal. The signals discussed will have random phases as well as lengths (amplitudes).

**Sum of random phasors:**

Initially defining the phasor sum as follows,

$$A = Ae^{i\theta} = \frac{1}{\sqrt{N}} \sum_{n=1}^N B_n = \frac{1}{\sqrt{N}} \sum_{n=1}^N a_n e^{i\phi_n}. \quad (4.0.35)$$

Given that  $a_n$  is the length of  $B_n$ , and  $\phi_n$  is the phase of  $B_n$ . Note a scaling factor of  $\frac{1}{\sqrt{N}}$  is used here, so as to maintain the finite second moments of the sum.

There are a few assumptions, which will now be stated, about the statistics of the components of the phasors in which the sum is made up of. These are of most importance, as all the calculations which will follow rely deeply on them:

- 1) The amplitude and the phase given by  $a_n$  and  $\phi_n$  respectively are statistically independent from one phasor to another. In other words the value of amplitude and phase of one phasor reveals no information about the phase and amplitude of the other phasors.
- 2) For each individual phasor the amplitude and phase are completely independent of each other.
- 3) The presumption of uniform distribution is taken for the phases  $\phi_n$ .

**Moments of the imaginary and real parts of the resultant phasor**

Note for the duration of this section the expectation value shall be denoted as  $E$ , and all the assumptions are used from before.

$$E[\Re] = E\left[\frac{1}{\sqrt{N}} \sum_{n=1}^N a_n \cos \phi_n\right] \quad (4.0.36a)$$

$$= \frac{1}{\sqrt{N}} \sum_{n=1}^N E[a_n \cos \phi_n] \quad (4.0.36b)$$

$$= \frac{1}{\sqrt{N}} \sum_{n=1}^N E[a_n] E[\cos \phi_n] = 0 \quad (4.0.36c)$$

Equivalently the imaginary part is found as,

$$E[\Im] = \frac{1}{\sqrt{N}} \sum_{n=1}^N E[a_n] E[\sin \phi_n] = 0. \quad (4.0.37)$$

Since it was stated before that the phase has a uniform distribution, this gives the average of  $\sin \phi_n$  and  $\cos \phi_n$  is  $= 0$ . Also noting that the variances of the real and imaginary part are equal to the second moments since the means are zero.

$$\sigma_{\Re}^2 = E[\Re^2] = \frac{1}{N} \sum_{n=1}^N \sum_{j=1}^N E[a_n a_j] E[\cos \phi_n \cos \phi_j] \quad (4.0.38a)$$

$$\sigma_{\Im}^2 = E[\Im^2] = \frac{1}{N} \sum_{n=1}^N \sum_{j=1}^N E[a_n a_j] E[\sin \phi_n \sin \phi_j]. \quad (4.0.38b)$$

Now for  $n \neq j$   $E[\cos \phi_n \cos \phi_j] = E[\cos \phi_n]E[\cos \phi_j] = 0$ , and the same can be seen for the imaginary part. Thus the terms where  $n = j$  are left, and the expressions in equation 4.0.38 can be expressed as,

$$\sigma_{\Re}^2 = \sum_{n=1}^N \frac{1}{N} E[a_n^2] E[\cos^2 \phi_n] = \frac{1}{N} \sum_{n=1}^N E[a_n^2] E\left[\frac{1}{2} + \frac{1}{2} \cos 2\phi_n\right] \quad (4.0.39a)$$

$$\sigma_{\Re}^2 = \frac{1}{N} \sum_{n=1}^N \frac{E[a_n^2]}{2} \quad (4.0.39b)$$

$$\sigma_{\Im}^2 = \frac{1}{N} \sum_{n=1}^N \frac{E[a_n^2]}{2}. \quad (4.0.39c)$$

It was assumed here that  $\phi_n$  is uniformly distributed on  $(-\pi, \pi)$ . The means and variances, of both the real  $\Re$  and imaginary  $\Im$  parts, are identical to one another. A useful identity to have is the correlation ( $\Gamma$ ) between the real and imaginary part, for the case here, this is shown to be,

$$\Gamma(\Re, \Im) = E[\Re \Im] = \frac{1}{N} \sum_{n=1}^N E[a_n^2] E[\cos \phi_n \sin \phi_n] = 0. \quad (4.0.40)$$

So for the conditions specified before, there is no correlation between the real and imaginary parts of the resultant phasor as shown in equation 4.0.40.

### Large number of independent steps

Recall, the resultant phasor is given by,

$$A = \sum \frac{1}{\sqrt{N}} e^{i\phi_n}. \quad (4.0.41)$$

Taking  $N$  to be very large, then  $\Re$  and  $\Im$  are going to be sums of independent random variables, this gives rise to the central limit theorem which states that the sum of a large  $N$  independent random variables, is asymptotic as  $N$  tends to infinity. Refer to section 4.0.4.

Given all the results obtained from equations (4.0.39, 4.0.36), one can find the joint probability density function, which can be expressed as follows,

$$P_{\Re \Im}(\Re, \Im) = \frac{1}{2\pi\sigma^2} e^{-\frac{\Re^2 + \Im^2}{2\sigma^2}}, \quad (4.0.42)$$

where  $\sigma^2 = \sigma_{\Im}^2 = \sigma_{\Re}^2$ .

The joint probability density function for both the amplitude and phase can be easily found through transformation of variables.

$$A = \sqrt{\Re^2 + \Im^2} \quad (4.0.43a)$$

$$\theta = \arctan\left(\frac{\Im}{\Re}\right) \quad (4.0.43b)$$

$$\Re = A \cos \theta \quad (4.0.44a)$$

$$\Im = A \sin \theta. \quad (4.0.44b)$$

By taking the Jacobian transformation determinant between the amplitude and phase  $(A, \theta)$ , with  $\Re$  and  $\Im$ , the probability of phase and amplitude is given by,

$$P_{A,\theta}(A, \theta) = P_{\Re,\Im}(A \cos \theta, A \sin \theta) \|J\|. \quad (4.0.45)$$

Here defining  $\|J\|$  as the Jacobian transformation.

$$\|J\| = \left\| \begin{array}{cc} \frac{\partial \Re}{\partial A} & \frac{\partial \Re}{\partial \theta} \\ \frac{\partial \Im}{\partial A} & \frac{\partial \Im}{\partial \theta} \end{array} \right\|.$$

Following this, an expression for the joint probability density for amplitude and phase of the resultant phasor is given by,

$$P_{A,\theta}(A, \theta) = \frac{A}{2\pi\sigma^2} e^{-\frac{A^2}{2\sigma^2}}. \quad (4.0.46)$$

Notice that the value of the Jacobian is equal to  $A$ .

Since the joint probability density is found, it is still possible to find the expression for the amplitude and phase alone. Starting by finding the probability density of the amplitude, for this the expression of probability density given by equation 4.0.46 is integrated in terms of phase using the limits from  $-\pi$  to  $\pi$ ,

$$P_A(A) = \int_{-\pi}^{\pi} P_{A,\theta}(A, \theta) d\theta = \frac{A}{\sigma^2} e^{-\frac{A^2}{2\sigma^2}}. \quad (4.0.47)$$

Now the density function of the phase is given by integrating over all possible amplitudes.

$$P_\theta(\theta) = \int_0^\infty \frac{A}{2\pi\sigma^2} e^{-\frac{A^2}{2\sigma^2}} dA = \frac{1}{2\pi}. \quad (4.0.48)$$

From this one can deduce that the probability density of phase and amplitude are statistically random variables, as the product of the two probabilities is equivalent to the joint probability density function.

## 4.0.6 Helmholtz equation

The Helmholtz equation is a partial differential equation of the form,

$$\nabla^2 A + k^2 A = 0. \quad (4.0.49)$$

Here  $\nabla^2$  is the Laplacian. The Helmholtz equation usually represents a time-independent form of the wave equation, so in terms of the wave equation given by,

$$\left(\nabla^2 - \frac{1}{c^2} \frac{\partial^2}{\partial t^2}\right) u(r, t) = 0. \quad (4.0.50)$$

Assuming that the wavefunction  $u(r, t)$  is separable.

$$u(r, t) = A(r)T(t) \quad (4.0.51)$$

Substituting this back into the wave equation in 4.0.50.

$$\frac{\nabla^2 A(r)}{A} - \frac{1}{Tc^2} \frac{\partial^2 T(t)}{\partial t^2} = 0. \quad (4.0.52)$$

Assuming both the spacial and time independent variables are equal to a constant call it  $k^2$ .

$$\nabla^2 A(r) + Ak^2 = 0. \quad (4.0.53)$$

# Bibliography

- [1] M. V. Berry, “‘faster than fourier’,in ‘quantum coherence and reality:in celebration of the 60th birthday of yakir aharonov’(j s anandan and j l safko, eds.),” *World Scientific, Singapore, pp.* 55–65, 1994.
- [2] M. V. Berry and S. Popescu, “Evolution of quantum superoscillations and optical superresolution without evanescent waves,” *J. Phys. A:Math. Gen.*, no. 6965-6977, 2006.
- [3] M. V. Berry and M. R. Dennis, “Natural superoscillations in monochromatic waves in d dimensions,” *J. Phys. A:Math. Theor.*42, 2009.
- [4] M. R. Dennis and J. Lindberg, “Natural superoscillation of random functions in one and more dimensions,” *SPIE*, vol. 7394, 2009.
- [5] M. R. Dennis, A. C. Hamilton, and J. Courtial, “Superoscillations in speckle patterns,” *Optics Letters*, vol. 33, 2008.
- [6] E. T. F. Rogers and N. I. Zheludev, “Optical super-oscillations: sub-wavelength light focusing and super-resolution imaging,” *Journal of Optics*, vol. 15, 2013.
- [7] F. M. Huang, T. S. Kao, V. A. Fedotov, Y. Chen, and N. I. Zheludev, “Nanohole array as a lens,” *Nano Lett.*, vol. 8(8), pp. 2469–2472, 2008.
- [8] E. T. F. Rogers, T. Roy, S. Savo, N. I. Zheludev, J. Lindberg, M. R. Dennis, and J. E. Chad, “A super-oscillatory lens optical microscope for subwavelength imaging,” *Nature Materials*, vol. 11, pp. 432–435, 2012.
- [9] E. T. F. Rogers, S. Quraishie, J. E. Chad, T. A. Newman, N. I. Zheludev, and P. J. S. Smith., “Super-oscillatory polarisation contrast microscopy: Super-resolution for unlabelled cells,” *Institute for Life Sciences, University of Southampton*.
- [10] E. T. F. Rogers, S. Savo, J. Lindberg, T. Roy, M. R. Dennis, and N. I. Zheludev, “Super-oscillatory optical needle,” *Appl. Phys. Lett.*, vol. 102, 2013.
- [11] G. T. di Francia, “Super-gain antennas and optical resolving power),” *Nuovo Cimento*, pp. 426–438, 1952.
- [12] S. A. Schelkunoff, “A mathematical theory of linear arrays,” *The Bell System Technical Journal*, vol. 22, pp. 80–107, 1943.

- [13] P. M. Woodward and J. D. Lawson, "The theoretical precision with which an arbitrary radiation-pattern may be obtained from a source of finite size," *Journal of the Institution of Electrical Engineers - Part III: Radio and Communication Engineering*, vol. 95, pp. 363–370, 1948.
- [14] Y. Aharonov, D. Z. Albert, and L. Vaidman, "How the result of a measurement of a component of the spin of a spin-1/2 particle can turn out to be 100," *Phys. Rev. Lett.*, vol. 60, 1988.
- [15] P. J. S. G. Ferreira and A. Kempf, *IEEE Transactions on Signal Processing*.
- [16] P. Ferreira and A. Kempf, "The energy expense of superoscillations," *Signal Processing Conference*, 2002.
- [17] N. I. Zheludev, *Nature Materials*, pp. 420–422.
- [18] Y. Aharonov, F. Colombo, I. Sabadini, D. Struppa, and J. Tollaksen, "Some mathematical properties of superoscillations," *Journal of Physics A: Mathematical and Theoretical*, vol. 44, no. 36, 2011.
- [19] —, "The mathematics of superoscillations," 2015.
- [20] M. V. Berry and M. R. Dennis, "Phase singularities in isotropic random waves," *Proc. R. Soc.*, vol. 456, no. 2059–2079, 2000.
- [21] E. A. ASH and G. NICHOLLS, "Super-resolution aperture scanning microscope," *Nature*, vol. 237, pp. 510–512, 1972.
- [22] D. W. Pohl, W. Denk, and M. Lanz, "Optical stethoscopy: Image recording with resolution  $\hat{I}z/20$ ," *Appl. Phys. Lett.*, vol. 44, p. 651, 1984.
- [23] E. Synge, "Xxxviii. a suggested method for extending microscopic resolution into the ultra-microscopic region," *The London, Edinburgh, and Dublin Philosophical Magazine and Journal of Science*, vol. 6, no. 35, pp. 356–362, 1928.
- [24] F. M. Huang and N. I. Zheludev, "Super-resolution without evanescent waves," *Nano Lett.*, vol. 9(3), pp. 1249–1254, 2009.
- [25] D. Slepian and H. O. Pollak, "Prolate spheroidal wave functions, fourier analysis and uncertainty," *The Bell System Technical Journal*, vol. 40, pp. 43–63, 1961.
- [26] F. M. Huang and N. Zheludev, "Focusing of light by a nanohole array," *Appl. Phys. Lett.*, vol. 90, 2007.
- [27] N. I. Zheludev, F. Min Huang, and J. Garcia de Abajo, "Nanohole arrays enable multiple-point-source imaging," vol. 44, pp. 75–77, 10 2008.
- [28] V. Korepin, F. Gaehler, and J. Rhyner, "Quasiperiodic tilings: a generalized grid-projection method," *Acta Crystallogr. A*, vol. 44, pp. 667–72, 1988.

- [29] S. V, “Subwavelength focusing of light by nanohole array,” *University of Southampton*, 2010.
- [30] N. Jin and Y. Rahmat-Samii, “Particle swarm optimization for antenna designs in engineering electromagnetics,” vol. 2008, 03 2008.
- [31] J. Kennedy and R. C. Eberhart, “A discrete binary version of the particle swarm algorithm,” vol. 5, pp. 4104–4108, Oct 1997.
- [32] Z. S. Hegedus and V. Sarafis, “Superresolving filters in confocally scanned imaging systems,” *Journal of the Optical Society of America A*, vol. 3, pp. 1892–1896, 1986.
- [33] M. Martinez-Corral, P. Andres, C. J. Zapata-Rodriguez, and C. J. R. Shepard, “Improvement of three-dimensional resolution in confocal scanning microscopy by combination of two pupil filters,” vol. 4, pp. 145–148, 1998.
- [34] T. R.M.Sales and G. M. Morris, “Axial superresolution with phase-only pupil filters,” *Optics Communications*, vol. 156, pp. 227–230, 1998.
- [35] M. Mazilu, J. Baumgartl, S. Kosmeier, and K. Dholakia, “Optical eigenmodes; exploiting the quadratic nature of the energy flux and of scattering interactions,” *Opt. Express*, vol. 19, pp. 933–945, 2011.
- [36] K. Piché, J. Leach, A. S. Johnson, J. Z. Salvail, M. I. Kolobov, and R. W. Boyd, “Experimental realization of optical eigenmode super-resolution,” *Opt. Express*, vol. 20, pp. 26 424–26 433, 2012.
- [37] G. H. Yuan, S. Vezzoli, C. Altuzarra, E. T. Rogers, C. Couteau, C. Soci, and N. I. Zheludev, “Quantum super-oscillation of a single photon,” *Light: Science and Applications*, vol. 5, 2016.
- [38] E. T. Copson, *Asymptotic Expansions*. Cambridge University Press, 2004.
- [39] J. F. Nye and M. V. Berry, “Dislocations in wave trains,” *Proc. R. Soc. A.*, vol. 336, no. 165-190, 1974.
- [40] J. W. Goodman, *Statistical Optics*. John Wiley |& Sons, 2000.
- [41] ———, *Speckle Phenomena in Optics*. W. H. Freeman,, 2010.

## Appendix A: MATLAB codes

Here are the main codes used for the work conducted in this thesis, These code files can be provided to the reader upon request by emailing sharif.alkhass@gmail.com.

### Code for obtaining graphs in figures (3.1, 3.2, 3.4, 3.5)

```

8pt
1 clear
2 %superpostions of plane waves from different angle, each with a unique
3 %wavevector assigned at random from a bandwidth which is chosen in advance. Also samples ...
   are taken by the
4 %variable m stated below.(the function is band limited between pi and 2pi)
5 %however the actual bandwidth of the sample function changes with each
6 %iteration.
7 clear all;
8 xmin=0.0;
9 xmax=0.00004;           %x and y give us the area in which we are working with.
10 dx=0.000005;
11 nx=1+(xmax-xmin)/dx;
12 x=xmin:dx:xmax;
13 ymin=0;
14 ymax=0.00004;
15 dy=0.000005;
16 ny=1+(ymax-ymin)/dy;
17 y=ymin:dy:ymax;
18
19 tt=0.0.*pi;           %this is time however we take this as zero since we are only ...
   dealing with time independent functions.
20 N=[5,6,7,8,9,10,50,500]; %number of plane waves,we need more than one so as to graph ...
   the results
21 hbar=1;               %plank's constant divided by 2pi.
22 c=1;                  %speed.
23 M=1;                  %mass.
24 A=2.*pi;             %total angle.
25 lim=100000;          %lim 100000
26
27 B=[linspace(0,1,15) linspace(1.1,2,15) linspace(2.2,100,15)]; %this gives the bandwidth ...
   for a specific number of waves.
28 for b=1:length(B)
29     BP(b)=(B(b).*pi); %this is the bandwidth multiplied by pi
30 end
31 %code below calculates the wave function given at every x and y value, kmax
32 %would be the maximum K value given in each sample this is later used to
33 %find the condition where the local wavelength is larger than
34 %kmax(superscillating region).
35
36
37 k_min=[1,2,3,4,10,50,100]; %this code changes the min and max k values ...
   chosen.
38
39
40 for h=1:length(N)
41     for n=1:N(h)
42         ddeg(h)=A/N(h); %creates the angles for each plane ...
   wave(dependent on the number of waves we are looking at).
43         cd(h,n)=cos((n-1)*ddeg(h));
44         sd(h,n)=sin((n-1)*ddeg(h));
45     end
46 end
47
48
49 for t=1:length(k_min);
50     for h=1:length(N)
51         for b=1:length(B)
52             frac=zeros(1,lim);
53
54             for m=1:lim
55                 kmax(h)=k_min(t).*pi; %this will be our initial ...
   maximum wavenumber (however it changes with each itteration as shown ...
   in the code)
56                 for n=1:N(h)
57                     k0(n)=(k_min(t).*pi)+B(b).*rand.*(pi);
58                     kx(n)=k0(n)*cd(h,n);
59                     ky(n)=k0(n)*sd(h,n);
60                     k2(n)=kx(n)^2+ky(n)^2;
61                     w1(n)=c*k0(n); %angular frequency
62                     w(n)=hbar*k2(n)/(2*M);
63                     if sqrt(k2(n)) > kmax(h)
64                         kmax(h)=k0(n); %defines our maximum wavenumber
65                     end
66                 end
67                 sum1=zeros(nx,ny);
68                 a=zeros(1,N(h));
69                 for n=1:N(h);
70                     a1=-pi+2.*pi.*rand; %assigns a random amplitude for every wave
71                     a2=0+2*rand; %assigns random phase for every wave

```

```

72         a(n)=a2.*exp(a1.*1i);
73         t1=a(n).*exp(-1i*w(n)*tt);
74         t2=zeros(nx,1);
75         t2(:)=exp(1i*kx(n)*x(:));           %can be thought of as individual phasors
76         t3=zeros(1,ny);
77         t3(:)=exp(1i*ky(n)*y(:));
78         term=zeros(nx,ny);
79         term=t1*t2*t3;
80         sum1=sum1+term;
81     end
82     %calculation to find the fraction where the wavefunctions ...
      superoscillate,by finding the differential of the phase of the log ...
      wavefunction.
83     lp=log(sum1);
84     psu=zeros(nx,ny);
85     P=0;
86     dpdx=imag(diff(lp,1,1)/dx);
87     dpdy=imag(diff(lp,1,2)/dy);
88     % -----
89     for ix=1:nx-1
90         for iy=1:ny-1
91             kr(ix,iy)=sqrt(dpdx(ix,iy)^2+dpdy(ix,iy)^2);           %local ...
              wavenumber at every point
92             if kr(ix,iy) > kmax(h)
93                 P=P+1;
94             end
95         end
96     end
97     frac(m)=P/((nx-1)*(ny-1));           %fraction of area superoscillating
98     end
99     sumf=0;
100    for m=1:lim
101        sumf=sumf+frac(m);
102    end
103    fraction(t,h,b)=sumf/lim;           %average fraction ...
      of area that is superoscillating by taking (lim) samples
104    formatSpec0 = ' Mean fraction of surface that is superoscillating %8.4f\%n ';
105    fprintf(formatSpec0,fraction(t,h,b));
106
107
108
109     end
110 end
111
112
113
114 %-----
115 %calculates average fraction for specific number of sources
116 for t=1:length(k_min)
117     for b=1:length(B)
118         fraction2(t,b)=fraction(t,1,b); %N=5
119         fraction3(t,b)=fraction(t,2,b); %N=6
120         fraction4(t,b)=fraction(t,3,b); %N=7
121         fraction5(t,b)=fraction(t,4,b); %N=8
122         fraction6(t,b)=fraction(t,5,b); %N=9
123         fraction7(t,b)=fraction(t,6,b); %N=10
124         fraction8(t,b)=fraction(t,7,b); %N=50
125         fraction9(t,b)=fraction(t,8,b); %N=500
126     end
127 end
128
129
130 %-----
131 %finds the difference in wavelength for each bandwidth
132 for t=1:length(k_min)
133     for b=1:length(B)
134         dlam2(t,b)=(B(b).*pi./(2.*pi)).*((2.*pi./(k_min(t).*pi)).*(2.*pi./((k_min(t)+B(b)).*pi))); ...
              %puts bandwidth in terms of lambda
135     end
136 end
137 dlam21=dlam2(1,:); dlam22=dlam2(2,:); dlam23=dlam2(3,:); dlam24=dlam2(4,:);
138 dlam25=dlam2(5,:); dlam26=dlam2(6,:);
139 %-----
140 %lamda min (smallest wavelength calculated for each kmin value (taken over
141 %the whole range of bandwidths)
142
143 for b=1:length(B)
144     lamda1(b)=2-dlam2(1,b);
145     lamda2(b)=1-dlam2(2,b);
146     lamda3(b)=(2./3)-dlam2(3,b);
147     lamda4(b)=(2./4)-dlam2(4,b);
148     lamda10(b)=(2./10)-dlam2(5,b);
149     lamda50(b)=(2./50)-dlam2(6,b);
150     lamda100(b)=(2./100)-dlam2(7,b);
151 end
152
153
154
155 %-----
156 %Finding the fraction for a given N, where the fraction is in terms of 1
157 %k_min only and is dependent on the bandwidth.
158 fraction21=fraction2(1,:); fraction22=fraction2(2,:); fraction23=fraction2(3,:); fraction24=fraction2(4,:);
159 fraction25=fraction2(5,:); fraction26=fraction2(6,:); fraction27=fraction2(7,:);
160 fraction31=fraction3(1,:); fraction32=fraction3(2,:); fraction33=fraction3(3,:); fraction34=fraction3(4,:);
161 fraction35=fraction3(5,:); fraction36=fraction3(6,:); fraction37=fraction3(7,:);

```

```

162 fraction41=fraction4(1,:); fraction42=fraction4(2,:); fraction43=fraction4(3,:); fraction44=fraction4(4,:);
163 fraction45=fraction4(5,:); fraction46=fraction4(6,:); fraction47=fraction4(7,:);
164 fraction51=fraction5(1,:); fraction52=fraction5(2,:); fraction53=fraction5(3,:); fraction54=fraction5(4,:);
165 fraction55=fraction5(5,:); fraction56=fraction5(6,:); fraction57=fraction5(7,:);
166 fraction61=fraction6(1,:); fraction62=fraction6(2,:); fraction63=fraction6(3,:); fraction64=fraction6(4,:);
167 fraction65=fraction6(5,:); fraction66=fraction6(6,:); fraction67=fraction6(7,:);
168 fraction71=fraction7(1,:); fraction72=fraction7(2,:); fraction73=fraction7(3,:); fraction74=fraction7(4,:);
169 fraction75=fraction7(5,:); fraction76=fraction7(6,:); fraction77=fraction7(7,:);
170 fraction81=fraction8(1,:); fraction82=fraction8(2,:); fraction83=fraction8(3,:); fraction84=fraction8(4,:);
171 fraction85=fraction8(5,:); fraction86=fraction8(6,:); fraction87=fraction8(7,:);
172 fraction91=fraction9(1,:); fraction92=fraction9(2,:); fraction93=fraction9(3,:); fraction94=fraction9(4,:);
173 fraction95=fraction9(5,:); fraction96=fraction9(6,:); fraction97=fraction9(7,:);
174 %-----
175
176 %The code below shows the relationship etween the fraction of
177 %superoscillations against bandwidth. This id done for N=500 sources for
178 %several kmin values. In the thesis this is represented by figure 3.1
179 plot(B, fraction91, 'k', B, fraction92, B, fraction93, B, fraction94, B, fraction95, B, fraction96, B, fraction97)
180 xlabel('Bandwidth in \pi')
181 ylabel('Fraction of area superoscillating')
182 title('Change in initial wavenumber with N=500')
183 legend('k=1 \pi', 'k=2 \pi', 'k=3 \pi', 'k=4 \pi', 'k=10 \pi', 'k=50 \pi', 'k=100 \pi')
184 set(gca, 'FontSize', 20)
185
186 %The following code represents the figures 3.2,3.3 in the thesis and is
187 %given to be the fraction of superoscillations against the bandwidth
188 %for several values of N (N=5,6,7,8,9,10,50) for kmin = 1pi
189 plot(B, fraction21, B, fraction31, B, fraction41, B, fraction51)
190 hold on
191 plot(B, fraction61, B, fraction71, B, fraction81, B, fraction91)
192 xlabel('Bandwidth in \pi')
193 ylabel('Fraction of area superoscillating')
194 title('change in number of sources N (for bandwidth 0 to 100 \pi)')
195 legend('N=5', 'N=6', 'N=7', 'N=8', 'N=9', 'N=10', 'N=50')
196 set(gca, 'FontSize', 20)
197
198
199 %in order to plot the required figure please comment out that which is not
200 %needed. Figures with the approximation given are calculated using the
201 %curve fitting app built into MATLAB. Here a curve fit can be found by
202 %entering a particular equation.

```

## Code for obtaining figures (3.7, 3.8, 3.9, 3.15)

```

8pt
1 %the only difference in this code is that I took the band-width fixed with
2 %every itteration
3 %superpositions of plane waves from different angle, each with a unique
4 %wavelength. Also samples are taken by the
5 %variable m stated below.(the function is band limited between pi and 2pi
6 clear all;
7 xmin=0.0;
8 xmax=0.00004; %x and y give us the area in which we are working with.
9 dx=0.000005;
10 nx=round(1+(xmax-xmin)/dx);
11 x=xmin:dx:xmax;
12 ymin=0;
13 ymax=0.00004;
14 dy=0.000005;
15 ny=round(1+(ymax-ymin)/dy);
16 y=ymin:dy:ymax;
17
18 tt=0.0.*pi; %this is time however we take this as zero since we are only dealing ...
%with time independent functions.
19 N=[5,10,50,100,500]; %number of plane waves,we need more than one so as to graph the ...
%results.
20 hbar=1; %plank's constant divided by 2pi.
21 c=1; %speed.
22 M=1; %mass.
23 A=2.*pi; %total angle.
24 lim=100000;
25
26 B=[linspace(0,1,15) linspace(1.1,2,15) linspace(2.2,100,15)]; %this gives the ...
%bandwidth for a specific number of waves.
27 for b=1:length(B)
28 BP(b)=(B(b).*pi); %Finds the value for the bandwidth
29 end
30 %code below calculates the wave function given at every x and y value, kmax
31 %would be the maximum K value given in each sample this is later used to
32 %find the condition where the local wavelength is larger than
33 %kmax(superoscillating region).
34
35
36 k_min=[1,2,10,50,100]; %this code changes the min and max k ...
%values chosen.
37
38
39 for h=1:length(N)
40 for n=1:N(h)
41 ddeg(h)=A/N(h); %creates the angles for each plane ...
%wave(dependent on the number of waves we are looking at).

```

```

42     cd(h,n)=cos((n-1)*ddeg(h));           %in order to change the angles so they are ...
43         random, change ddeg(h) so that its ddeg(h,n)
44         %ddeg(h,n)=0+2.*pi.*rand and
45         %change cd(h,n)=cos(ddeg(h,n))
46         %sd(h,n)=sin(ddeg(h,n))
47     end
48 end
49
50 for t=1:length(k_min);
51     for h=1:length(N)
52         for b=1:length(B)
53             frac=zeros(1,lim);
54
55             for m=1:lim
56                 kmax(h)=k_min(t).*pi;           %this will be our initial ...
57                 %maximum wavenumber (however it changes with each iteration as shown ...
58                 %in the code
59                 for n=1:N(h)
60                     if n==1                       %if statements that make sure ...
61                         our bandwidth is fixed through every sample
62                         k0(n)=k_min(t).*pi;
63                     else if n==N(h)
64                         k0(n)=(k_min(t).*pi)+(B(b).*pi);
65                     else
66                         k0(n)=(k_min(t).*pi)+(B(b).*rand.*(pi));
67                     end
68                 end
69                 kx(n)=k0(n)*cd(h,n);
70                 ky(n)=k0(n)*sd(h,n);
71                 k2(n)=kx(n)^2+ky(n)^2;
72                 w1(n)=c*k0(n);                 %angular frequency
73                 w(n)=hbar*k2(n)/(2*M);
74                 if sqrt(k2(n)) > kmax(h)       %defines our maximum wavenumber
75                     kmax(h)=k0(n);
76                 end
77             end
78             sum1=zeros(nx,ny);
79             a=zeros(1,N(h));
80             for n=1:N(h);
81                 a1=-pi+2.*pi.*rand;           %assigns a random amplitude for every wave
82                 a2=2.*rand;                   %assigns random phase for every wave
83                 a(n)=(a2).*exp(1i.*a1);
84                 t1=a(n);
85                 t2=zeros(nx,1);
86                 t2(:)=exp(1i*kx(n)*x(:));     %can be thought of as individual phasors
87                 t3=zeros(1,ny);
88                 t3(:)=exp(1i*ky(n)*y(:));
89                 term=zeros(nx,ny);
90                 term=t1*t2*t3;
91                 sum1=sum1+term;               %summing the waves at every point in ...
92                 %our 'pool' or rather area. defined by x and y
93             end
94             %calculation to find the fraction where the wavefunctions ...
95             %superoscillate, by finding the differential of the phase of the log ...
96             %wavefunction.
97             lp=log(sum1);
98             psu=zeros(nx,ny);
99             P=0;
100            dpdx=imag(diff(lp,1,1)/dx);
101            dpdy=imag(diff(lp,1,2)/dy);
102            %-----
103            for ix=1:nx-1
104                for iy=1:ny-1
105                    kr(ix,iy)=sqrt(dpdx(ix,iy)^2+dpdy(ix,iy)^2); %local wavenumber ...
106                    %at every point
107                    if kr(ix,iy) > kmax(h)
108                        P=P+1;
109                    end
110                end
111            end
112            frac(m)=P/((nx-1)*(ny-1));         %fraction of area superoscillating
113        end
114        sumf=0;
115        for m=1:lim
116            sumf=sumf+frac(m);
117        end
118        fraction(t,h,b)=sumf/lim;             %average fraction of area ...
119        %that is superoscillating by taking (lim) samples
120        formatSpec0 = ' Mean fraction of surface that is superoscillating %8.4f\n ';
121        fprintf(formatSpec0, fraction(t,h,b));
122    end
123 end
124
125 %-----
126 %calculates average fraction for specific number of sources
127
128 for t=1:length(k_min)
129     for b=1:length(B)
130         fraction2(t,b)=fraction(t,1,b); %N=5
131         fraction3(t,b)=fraction(t,2,b); %N=10
132         fraction4(t,b)=fraction(t,3,b); %N=50
133         fraction5(t,b)=fraction(t,4,b); %N=100
134     end
135 end

```

```

128         fraction6(t,b)=fraction(t,5,b); %N=500
129
130     end
131 end
132
133
134 %-----
135 %finds the difference in wavelength for each bandwidth
136 for t=1:length(k_min)
137     for b=1:length(B)
138         dlam2(t,b)=(B(b).*pi./(2.*pi)).*((2.*pi./(k_min(t).*pi)).*(2.*pi./((k_min(t)+B(b)).*pi))); ...
139             %puts bandwidth in terms of lambda
140     end
141 end
142 dlam21=dlam2(1,:); dlam22=dlam2(2,:); dlam23=dlam2(3,:); dlam24=dlam2(4,:); dlam25=dlam2(5,:);
143
144 %-----
145 %lamda min (smallest wavelength calculated for each kmin value (taken over
146 %the whole range of bandwidths)
147 %
148 for b=1:length(B)
149     lamda1(b)=2-dlam2(1,b);
150     lamda2(b)=1-dlam2(2,b);
151     lamda3(b)=(2./10)-dlam2(3,b);
152     lamda4(b)=(2./50)-dlam2(4,b);
153     lamda10(b)=(2./100)-dlam2(5,b);
154 end
155 %-----
156 %Finding the fraction for a given N, where the fraction is in terms of l
157 %k_min only and is dependent on the bandwidth.
158 fraction21=fraction2(1,:); fraction22=fraction2(2,:); fraction23=fraction2(3,:); fraction24=fraction2(4,:);
159 fraction25=fraction4(5,:);
160 fraction31=fraction3(1,:); fraction32=fraction3(2,:); fraction33=fraction3(3,:); fraction34=fraction3(4,:);
161 fraction35=fraction4(5,:);
162 fraction41=fraction4(1,:); fraction42=fraction4(2,:); fraction43=fraction4(3,:); fraction44=fraction4(4,:);
163 fraction45=fraction4(5,:);
164 fraction51=fraction5(1,:); fraction52=fraction5(2,:); fraction53=fraction5(3,:); fraction54=fraction5(4,:);
165 fraction55=fraction5(5,:);
166 fraction61=fraction6(1,:); fraction62=fraction6(2,:); fraction63=fraction6(3,:); fraction64=fraction6(4,:);
167 fraction65=fraction6(5,:);
168
169 %-----
170 %the plot below show the relationship between the bandwidth and the
171 %fraction of superoscillations for several N values at kmin =1pi. In the
172 %thesis this corresponds to figures 3.7 and 3.8 where 3.8 is just a zoomed
173 %in version of 3.7
174 plot(B, fraction21 ,B, fraction31 ,B, fraction41 ,B, fraction51 ,B, fraction61 )
175 xlabel('Bandwidth in \pi')
176 ylabel('Fraction of area superoscillating')
177 title('change in number of sources N')
178 legend('N=5','N=10','N=50','N=100','N=500')
179 set(gca,'FontSize',30)
180
181 %the plot below shows the relation ship between bandwidth and the fraction
182 %of superoscillations for N=500 for several k_min values . in the thesis
183 %this relates to figure 3.9.
184 plot(B, fraction61 ,B, fraction62 ,B, fraction63 ,B, fraction64 ,B, fraction65 )
185 xlabel('Bandwidth in \pi')
186 ylabel('Fraction of area superoscillating')
187 title('Average fraction against bandwidth with change in kmin (N=500)')
188 legend('kmin=1 \pi','kmin=2 \pi','kmin=10 \pi','kmin=50 \pi')
189 set(gca,'FontSize',30)

```

## Code for Probability density of wavenumbers figures (3.11, 3.12, 3.14)

```

8pt
1 %superpositions of plane waves from different angle, each with a unique
2 %wavelength where each wavelength is larger than that of k0 giving the
3 %condition that kn must be smaller than k0. Also samples are taken by the
4 %variable m stated below.(the function is band limited between pi and 2pi
5 clear all;
6 xmin=0.0;
7 xmax=0.00004;
8 dx=0.000001;
9 nx=round(1+(xmax-xmin)/dx);
10 x=xmin:dx:xmax;
11 ymin=0;
12 ymax=0.00004;
13 dy=0.000001;
14 ny=round(1+(ymax-ymin)/dy);
15 y=ymin:dy:ymax;
16
17 tt=0.0.*pi;
18 N=[5,50]; %number of plane waves,we need more than one so as to graph the results
19 hbar=1;
20 c=1;
21 M=1;

```

```

22 A=2.*pi;
23 lim=10000;
24
25 B=[2]; %this gives the bandwidth for a specific number of waves.
26
27 %code below calculates the wave function given at every x and y value, kmax
28 %would be the maximum K value given in each sample this is later used to
29 %find the condition where the local wavelength is larger than
30 %kmax(superoscillating region).
31
32 k_min=[0,1]; %this code changes the min and max k values chosen.
33 for h=1:length(N)
34     for n=1:N(h)
35         ddeg(h)=A/N(h); %creates the angles for each plane wave(dependent on the number of ...
36             waves we are looking at).
37         cd(h,n)=cos((n-1)*ddeg(h));
38         sd(h,n)=sin((n-1)*ddeg(h));
39     end
40 end
41 for t=1:length(k_min)
42     for h=1:length(N)
43         for b=1:length(B)
44             frac=zeros(1,lim);
45             for m=1:lim
46                 kmax(h)=k_min(t).*pi; %this will be our initial ...
47                 maximum wavenumber (however it changes with each iteration as shown ...
48                 in the code
49                 for n=1:N(h)
50                     if n==1 %if statements that make sure ...
51                         our bandwidth is fixed through every sample
52                         k0(n)=k_min(t).*pi;
53                     else if n==N(h)
54                         k0(n)=(k_min(t).*pi)+(B(b).*pi);
55                     else
56                         k0(n)=(k_min(t).*pi)+(B(b).*rand.*(pi));
57                     end
58                 end
59                 kx(n)=k0(n)*cd(h,n);
60                 ky(n)=k0(n)*sd(h,n);
61                 k2(n)=kx(n)^2+ky(n)^2;
62                 w1(n)=c*k0(n); %angular frequency
63                 w(n)=hbar*k2(n)/(2*M);
64                 if sqrt(k2(n)) > kmax(h) %defines our maximum wavenumber
65                     kmax(h)=k0(n);
66                 end
67             end
68             sum1=zeros(nx,ny);
69             sumt=zeros(nx,ny);
70             a=zeros(1,N(h));
71             for n=1:N(h)
72                 a1=-pi+2.*pi.*rand; %assigns a random amplitude for every wave
73                 a2=2.*rand; %assigns random phase for every wave
74                 a(n)=(a2).*exp(1i.*a1);
75                 t1=a(n);
76                 t2=zeros(nx,1);
77                 t2(:)=exp(1i*kx(n)*x(:)); %can be thought of as individual phasors
78                 t3=zeros(1,ny);
79                 t3(:)=exp(1i*ky(n)*y(:));
80                 term=zeros(nx,ny);
81                 term=t1*t2*t3;
82                 sum1=sum1+term; %summing the waves at every point in ...
83                 our 'pool' or rather area. defined by x and y
84             end
85             %realkmin2(t,h,b,m)=min(sqrt(k2(:))); %minimum wavenumber for each sample
86
87             %calculation to find the fraction where the wavefunctions ...
88             superoscillate, by finding the differential of the phase(log wavefunction).
89             lp=log(sum1);
90             psu=zeros(nx,ny);
91             P(m)=0;
92             dpdx=imag(diff(lp,1,1)/dx);
93             dpdy=imag(diff(lp,1,2)/dy);
94             % -----
95             for ix=1:nx-1
96                 for iy=1:ny-1
97                     kr(ix,iy)=sqrt(dpdx(ix,iy).^2+dpdy(ix,iy).^2);
98                     if kr(ix,iy) > kmax(h)
99                         P(m)=P(m)+1;
100                     end
101                 end
102                 K1(t,h,b,m,ix,iy)=kr(ix,iy); %every single local wavenumber for ...
103                 each sample we take at every x and y point
104             end
105         end
106     end
107 end
108 % for every m this finds the fraction of superoscillating waves. then add ...
109 all results for each repeat and find the average
110 frac(m)=P(m)/((nx-1)*(ny-1));
111 realfrac(t,h,b,m)=frac(m); %superoscillating fraction for every sample
112 k01(t,h,b,m)=kmax(h); %every Kmax for every sample
113 for ix=1:nx-1
114     for iy=1:ny-1
115         k10(t,h,b,m,ix,iy)=K1(t,h,b,m,ix,iy)./k01(t,h,b,m); % local wavenumber ...
116         divided by the maximum wavevector for that sample
117     end

```

```

108         end
109         %-----
110         %-----
111         %PDDK is the expression found through the result obtained
112         %for probability distribution given by equation
113         %\ref{eq:4.32} with the power spectrum given by
114         %\ref{eq:4.39} (section superoscillations in speckle pattern).
115         for ix=1:nx-1
116             for iy=1:ny-1
117 PDDK(t,h,b,m,ix,iy)=(((k01(t,h,b,m).^2)/2) ...
118             *(2-(2.*B(b)./k01(t,h,b,m))+B(b)./k01(t,h,b,m)).^2).*K1(t,h,b,m,ix,iy)) ...
119             ./(((K1(t,h,b,m,ix,iy).^2 + ((k01(t,h,b,m).^2)/4) ...
120             *(2-(2.*B(b)./k01(t,h,b,m))+B(b)./k01(t,h,b,m))))).^2);
121         end
122         end
123         sumf=0;
124         for m=1:lim
125             sumf=sumf+frac(m);
126         end
127         fraction(t,h,b)=sumf/lim;
128         formatSpec0 = ' Mean fraction of surface that is superoscillating %8.4f\n ' ;
129         fprintf(formatSpec0,fraction(t,h,b));
130     end
131 end
132
133
134 %-----CALCULATING K
135 %DISTRIBUTION-----
136 %the following calculates the probability distribution for the wavenumbers
137 %using the equation given in section: superoscillations in speckle patterns
138 %each represents a specific bandwidth value for kmin=1pi.
139
140
141 PDDK2=PDDK(2,1,1,,:,:,);
142 PDDK32(:)=PDDK2(:); %the array for the probability distribution
143 normPDDK32(:)=PDDK32(:)/max(PDDK32);
144
145 PDDK3=PDDK(2,2,1,,:,:,);
146 PDDK33(:)=PDDK3(:); %the array for the probability distribution
147 normPDDK33(:)=PDDK33(:)/max(PDDK33);
148
149
150
151
152 %the following finds the array of each local wavenumber divided by kmax in
153 %the sample for kmin 1pi and bandwidth of 0,2,and 50 pi respectively. In
154 %order to produced the graphs for different N values please change the
155 %value of N at the beginning of the code (the reason for running only one N
156 %is to reduce running time). Also to produce the graphs but for the other
157 %kmin values please change k10(2,1,1,,:,:,) to k10(3,1,1,,:,:,) for kmin =2pi and so on.
158
159
160
161 K32=k10(2,1,1,,:,:,);
162 K332(:)=K32(:); %array of wavenumbers
163
164 K33=k10(2,2,1,,:,:,);
165 K333(:)=K33(:); %array of wavenumbers
166
167
168
169 %please uncomment and comment the required plots for the different
170 %bandwidths.
171 % numOfBins = 2500;
172 % [histFreq, histkout] = hist(K331, numOfBins);
173 % figure;
174 % bar(histkout, histFreq/max(histFreq))
175 % hold on
176 % plot(K331,normPDDK31,'+')
177
178 numOfBins = 2500;
179 [histFreq2, histkout2] = hist(K332, numOfBins);
180 % figure;
181 % bar(histkout2, histFreq2/max(histFreq2))
182 % hold on
183 % plot(K332,normPDDK32,'+')
184
185 %+++++
186 %here some of the graphs require the axis properties to be changed by going
187 %to 'edit' and then 'axis properties' once the graph is shown. This is
188 %because there are values which have a very large k(r)to k(0) ratio but
189 %with very small probability.
190 %+++++
191 numOfBins = 20000000;
192 [histFreq3, histkout3] = hist(K333, numOfBins); %this plots for bandwidth 50 pi
193 figure;
194 plot(histkout3, histFreq3/max(histFreq3))
195 hold on
196 plot(histkout2, histFreq2/max(histFreq2))
197 %plot(K333,normPDDK33,'+')
198
199
200 xlabel('k(r)/k0')

```

```
201 ylabel('Probability (P)')
202 title('Probability distribution wavenumber k (N=5, kmin=1\pi, Bandwidth=50\pi)')
203 legend('Calculated Distribution', 'Theoretical expression')
204 set(gca, 'FontSize', 15)
```